

**DEVELOPMENT AND CHARACTERISATION OF AML-M5-
DERIVED INDUCED PLURIPOTENT STEM CELLS (IPSCS)**

By

CHIEW MEN YEE

A dissertation submitted to the Department of Pre-clinical Sciences,

Faculty of Medicine and Health Sciences,

Universiti Tunku Abdul Rahman,

In partial fulfillment of the requirements for the degree of

Master of Medical Sciences

October 2015

ABSTRACT

DEVELOPMENT AND CHARACTERISATION OF AML-M5- DERIVED INDUCED PLURIPOTENT STEM CELLS (IPSCS)

CHIEW MEN YEE

Acute monocytic leukaemia (AML-M5) is a subtype of acute myeloid leukaemia (AML) with poor prognosis. The AML-M5 subtype is the most common type of AML in young children (< 2years old) of Asian and Hispanics origin with an incidence of 0.8 -1.1 per million per year. AML-M5 is believed to be highly associated with the formation of MLL-AF9 fusion gene. However, the pathogenic mechanisms underlying AML-M5 with MLL-AF9 remained poorly understood. Induced pluripotent stem cells (iPSCs) are derived from adult somatic cells via inducing ectopic expression of stem cell transcription factors. iPSCs are similar with embryonic stem cells (hESCs) from the aspects of gene expression and differentiation ability. In Malaysia, although AML-M5 is rare, it remains a disease that is difficult to treat. Development of AML-M5-derived iPSCs may provide a novel approach to elucidate the mechanisms of disease manifestations and hence leading to novel therapeutic intervention against AML-M5. The objective of this study was to generate iPSC line from THP-1 cell line originated from a patient with AML-M5. The parental AML-M5 cells were infected with retroviruses encoding the pluripotency-associated genes (*OCT3/4*, *SOX2*, *KLF4* and *c-MYC*) crucial for the maintenance and induction of pluripotent stem cells. The infected cells were next maintained on culture for 30 days under hypoxia condition. The iPSC-like colonies appeared

from day-14 to -30. Pluripotency of these iPSC-like colonies were then characterised via RT-PCR, immunofluorescence staining, immunophenotyping and *in vitro* differentiation assays into three germ layers. Genotype-phenotype characteristics were compared between parental AML-M5 cells and AML-M5-derived iPSCs by chromosomal translocation PCR method and detection of monocyte-specific markers using immunophenotyping method. The findings revealed that these AML-M5-derived iPSCs showed similarity with hESCs in terms of morphology, gene expression, protein/antigen expression and differentiation ability. Furthermore, reduction of parental markers and retention of expression of *MLL-AF9* fusion gene on AML-M5-derived iPSCs provided evidence that AML-M5-specific iPSC clones have been successfully developed and may provide a new avenue for the study of AML-M5 at stem cell level.

ACKNOWLEDGEMENT

First and foremost, I would like to express my special appreciation and thanks to my advisor Asst. Prof. Dr. Leong Pooi Pooi, you have been a tremendous mentor for me. Thank you for the encouragement you have given me throughout the duration of my research and for allowing me to grow as a research scientist. I would also like to thank to Emeritus Prof. Dr. Boo Nem Yun @ Mooi Nam Ying, Assoc. Prof. Dr. Alan Ong Han Kiat and Emeritus Prof. Dr. Cheong Soon Keng for your brilliant comments and suggestions. I would especially like to thank all present and past members of the UTAR Sungai Long Research lab especially Mr. Lim Sheng Jye who have provided me with help or advice.

I also want to acknowledge with much appreciation the crucial role of Universiti Tunku Abdul Rahman for their financial support granted through UTARRF, and provided necessary facilities. In addition, a thank you to Dr. Shigeki Sugii from A* STAR, Singapore Bioimaging Consortium (SBIC) for your kindness in providing pMXs vector encoding O, S, K, M and GFP. Besides, I would like to express my warm thank to Dr. Kenneth Raj from Health Protection Agency (HPA), UK, who provides me phoenix cells. I would like to thank Cryocord Sdn. Bhd, Malaysia for providing human adipose-derived mesenchymal stem cells. Last but not least, a special thanks to my family and friends especially my parents, for giving me their support, and encouragement to achieve my goal.

APPROVAL SHEET

This dissertation entitled “**DEVELOPMENT AND CHARACTERISATION OF AML-M5-DERIVED INDUCED PLURIPOTENT STEM CELLS (IPSCS)**” was prepared by CHIEW MEN YEE and submitted as partial fulfillment of the requirements for the degree of Master of Medical Sciences at Universiti Tunku Abdul Rahman.

Approved by:

(Assistant Prof. Dr. LEONG POOI POOI)
Professor/Supervisor
Department of Pre-clinical
Faculty of Medicine and Health Sciences
Universiti Tunku Abdul Rahman

Date:.....

(Emeritus Prof. Dr. BOO NEM YUN @ MOOI NAM YING)
Senior Professor/Co-supervisor
Department of Population Medicine
Faculty of Medicine and Health Sciences
Universiti Tunku Abdul Rahman

Date:.....

FACULTY OF MEDICINE AND HEALTH SCIENCES

UNIVERSITI TUNKU ABDUL RAHMAN

DATE: October 2015

SUBMISSION OF DISSERTATION

It is hereby certified that **CHIEW MEN YEE** (ID No: **12UMM07735**) has completed this dissertation entitled “**DEVELOPMENT AND CHARACTERISATION OF AML-M5-DERIVED INDUCED PLURIPOTENT STEM CELLS (IPSCS)**” under the supervisor of Assist. Prof. Dr. **LEONG POOI POOI** (Supervisor) from the Department of Pre-clinical Sciences, Faculty of Medicine and Health Sciences, and Emeritus Prof. Dr. **BOO NEM YUN @ MOOI NAM YING** (Co-Supervisor) from the Department of Population Medicine, Faculty of Medicine and Health Sciences.

I understand that the University will upload softcopy of my dissertation in pdf format into UTAR Institutional Repository, which may be made accessible to UTAR community and public.

Yours truly,

CHIEW MEN YEE

DECLARATION

I CHIEW MEN YEE hereby declare that the dissertation is based on my original work except for quotations and citations which have been duly acknowledged. I also declare that it has not been previously or concurrently submitted for any other degree at UTAR or other institutions.

(CHIEW MEN YEE)

Date: October 2015

TABLE OF CONTENTS

	Page
ABSTRACT	ii
ACKNOWLEDGEMENT	iv
APPROVAL SHEET	v
SUBMISSION OF DISSERTATION	vi
DECLARATION	vii
LIST OF TABLES	xii
LIST OF FIGURES	xiii
LIST OF ABBREVIATIONS	xv
CHAPTER	
1.0 INTRODUCTION	1
2.0 LITERATURE REVIEW	4
2.1 Acute monocytic leukaemia (AML-M5)	4
2.1.1 Epidemiology of AML-M5	6
2.1.2 Clinical Presentation of AML-M5	7
2.1.3 Diagnosis of AML-M5	8
2.1.4 Treatment of AML-M5	10
2.1.5 Pathogenesis of AML-M5	12
2.2 Pluripotent Stem Cells	16
2.3 Induced Pluripotent Stem Cells	16
2.3.1 Reprogramming Factors	18
2.3.2 Potential Applications of iPSCs	22
2.3.3 Reprogramming Methods	25
2.3.4 Pluripotency Characterisation Assays	36
3.0 MATERIALS AND METHODS	42
3.1 Cell Culture	44

3.1.1	Maintenance and Subculture of AML-M5 Leukaemia Cells	44
3.1.2	Maintenance, Subculture and Inactivation of Feeder Cells	45
3.1.3	Maintenance and Subculture of Human Embryonic Stem Cells (ESCs)	46
3.1.4	Maintenance and Subculture of Phoenix Packaging Cell Line	47
3.2	Preparation of Recombinant Plasmids	49
3.2.1	Expansion of Transformed <i>E. coli</i>	49
3.2.2	Isolation of Recombinant Plasmids	49
3.2.3	Verification of Recombinant Plasmids	50
3.3	Transfection and Infection Optimisation	51
3.3.1	Transfection Optimisation of Phoenix Cells Using Recombinant Plasmid GFP	51
3.3.2	Infection of Parental Cells Using Retrovirus Harboursing GFP	52
3.4	Generation of AML-M5-Induced Pluripotent Stem Cells (AML-M5-derived iPSCs)	53
3.4.1	Maintenance and Subculture of AML-M5-derived Induced Pluripotent Stem Cells (AML-M5-derived iPSCs)	55
3.5	Characterisation of AML-M5-derived iPSCs	57
3.5.1	Detection of Pluripotency Markers Using Reverse Transcription-Polymerase Chain Reaction (RT-PCR)	57
3.5.2	Detection of Pluripotency Markers Using Immunofluorescence Staining	66
3.5.3	Detection of Pluripotency Markers Using Flow Cytometry	67
3.5.4	<i>In Vitro</i> Three Germ Layers Differentiation	68
3.6	Verification of AML-M5-derived iPSCs	72
3.6.1	Detection of Monocyte-specific Markers Using Flow Cytometry	72

3.6.2	Detection of Leukaemia-associated <i>MLL-AF9</i> Fusion Gene Using Reverse Transcription- Polymerase Chain Reaction (RT-PCR)	73
3.7	Data Analysis	74
4.0	RESULTS	75
4.1	Verification of Recombinant Plasmids Using Restriction Enzymes	75
4.2	Optimisation of Transfection and Infection Protocols	76
4.3	Generation of AML-M5-derived iPSCs Using Retrovirus Particles Harboursing O, S, K and M	83
4.4	Formation and Maintenance of AML-M5-derived iPSCs	86
4.5	Pluripotency Characterisation of AML-M5-derived iPSCs	89
4.5.1	Gene Expression Study of Pluripotency Markers Using RT-PCR Method	89
4.5.2	Detection of Pluripotency Markers Using Immunofluorescence Staining	92
4.5.3	Detection of Pluripotency Markers Using Flow Cytometry Analysis	99
4.5.4	<i>In vitro</i> Three Germ Layers Differentiation Assays	103
4.6	Verification of AML-M5-derived iPSCs	113
4.6.1	Detection of Monocyte-specific Markers Using Immunophenotyping	113
4.6.2	Detection of <i>MLL-AF9</i> Fusion Gene	116
5.0	DISCUSSION	118
5.1	Generation of AML-M5-derived iPSCs	118
5.2	Characterisation of AML-M5-derived iPSCs	124
6.0	CONCLUSION	133
6.1	Conclusion	133
6.2	Limitations of the Study	134
6.3	Future Studies	136

REFERENCES

137

APPENDICES

160

LIST OF TABLES

Table		Page
2.1	Compounds that modulate stem cell fate and reprogramming	35
3.1	Restriction enzymes and their expected product sizes for different recombinant plasmids used in the study	51
3.2	Monoclonal antibodies used for intracellular and surface staining	67
4.1	Summary of gene expression of pluripotency markers in hESCs, AML-M5-derived iPSCs, feeder cells and AML-M5 cells	90
4.2	Comparative expression of pluripotency markers in AML-M5-derived iPSCs and parental AML-M5 cells	102
4.3	Comparative expression of monocytic-specific markers in AML-M5-derived iPSCs and parental AML-M5 cells	115

LIST OF FIGURES

Figure		Page
2.1	Classification of AML according French-American-British (FAB) classification	5
2.2	Standard hematoxylin and eosin stain of blood film of patient with AML-M5	6
2.3	The <i>MLL</i> complex and its molecular functions	15
3.1	Flow chart of this study	43
4.1	Verification of recombinant plasmids using restriction enzyme digestion	75
4.2	Transfection of Phoenix cells with different concentration of pMX-GFP at 50-60% cell confluency	78
4.3	Infection of AML-M5 cells with GFP encoded virus particles produced from 50-60% confluency of Phoenix cells	79
4.4	Transfection of Phoenix cells with different concentration of pMX-GFP at 70-80% cell confluency	81
4.5	Infection of AML-M5 cells with GFP encoded virus particles produced from 70-80% confluency of Phoenix cells	82
4.6	Optimal Phoenix cells transfection protocol	84
4.7	Optimal parental AML-M5 cells infection protocol	85
4.8	Formation of iPSC-like colonies from D0 to D25	87
4.9	Appearance of iPSC-like colonies on feeder cells from Passage 4 to Passage 29	88
4.10	Detection of pluripotency markers using PCR on various cells	91
4.11	Detection of NANOG using immunofluorescence staining	94
4.12	Detection of SSEA4 using immunofluorescence staining	95

4.13	Detection of TRA-1-81 using immunofluorescence staining	96
4.14	Detection of OCT3/4 using immunofluorescence staining	97
4.15	Detection of SOX2 using immunofluorescence staining	98
4.16	Flow cytometry analysis of expression of pluripotency markers on AML-M5-derived iPSC	101
4.17	Mean expression of pluripotency markers on AML-M5-derived iPSCs and parental AML-M5 cells	102
4.18	Induction of adipogenesis differentiation	105
4.19	Induction of osteogenesis differentiation	106
4.20	Activin A-induced endoderm differentiation	108
4.21	Detection of definitive endoderm marker SOX17 using immunofluorescence staining	109
4.22	Noggin-induced endoderm differentiation	111
4.23	Detection of ectoderm marker MAP2 using immunofluorescence staining	112
4.24	FACS analysis of monocytic-specific markers on AML-M5-derived iPSCs and parental AML-M5 cells	114
4.25	Mean expression of monocytic-specific markers on AML-M5-derived iPSCs and parental AML-M5 cells	115
4.26	Detection of leukaemia-specific mutation <i>MLL-AF9</i> using PCR	117

LIST OF ABBREVIATIONS

ALP	Alkaline phosphatase
AML	Acute myeloid leukaemia
AML-M5	Acute myeloid leukaemia M5 subtype
APC	Allophycocyanin
APC-Cy ^{TM7}	Allophycocyanin- Cy ^{TM7}
ASH2L	ASH2-like
bFGF	Basic fibroblast growth factors
bp	Base pair
BSA	Bovine serum albumin
cDNA	Complementary DNA
CO ₂	Carbon Dioxide
DAPI	4',6-diamidino-2-phenylindole
ddH ₂ O	Double distilled water
DIC	Disseminated intravascular coagulopathy
DMEM/F12	Dulbecco's Modified Eagle Medium/Ham F-12
DMSO	Dimethyl sulfoxide
DNA	Deoxyribonucleic acid
dNTP	Deoxynucleotide
DPPA genes	Developmental pluripotency-associated genes
EBNA1	Epstein-Barr nuclear antigen-1
EBs	Embryoid bodies
EG	Embryonic germ cells
ESCs	Embryonic stem cells
FAB classification	French-American-British classification
FITC	Fluoresceine isothiocyanate
GFP	Green fluorescence protein
GSK3	Glycogen synthase kinase-3
H3K4 methylase	Histone 3 lysine 4 methylase
H4K16	Histone 4 Lysine 16
HDAC inhibitor	Histone deacetylase inhibitor
hESCs	Human embryonic stem cells
HLA-matched donor	Human leukocyte antigen-matched donor
hAd-MSC	human adipose-derived mesenchymal stem cell
iPSCs	Induced pluripotent stem cells
ISCBI	International Stem Cell Banking Initiative
KOSR	Knockout serum replacement
LB agar	Luria Bertoli agar
LSD1 inhibitor	Lysine-specific demethylase 1 inhibitor
LEDGF	Lens epithelium-derived growth factor
MEFs	Mouse embryonic fibroblasts
MEK inhibitor	Mitogen-activated protein kinase inhibitor
MET	Mesenchymal-epithelial transition
miRNA	Micro RNA
MLL	Mixed-lineage leukaemia
MOF	Histone acetyltransferase MYSTI
MTA	Material transfer agreements
O ₂	Oxygen

OSKM	OCT3/4, SOX2, KLF4, and c-MYC
PCR	Polymerase chain reaction
PDAC	Pancreatic ductal adenocarcinoma
PBS	Phosphate buffered saline
PDK1 activator	Phosphoinositide-dependent kinase 1 activator
PE	Phycoerythrin
PE-Cy TM 7	Phycoerythrin- Cy TM 7
PerCP-Cy TM 5.5	Peridinin chlorophyll protein- Cy TM 5.5
PFA	Paraformaldehyde
RBBP5	Retinoblastoma-binding protein
RNA	Ribonucleic acid
ROCK inhibitor	Rho-associated-coiled-containing protein kinase inhibitor
rpm	Resolution per minute
SEC	Super elongation complex
SCID mice	Severe combined immunodeficient mice
SMA	Spinal muscular atrophy
SVLT	SV40 large T antigen
TAE buffer	Tris-Acetate-EDTA buffer
TGF- β	Transforming growth factor-beta
Trypsin-EDTA	Trypsin- EDTA
VPA	Valproic acid
WDR5	WD-repeat containing protein 5

CHAPTER 1

INTRODUCTION

Referring to the French-American-British (FAB) Classification, acute myeloid leukaemia (AML) can be subcategorised into nine distinct subtypes and acute monocytic leukaemia is the M5 subtype (AML-M5) (Bloomfield and Brunning, 1985; Tallman et al., 2004). AML-M5 is characterised by the presence of immature monocytes population ($> 20\%$) in bone marrow and peripheral blood (Verchuur, 2004). Approximately 40%-50% of AML-M5 affects children younger than two years old and it is more common in individual with Asian and Hispanics origin (Verschuur, 2004). AML- M5 has poor prognosis with three-years disease-free survival rate at approximately 25%, and overall survival rate ranging from 35%-60% (Tallman, 2004; Yan et al., 2011). Pathogenesis of AML-M5 is highly associated with the presence of MLL-AF9 fusion protein resulted from chromosomal translocation $t(9;11)(p22;q23)$ (Chandra et al., 2010; Fleischmann et al., 2014). Formation of MLL-AF9 fusion protein is sufficient to develop AML-M5 in mouse model (Somerville and Clearly, 2006). Nevertheless, little is known about the association of pathogenesis of AML-M5 with MLL-AF9 fusion protein (Fleischmann et al., 2014). Additionally, there is no specific treatment targeting on MLL-AF9, perhaps due to minimum understanding of the molecular mechanism involved in AML-M5 (Verchuur, 2004). Therefore, identifying

genes and their molecular pathogenesis related to MLL-AF9 could assist in discovery of novel targeted therapies for AML-M5 (Fleishchmann et al., 2014).

Induced pluripotent stem cells (iPSCs) are generated by ectopically introducing a group of pluripotency-associated transcription factors namely *OCT3/4*, *SOX2*, *KLF4* and *c-MYC* into adult somatic cells (Takahashi and Yamanaka, 2006). Many cell types have been used to generate iPSCs including normal and abnormal cells (Aasen et al., 2008; Haase et al., 2009; Yamasaki et al., 2014). iPSCs are similar to bona fide human embryonic stem cells (hESCs) in terms of morphology, pluripotent genes expression profile and ability to differentiate into three germ layers (Takahashi and Yamanaka, 2006). iPSCs have advantages over the use of hESCs in clinical applications such as disease modelling, drug discovery and regenerative medicine (Yamanaka, 2012). Since iPSCs are generated from somatic cells and therefore bypass the controversy of blastocyst destruction (Thomson et al., 1998). Generation of patient-specific iPSCs shed light on regenerative medicine by providing patient-matched organ or tissues for transplantation purpose (Yamanaka, 2012). Besides, availability of disease/patient-specific iPSC lines provides unprecedented opportunities to elucidate disease mechanism *in vitro*, and the disease model can be used to develop potential therapeutic approaches such as new targeted drug and gene therapy (Yamanaka, 2012).

In Malaysia, although the incidence of AML-M5 is less common, it has poor outcome due to involvement of MLL-AF9 fusion protein and has overall survival rate of 35%-60% (National Cancer Registry, 2007). The innovation of

iPSC may allow the generation of AML-M5-specific iPSC that recapitulate cancer phenotypes which can provide a disease model for discovery of potential therapeutic approaches. In this study, we hypothesised that cancer-specific iPSCs could be derived from acute monocytic leukaemia cells (AML-M5). This AML-M5-derived-iPSCs acquires pluripotent characteristics with loss of their monocytic markers and yet retains disease-specific mutation. Successful pluripotency-based reprogramming using AML-M5 cell line may reveals the underlying mechanisms of tumorigenic transformation, and provides a new platform for modelling cancer behaviour.

General objective of this study:

1. To generate AML-M5-derived iPSCs line using retroviral method.

Specific objectives of this study:

1. To characterise AML-M5-derived iPSCs using reverse transcription-PCR (RT-PCR), immunofluorescence staining and immunophenotyping.
2. To investigate the *in vitro* differentiation potential of AML-M5-derived iPSCs into three germ layers (mesoderm, endoderm and ectoderm).
3. To detect expression of monocytic markers and disease-specific mutation on AML-M5-derived iPSCs.

CHAPTER 2

LITERATURE REVIEW

2.1 Acute Monocytic Leukaemia (AML-M5)

According to the involvement of particular myeloid lineage and the degree of leukaemic cell was showed in Figure 2.1, acute myeloid leukaemia (AML) can be subcategorised into nine distinct subtypes and acute monocytic leukaemia is the M5 subtype (AML-M5) (according to the French-American-British (FAB) Classification) (Bloomfield and Brunning, 1985; Tallman et al., 2004). AML-M5 consists of more than 80% of immature monocytic lineage cells and less than 20% of neutrophil in the total bone marrow myoblast population (Löwenberg et al., 1999; Tallman et al., 2004; Verschuur, 2004). AML-M5, which is subcategorised into M5a and M5b, accounts for 1% to 20% of total AML yearly cases (Verchuur, 2004). M5a consists of more than 80% of monoblast, and M5b consists more than 80% of promonocytes and more differentiated monocytes (Figure 2.2) (Verschuur, 2004; Yan et al., 2011).

Classification of AML according French-American-British (FAB) classification

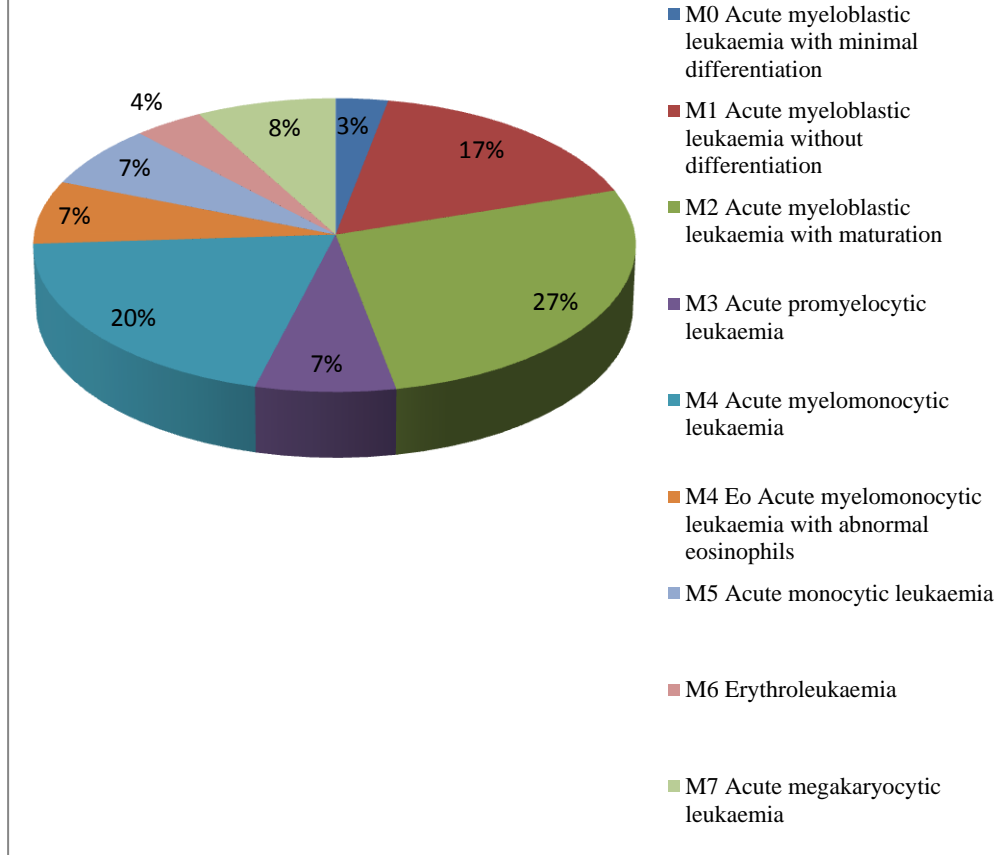


Figure 2.1: Classification of AML according French-American-British (FAB) classification. Pie chart shows AML-M5 accounts for 7% of total AML cases. (Adapted from Tallman et al., 2004.)

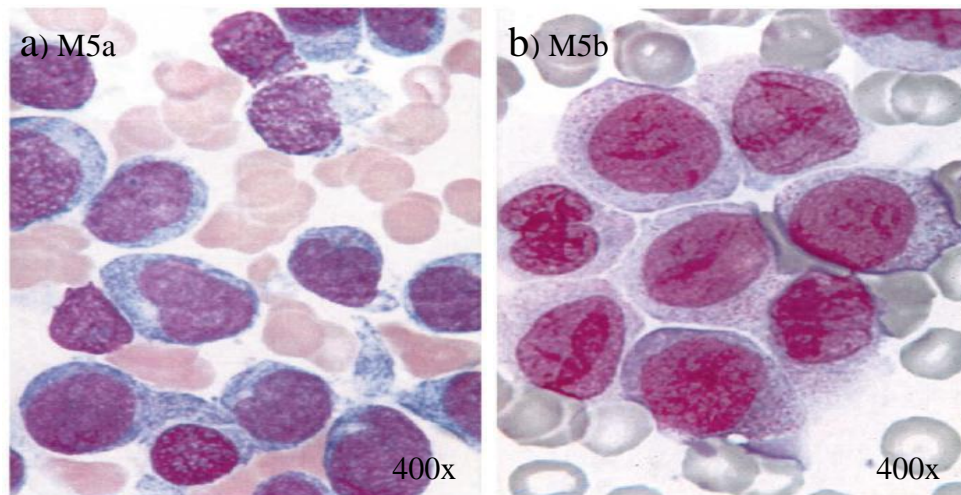


Figure 2.2: Standard hematoxylin and eosin staining blood film of patient with AML-M5. (a) M5a consists of >80% of monoblasts which characterised by having roughly circular nucleus, fine chromatin, and basophilic cytoplasm. (b) M5b consists of >80% of promonocytes which have a more complex nucleus, and may contain metachromatic granules in their cytoplasm. (Adapted from Tallman et al., 2004).

2.1.1 Epidemiology of AML-M5

AML-M5 accounts for 7% of all AML cases world wide (Tallman et al., 2004). In Malaysia, AML-M5 is categorised under acute myeloid leukaemia and is the seventh most common cancer with an incidence of 2.9 per million in populations (National Cancer Registry, 2007). 40% to 50% of AML-M5 is reported in young children at age less than two years old; and it is more common in Asian and Hispanics (Tallman et al., 2004). Development of AML-M5 may result from several risk factors such as chemical exposures, radiation exposures and genetics (Verschuur, 2004; Cheng and Sakamoto, 2005; Balgobind et al., 2011; Yan et al., 2011; Chauhan et al., 2013). Exposure to anticancer chemotherapy (for example alkylating agents), aromatic organic solvent (particularly benzene) and high amount of ionising radiation increases the risk of developing AML-M5 (Verschuur, 2004; Cheng and Sakamoto, 2005; Godley and Larson, 2008). Of note, AML-M5 is highly associated with cytogenetic or genetic abnormalities including mutation in mixed-lineage

leukaemia gene (*MLL*), *FLT3* gene, *NPM1* gene and *DNMT3B* gene (Balgobind et al., 2011; Yan et al., 2011; Nin et al., 2012; Chauhan et al., 2013). Generally, AML-M5 has poor outcome with an overall survival of 35% to 60% (Verschuur, 2004).

2.1.2 Clinical Presentation of AML-M5

Similar to AML, normal marrow cells of patient with AML-M5 are gradually replaced by immature white cells, leading to anaemia, neutropenia and thrombocytopenia (Rubnitz et al., 2010). Generally, patient with AML-M5 presents with broad range of sign and symptoms, ranging from mild to life threatening including fatigue (consequence of anaemia), persistent fever, pallor, headache, dizziness, dyspnea and congestive heart failure (Verschuur, 2004). In AML-M5, clinical presentations are usually associated with infiltration of leukaemic cells in bone marrow, central nervous system, mouth, rectum and anal canal but rarely in skin, gastrointestinal tract and renal system (Verschuur, 2004; Rubnitz et al., 2010).

Sharp decline to functional white cells often compromises immune systems that lead to severe opportunistic fungal and bacterial infections in patient with AML-M5 (Verschuur, 2004). Since the normal bone marrow function is overtaken by the production of immature white cells, dyspnea and hypoxia may be present due to reduction of erythrocytes in vital organs including brain, lungs, liver and skin (Verschuur, 2004; Rubnitz et al., 2010). Bleeding often occurs as a result of thrombocytopenia (Löwenber et al., 1999;

Verschuur, 2004). The severity of bleeding ranges from mild bleeding (easy brushing) to excessive bleeding (epistaxis, gum bleeding, retinal hemorrhage, rectal bleeding, menorrhagia and intracranial hemorrhage) (Verschuur, 2004). Bleeding conditions may also be linked to disseminated intravascular coagulopathy (DIC) that can lead to deadly consequences (Verschuur, 2004; Rubnitz et al., 2010).

Involvement of extramedullary sites especially meninges and the central nervous system are strongly correlated with AML-M5 (Lichtman, 1995; Bisschop, 2001; Abbott, 2003; Verschuur, 2004; Rubnitz et al., 2010). Presentation of neurological symptoms including headache, nausea, vomiting, photophobia, cranial nerve palsies, papilledema and nuchal rigidity (neck stiffness) (Verschuur, 2004). Neurological symptoms may arise from leukostasis or meningeal infiltration of monoblasts (Pui et al., 1985; Verschuur, 2004). Occasionally, chloroma, a soft tissue mass composing of immature myeloid cells (monoblasts and/or premonocytes), is found at central nervous system and causes spinal cord compression leading to paraparesis (Verschuur, 2004).

2.1.3 Diagnosis of AML-M5

Blood analysis, bone marrow aspiration and biopsy are definitive tests used to diagnose AML-M5 (Fanning et al., 2009). Presence of 20% or more monoblasts in blood and bone marrow sample is required for disease confirmation (Verschuur, 2004). Cytogenetic testing is also used to identify

specific genes or chromosomal changes involved in AML-M5 (Verschuur, 2004).

Routine blood analysis includes complete blood count with differential, coagulation studies and comprehensive metabolic profiles are used to diagnose AML-M5 (Verschuur, 2004). Complete blood count with differential may show the presence of myoblasts, premyelocytes and myelocytes, and often with decreased neutrophil count (Verschuur, 2004). Microscopy analysis of bone marrow aspirate is also used to identify cell types that are committed to the myeloid lineage (Verschuur, 2004). Bone marrow aspirate of an AML-M5 case is characterised by abundant monoblasts with the size of 15-25 μm , and with high nuclear/cytoplasmic ratio (Verschuur, 2004). Additionally, larger and irregular shapes of more differentiated promonocytes and monocytes may be seen and fine chromatin with 1-3 prominent nucleoli are commonly observed in the nucleic, which indicates the presence of immature monocytic cells (Verschuur, 2004). Immunophenotyping using flow cytometry is commonly used to determine involvement of monocytic cells in bone marrow aspirate (Jaso et al., 2014). AML-M5 cell line expressed CD4, CD11b, CD11c, CD13, CD33, CD45, CD56, CD64 and HLA-DR (Jaso et al., 2014).

Cytogenetic and genetic make up in AML-M5 affect prognosis and treatment option (Kumar, 2011). Cytogenetic analysis and polymerase chain reaction (PCR) have been used to detect chromosomal abnormalities specific to AML-M5 for example chromosomal translocations including t(9;11) (p21;q23), t(8;16) (p11;p13), t(8;22) (p11;q13), t(10;11) (p13;q23), and

mutation in *FLT3* gene, *NPM1* and *DNMT3B* gene (Dewald et al., 1983; Weh et al., 1986; Heim et al., 1987; Lai et al., 1992; Rubnitz et al., 1996; Balgobind et al., 2011; Yan et al., 2011; Chauhan et al., 2013).

2.1.4 Treatment of AML-M5

Although AML-M5 is a serious disease like AML, it is treatable and curable with chemotherapy and bone marrow transplantation (Roboz, 2011). The primary treatment of AML-M5 is chemotherapy and occasionally followed by bone marrow transplantation when there is availability of HLA-matched donor (Rubnitz et al., 2010; Roboz, 2011).

For more than three decades, administration of aggressive multidrug chemotherapy with cytarabine, anthracyclins and etoposide is commonly used to treat patient with AML-M5 (Verschuur, 2004; Rubnitz et al., 2010). Chemotherapy tends to destroy both leukaemic cells and normal healthy bone marrow cells, in order to allow restoration of new bloods cells after treatment (Estey, 2012). The complete response rate of chemotherapy has been reported ranging from 40% to 85% with an overall five years disease-free survival rate of 25% (Fanning et al., 2009). It is often associated with adverse side effects including temporary bone marrow suppression, increased susceptibility to opportunistic infection and cardiac toxicity (Tallman et al., 2004; Verschuur, 2004; Rubnitz et al., 2010). Administration of chemotherapy is often associated with 5% to 30% of treatment-related mortality rate (Fanning et al., 2009).

For AML-M5 patients who do not tolerate the toxic effects of chemotherapy or if HLA-matched donor is available, bone marrow transplantation serves as an alternative (Rubnitz et al., 2010). Bone marrow transplantation is a medical procedure aims to replace the abnormal or damaged of a patient's bone marrow with healthy bone marrow stem cells from a HLA-matched donor (Barret and Battiwalla, 2010). There are two types of bone marrow transplantation namely allogeneic (from a donor) or autologous (from patient) bone marrow transplantation (Löwenberg et al., 1999; Verschuur, 2004; Rubnitz et al., 2010). Generally, allogeneic bone marrow transplantation tends to give better treatment response than autologous transplantation due to its lower risk of disease relapse resulted from contamination of patient's leukaemic cells (Thomas, 1979; Bruno et al., 2007). In cases where the transplantation are successful, the patient with AML-M5 are completely free from the disease and go back to normal life in a short period of time (Fanning et al., 2009). Treatment with bone marrow transplantation tends to have higher risk to develop graft-versus-host disease (Barret and Battiwalla, 2010). Additionally, relapse of disease is possible after bone marrow transplantation and is often fatal (Fanning et al., 2009).

Treatment outcome of AML-M5 is greatly influenced by several prognostic factors such as age, response to induction therapy, leukaemic cytogenetic and molecular abnormalities (Verschuur, 2004; Schlenk, 2014). For instant, younger patient (less than 60 years of age) tends to have better treatment outcome than older patient (Schlenk, 2014). Involvement of certain cytogenetic abnormalities tends to have unfavourable treatment response in

AML-M5 patient (Schlenk, 2014). In particular, a patient carrying any of the AML-M5-associated cytogenetic aberrations including $inv(3)(q21q26)/t(3;3)(q21;q26)$, $add(5q)/del(5q)$, -5 ; $add(7q)/del(7q)$, -7 ; $t(6;11)(q27;q23)$, $t(10;11)(p11\sim13;q23)$, and $t(11q23)$ with the exception of $t(9;11)(p22;q23)$ and $t(11;19)(q23;p13)$; $t(9;22)(q34;q11)$; -17 and $abn(17p)$ usually has unfavourable outcome (Mrózek and Bloomfield, 2012). In contrast, a patient with cytogenetic aberration such as $t(15;17)(q22;q21)$, $t(8;21)(q22;q22)$, $inv(16)(p13q22)$ or $t(16;16)(p13;q22)$ has better response rate towards treatment (Mrózek and Bloomfield, 2012).

2.1.5 Pathogenesis of AML-M5

Exposure to chemicals (for example anticancer chemotherapy and aromatic organic solvents) and ionising radiation may lead to development of AML-M5 (Verschuur, 2004; Cheng and Sakamoto, 2005; Balgobind et al., 2011; Yan et al., 2011; Chauhan et al., 2013). Involvement of genetic aberrations such as mutation in *FLT3* gene, *NPM1* gene and *DNMT3B* gene have been reported in AML-M5 (Yan et al., 2011; Chauhan et al., 2013). AML-M5 is highly associated with cytogenetic abnormalities involving the mixed-lineage leukaemia gene (*MLL*) located at 11q23, and represents 51% of AML-M5 cases (Balgobind et al., 2011). *MLL* gene has been found to be chromosomally translocated with more than 50 partner genes and give rise to different types of diseases (Thirman et al., 1993; Kohmann et al., 2005; Slany, 2009). For example, fusion of *MLL* with *AFF1* or *ENL* genes leading to acute lymphoblastic leukaemia, whereas, formation of *MLL-AF10* is observed in

patient with AML-M4 (Fu et al., 2007; Stam, 2012; Chen et al., 2013). Among many fusion transcripts involving *MLL*, fusion of *MLL-AF9* is the most frequently found chromosomal translocation in infant with AML-M5 (Fleischmann et al., 2014). *MLL-AF9* results from the chromosomal translocation t(9;11)(p22;q23), which is fusion of wildtype *MLL* gene and *AF9* gene (Corral et al., 1993; Corral et al., 1996). *MLL-AF9* fusion protein has been highly correlated with pathogenesis of AML-M5 (Ayton and Clearly, 2001; Chandra et al., 2010). The fusion gene itself is sufficient to initiate AML-M5 (Ayton and Clearly, 2001; Chandra et al., 2010). For example, *MLL-AF9* knocked-in mice showed abnormal expansion of myeloid precursor cells leading to the development of AML-M5 (Dobson et al., 1999; Johnson et al., 2003; Liu et al., 2009). However, the underlying mechanism of AML-M5 involving *MLL-AF9* is poorly understood (Moriya et al., 2012).

2.1.4.1 *MLL* Gene

MLL is a histone 3 lysine 4 (H3K4) methylase, which belongs to the trithorax/*MLL* gene family (Yokoyama et al., 2002). *MLL* forms a complex consisting of subunits *MLL-N* (320 kDa) and *MLL-C* (180 kDa) (Hsieh et al., 2003). *MLL* complex is a transcription activator by regulating the nuclear localisation activity, target gene selection and chromatin modification (Slany, 2009). As shown in Figure 2.3, *MLL-N/MLL-C* dimer is the core component of *MLL* complex, in which *MLL-N* interacts with Menin and LEDGF to regulate the nuclear localisation activity and target genes selection; while *MLL-C* and their associated protein involve in chromatin modification (Slany,

2009). The MLL complex that is responsible for gene loci methylation is recruited by transcription factors to initiate RNA synthesis (Slany, 2009).

MLL is widely expressed in mouse embryo (Yu et al., 1995). Homozygous knockout of *MLL* is found to be embryonically lethal in mouse, indicating its importance in embryogenesis (Yu et al., 1995). Expression of *MLL* is required to positively regulating the expression of *HOX* genes which are crucial for body structure formation during early embryogenesis (Yu et al., 1998; Gan et al., 2010). *HOX* also plays a definitive role in regulating proliferation and differentiation of haematopoietic stem cells and progenitor cells (He et al., 2011). Heterozygous knockout of *MLL* in mouse led to aberrant *HOX* gene expression associated with growth retardation, hematopoietic abnormalities and skeletal malformation (Yu et al., 1995). Heterozygous mouse showed phenotypically normal fetal haematopoiesis but died within 3 weeks of age (Gan et al., 2010). Surviving animals revealed significant haematological changes, including anaemia, thrombocytopenia and reduction of bone marrow haematopoietic stem/ progenitor cells (Gan et al., 2010). Therefore, *MLL* is believed to play pivotal role in embryogenesis and haematopoiesis (Bertani et al., 2011).

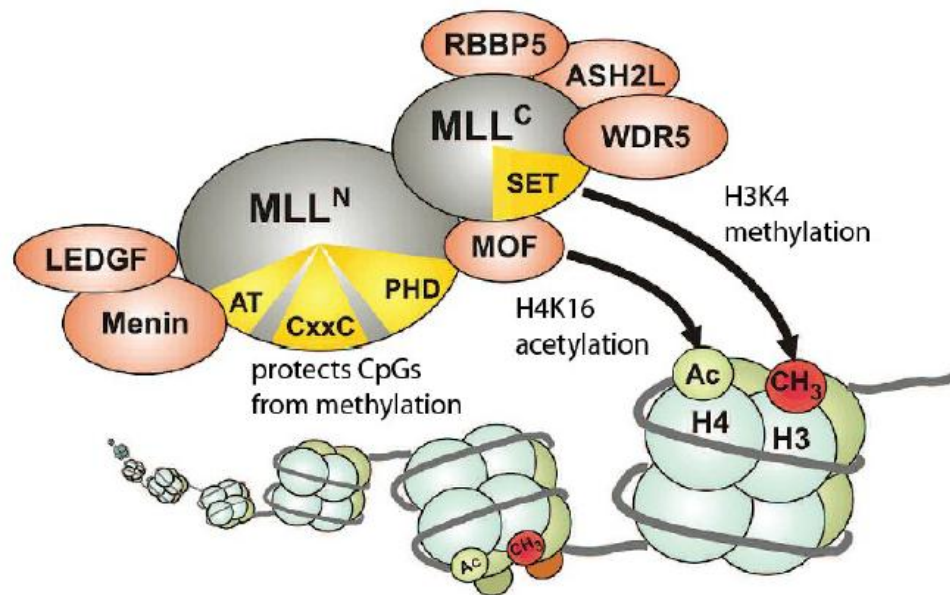


Figure 2.3: The MLL complex and its molecular functions. MLL-N interacts with Menin and lens epithelium-derived growth factor (LEDGF) in regulation of subnuclear localisation and selection of target gene, while MLL-C and its associated proteins including histone acetyltransferase MYSTI (MOF), retinoblastoma-binding protein (RBBP5), ASH2-like (ASH2L) and WD-repeat containing protein 5 (WDR5) are responsible for chromatin modification (histone 4 lysine 16 (H4K16) acetylation and H3K4 trimethylation). Figure adopted from Slany, 2009.

2.1.4.2 *AF9* Gene

AF9 also known as *MLLT3*, is located at 9p22 (Lida et al., 1993; Malik and Hemenway, 2013). Functionally, *AF9* is a transcription factor containing a serine and proline rich domain which is crucial for transcriptional activation and resuming RNA Polymerase II elongation function (Collina et al., 2002). *AF9* is believed to be regulator of *HOX* genes on axial skeletal during embryogenesis (Collina et al., 2002). Mouse with heterozygous knockout of *AF9* gene were found to have normal skeletal formation, whereas, those with homozygous deletion of *AF9* exhibited homeotic skeletal anomalies and risk of perinatal death (Collina et al., 2002). *AF9* gene is found to be highly expressed in haematopoietic stem cells, and is important for erythropoiesis and megakaryopoiesis (Pina et al., 2008).

2.2 Pluripotent Stem Cells

Pluripotent stem cells are specialised cells that are able to grow immortally while retaining pluripotency and ability to differentiate into all cell types from three germ layers including mesoderm, endoderm and ectoderm (Thomson et al., 1998). Embryonic stem cells (ESCs) are one of the examples of pluripotent stem cells, which isolated from the inner cell mass of early-stage embryo (Thomson et al., 1998). The characteristics of unlimited growth and pluripotency of ESCs could have great potential in development of regenerative medicine (Levenberg, 2002). Currently, donated organs and tissues from HLA-matched donor are required to replace destroyed organ/tissue, however, the demands far outweighed supply (Levenberg, 2002). In this context, ESCs could be made and used to differentiate into any desired cell types or tissues for cell replacement therapy for various applications (Levenberg, 2002). Despite the enormous applications of ESCs, the use of ESCs has been limited because of ethical concern that involved destruction of the blastocyst, which could create life (Baldwing, 2009). Furthermore, ESCs can only be derived from embryo and it is difficult to create patient/disease-specific ESC line (Verlinsky et al., 2005).

2.3 Induced Pluripotent Stem Cells

Induced pluripotent stem cells (also known as iPSCs) are a type of pluripotent stem cell generated from adult cells (Takahashi and Yamanaka, 2006). iPSCs experiment was first carried out by Professor Yamanaka and his

group in Kyoto, Japan (Takahashi and Yamanaka, 2006). The experiment showed that exogenous insertion of four key transcription factors namely *OCT3/4*, *SOX2*, *KLF4* and *c-MYC* was able to activate the endogenous pluripotency factors, and reprogramme the adult cells into pluripotent state (Takahashi and Yamanaka, 2006).

Cells from different species have been used to generate iPSCs including mouse, human, rhesus monkey, pig, and even from highly endangered species primate and white rhinoceros (Takahashi and Yamanaka, 2006; Takahashi et al., 2007; Yu et al., 2007; Liu et al., 2008; Ben-Nun et al., 2011; Fang et al., 2014; Yang et al., 2014). Many cell types have shown capability to reprogramme into iPSCs such as fibroblasts, peripheral blood, cord blood endothelial cells, urine cells, dental pulp cells, kidney mesangial cells, hepatocytes and keratinocytes (Aasen et al., 2008; Lowry et al., 2008; Haase et al., 2009; Loh et al., 2009; Liu et al., 2010; Song et al., 2011; Zhou et al., 2011; Yamasaki et al., 2014). The most common cell type tested so far is fibroblasts (Yamanaka, 2012). Apart from using healthy somatic cells, iPSCs can also be generated from abnormal cell types including those with inherited genetic diseases (such as sickle cell anaemia, amyotrophic lateral sclerosis, thalassaemia and Fanconi anaemia) and cancers (such as chronic myeloid leukaemia, lymphoma, pancreatic cancer, gastrointestinal cancer, melanoma and osteosarcoma) (Dimos et al., 2008; Hanna et al., 2008; Nishikawa et al., 2008; Park, I.H et al., 2008; Raya et al., 2009; Ye et al, 2009; Utikal et al., 2009; Carette et al., 2010; Miyoshi et al., 2010; Seki et al., 2010; Choi et al., 2011; Kumano et al., 2012; Zhang, X et al., 2012; Kim et al., 2013).

Unlike ESCs, iPSCs are generated from adult cells and therefore bypassing the controversy of blastocyst destruction (Medvedev et al., 2010; Yamanaka, 2012). With the discovery of iPSC, generation of patient/disease-specific pluripotent stem cell line is possible for personalised medicine (Medvedev et al., 2010; Yamanaka, 2012).

2.3.1 Reprogramming Factors

A few reprogramming factors have been found to be crucial in generation of iPSC, including *OCT3/4*, *SOX2*, *KLF4*, *c-MYC*, *NANOG* and *LIN28* (Takahashi and Yamanaka, 2006; Yu et al., 2007). The most well-established reprogramming factors used are combination of *OCT3/4*, *SOX2*, *KLF4* and *c-MYC*, also known as Yamanaka's factors (Kulcenty et al., 2015). Inclusion of *OCT3/4* and *SOX2* are expected in iPSCs generation because both factors have been shown to be a regulator in maintaining pluripotency (Boyer et al., 2005; Loh et al., 2006; Rizzino, 2009). Yu and co-workers described a successful generation of iPSCs using combination of *OCT3/4*, *SOX2*, *NANOG* and *LIN28*, indicating the possible omission of oncogenes such as *KLF4* and *c-MYC* in iPSCs generation (Yu et al., 2007).

2.3.1.1 *OCT3/4*

OCT3/4 (octamer-binding transcription factor 4) also called *POU5F1* (POU domain, class 5, transcription factor 1), is a homeodomain transcription factor of *POU* family (Ma and Young, 2014). The *POU* family are DNA-

binding proteins consisting of an octamer motif (ATGCAAAT) within their promoter region (Ma and Young, 2014). *OCT3/4* is believed to be the factor that first appears during embryo development (Pan et al., 2002). Gene knockdown of *OCT3/4* in mouse failed to form inner cell mass, loss of pluripotency and differentiation of primitive cells into trophectoderm lineage (Wu and Schöder, 2014). Expression level of *OCT3/4* is tightly controlled in ESCs as any alteration of its expression levels will result in different cell fates (Wei et al., 2007). For example, an increased expression of *OCT3/4* showed to favour differentiation into endoderm and mesoderm lineages, whereas, decreased expression of *OCT3/4* caused dedifferentiation into trophectoderm lineage (Wu and Schöder, 2014).

Functionally, *OCT3/4* works closely with *SOX2* and *NANOG* in maintenance of pluripotency (Zhang and Cui, 2014). These three transcription factors bind to the same enhancer elements of genes that are involved in pluripotency and self-renewal (Boyer et al., 2005; Zhang and Cui, 2014). *OCT3/4*, *SOX2* and *NANOG* were also found to occupy their own promoter site respectively to form an interconnected feedback loop that either positively or negatively regulates their expression levels in embryonic stem cells (Boyer et al., 2005).

2.3.1.2 *SOX2*

SOX2 also known as *SRY* (Sex determining region Y)-box 2, is a member of the *SOX* family transcription factors (Zhang and Cui, 2014). All

proteins derived from *SOX* family contain highly conserved HMG box-DNA binding domains (Kamachi and Kondoh, 2013). Unlike *OCT3/4*, *SOX2* is detectable only after embryo implantation (Avilion et al., 2003). *SOX2* is required for the formation of inner cell mass and epiblast (Avilion et al., 2003). Conditional knockout of *SOX2* in mouse led to high mortality of embryo due to failure to form pluripotent epiblast (Avilion et al., 2003). Repression of *SOX2* in ESCs resulted in changes of cell morphology and loss of pluripotency (Zhang and Cui, 2014). Nevertheless, overexpression of *OCT3/4* in *SOX2* *-/-* mouse embryonic stem cells can restore pluripotency of these cells (Masui et al., 2007; Fong et al., 2008).

As mentioned in Session 2.3.1.1, *SOX2* works synergically with other transcription factors in maintaining pluripotency and self-renewal while suppressing differentiation (Zhang and Cui, 2014). Given that *SOX2* plays essential role in maintaining pluripotency and self-renewal, *SOX2* is believed to be one of the key factors for iPSCs generation (Zhang and Cui, 2014).

2.3.1.3 *KLF4*

KLF4 or Kruppel-like factor 4 belongs to Kruppel-like family which has three zinc finger domains function as DNA binding site (Evans and Liu, 2008). Kruppel-like family consists of 17 members that involved in various cellular processes such as cell proliferation, differentiation, self-renewal and apoptosis (Evans and Liu, 2008). *KLF4* is widely expressed in undifferentiated ESCs, and withdrawal of this factor led to loss of pluripotency, suggesting their

role in regulating stem cells self-renewal and pluripotency (Bruce et al., 2007). In addition, *KLF4* has bi-functional role to act as an oncogene or tumour suppressor, depending on the tumour type (Rowland et al., 2005; Tetreault et al., 2013).

KLF4 requires the presence of additional transcription factors including OCT3/4, SOX2 and c-MYC to maintain stemness properties and induction of iPSCs (Li et al., 2011). However, oncogenic properties of *KLF4* might not be favourable in generation of iPSCs (Ichida et al., 2014). *KLF4* was found to be replaceable by other KLF family members in regulating self-renewal process (Jiang et al., 2008). Knockdown of single *KLF* (*KLF2*, 4 and 5) at a time caused no changes in cell morphology and pluripotency of embryonic stem cells (Jiang et al., 2008). This may due to the fact that these KLF proteins exhibit same biological functions by acting on the same target site that could regulate the pluripotency of stem cells (Jiang et al., 2008). Studies have showed that *KLF2* had equivalent reprogramming efficiency as *KLF4*, while *KLF1* and *KLF5* had lower efficiency compared to *KLF4* (Jiang et al., 2008; Schmidt and Plath, 2012).

2.3.1.4 *c-MYC*

c-MYC belongs to the *MYC* family (members including *b-MYC*, *l-MYC*, *n-MYC* and *s-MYC*) (Dang, 1999). *c-MYC* is a transcription factor containing bHLH/LZ (basic Helix-Loop-Helix Leucine Zipper) domain that function as DNA binding site (Chapman-Smith and Whitelaw, 2006). *c-MYC* is an

important regulator involved in cell proliferation, cell transformation, apoptosis, differentiation and stem cell self-renewal (Dang, 2012a; Dang, 2012b). *c-MYC* is also a well-known proto-oncogene and is found to be overexpressed in many types of cancer (Gordan et al., 2007).

c-MYC is capable of promoting iPSC generation, but also increasing chances of tumour formation (Nakagawa et al., 2010). Nakagawa and co-workers reported that *c-MYC* is replaceable by non-oncogenes *n-MYC* and *l-MYC* with almost similar reprogramming efficiency, suggesting that the omission of *c-MYC* would still allow successful iPSC generation (Nakagawa et al., 2008).

2.3.2 Potential Applications of iPSCs

Development of iPSCs shed light on regenerative medicine by providing multipurpose research and clinical tools in the study of disease pathogenesis, drug screening, and custom-tailored cell-replacement therapy (Yamanaka, 2012). Currently many studies use stem cells to conduct drugs testing or as study material to elucidate disease mechanisms, and as a source of tissue or organ transplantation (Wan et al., 2014).

2.3.2.1 Cell Therapy

Cell therapy is therapy in which cellular material such as cells, tissues or organs are injected into a patient. The most established example is

allogeneic transplantation which requires HLA-matched donors (Stadtfeld and Hochedlinger, 2010). Unfortunately, availability of HLA-matched donors is limited (Stadtfeld and Hochedlinger, 2010). For those who had transplanted with HLA-matched organ from different person require long-term treatment with immunosuppressive drugs that commonly have adverse side effects including hypertension, kidney injury and immunodeficiency (Stadtfeld and Hochedlinger, 2010). Use of iPSCs could potentially overcome these problems as they are derived from patient, and the risk of immune rejection would be minimised and perhaps could avoid the use of immunosuppressive drugs (Svendsen, 2013).

In addition, iPSCs hold promising advantage compared to current transplantation approaches, in which correction of disease-causing mutations by homologous recombination is available (Chun et al., 2010). Indeed, experiments using mice model suggested that treating genetic disease with iPSCs is practicable (Hanna et al., 2007; Xu et al., 2009). For example, Hanna and co-workers demonstrated a successful cure of sickle cell anaemia in humanised mouse model (Hanna et al., 2007). In this proof-of-concept study, mouse fibroblast cells were first reprogrammed into iPSCs (Hanna et al., 2007). Subsequently, the defective sickle globin gene was corrected in iPSCs by gene target followed by transplantation of iPSC-derived hematopoietic progenitor cells into anaemic mice (Hanna et al., 2007). The study showed that healthy progenitor cells were able to produce normal erythrocytes and cured the disease (Hanna et al., 2007). Study by Xu and co-workers demonstrated the used of corrected iPSC-derived endothelial progenitor cells to reverse

hemophilia A phenotype in mouse model (Xu et al., 2009). In this study, iPSC was derived from mouse carrying hemophilia A and differentiated into endothelial cells and endothelial progenitor cells (Xu et al., 2009). Phenotypic correction of hemophilia A was carried out by transplantation of corrected iPSC-derived endothelial progenitor cells into mouse (Xu et al., 2009). Consequently the mouse was cured from hemophilia A (Xu et al., 2009). Taken together, any disease in human with known mutation could be possibly treated by this technique (Stadtfeld and Hochedlinger, 2010).

2.3.2.2 Disease Modelling and Drug Development

Disease modelling is an idea to recapitulate diseases *in vitro* by deriving patient/disease-specific iPSCs, and different disease cell types can be recreated in culture (Stadtfeld and Hochedlinger, 2010). In past decades, many studies and therapies of diseases such as Parkinson's disease, type I diabetes, Alzheimer's disease and cancers are restricted by accessibility of the affected cells/tissues and some diseases are only detected at late stages (Tiscornia et al., 2011). Furthermore, isolated cells have limited life span that can grow in the lab (Tiscornia et al., 2011). Theoretically, iPSCs derived from patient or diseases are at primitive stage and undergo *in vitro* proliferation without senescence (Takahashi and Yamanaka, 2006). Differentiation of these iPSCs into various cell types could provide insight to study disease progression and mechanisms underlying the pathogenesis (Stadtfeld and Hochedlinger, 2010). The disease model that mimics the disease exactly can be used to decipher disease mechanism and ultimate goal is to identify novel drugs (Stadtfeld and

Hochedlinger, 2010). For example, iPSCs derived from spinal muscular atrophy (SMA) exhibited partial or early disease phenotypes (Lee and Studer, 2011). This SMA-derived iPSC could be used to model early-onset human diseases and eventually identify potential drug that can restore the normal condition (Ebert et al., 2009; Lee and Studer, 2011).

2.3.3 Reprogramming Methods

There are different reprogramming methods used to deliver reprogramming factors into somatic cells such as using integrative viral vector, non-integrative viral vector and non-viral non-integrative vector (Robinton and Daley, 2012). Different approaches are able to influence the reprogramming efficiency and quality of iPSCs (Sugii et al., 2010; Zhao et al., 2010; Lapasset et al., 2011; Papapetrou and Sadelain, 2011). Among these methods, integrative viral vector was chosen in this study as it has wide range of host tropism, stably transgene expression and higher reprogramming efficiency (Osten et al., 2007).

2.3.3.1 Viral Integration Method

Viral integration method is performed by using viruses that carrying key pluripotent transcription factors namely *OCT3/4*, *SOX2*, *KLF4* and *c-MYC* (Takahashi and Yamanaka, 2006). These viruses were used to infect cells and the transcription factors were exogenously introduced into host cell genome (Takahashi and Yamanaka, 2006). Exogenous insertion of pluripotency genes

is found to turn on endogenous pluripotency genes and eventually transform the infected cells into pluripotent state (Takahashi and Yamanaka, 2006). Reprogramming using retroviral vector is the most commonly adopted method to generate iPSC with reprogramming efficiency at 0.01% to 0.02% in human cells (Maherali et al., 2007; Okita et al., 2007). iPSC colonies appeared between 25 and 30 days after retroviral infection (Takahashi et al., 2007). Lentiviral vectors are also being widely used due to its enhanced reprogramming efficiency in infecting inert somatic cells such as non-dividing peripheral blood cells (Hanna et al., 2008; Maherali et al., 2008; Carey et al., 2009; Sommer et al., 2009). Lentiviral reprogramming method was reported to have reprogramming efficiency at 0.02% and iPSC colonies appeared within 20 days (Sommer et al., 2009).

One of the drawbacks of using viral vector is that endogenous pluripotency genes is always failed to be activated and resulted in partially reprogramming cells (Takahashi and Yamanaka, 2006; Mikkelsen et al., 2008; Sridharan et al., 2009). The fully reprogrammed cells showed genomic instability and aberrant gene expression due to integration of viral sequence pieces into host cell genome and partially silenced of transgenes (Hottam and Ellis, 2008; Yu et al., 2009; Si-Tayeb et al., 2010). Random integration may result in increased risk of tumour formation and interfered their developmental potential in chimeric animals (Takahashi and Yamanaka, 2006; Okita et al., 2007). To overcome integration of viral sequences integration during reprogramming, Cre recombinase system was developed to remove transgenes using doxycycline-inducible lentiviral vectors (Soldner et al., 2009). This Cre

recombinase system was able to generate bona fide iPSCs, and removal of transgenes had no effect on pluripotency of reprogrammed cells (Soldner et al., 2009).

2.3.3.2 Nonviral Integration

Several studies reported that iPSCs can be obtained using nonviral single plasmid vectors followed by removal of transgenes via piggyBac transposon system (Kaji et al., 2009; Woltjen et al., 2009; Tsukiyama et al., 2014). The piggyBac transposon, a mobile genetic element, can be efficiently transposed between vectors and chromosomes through ‘cut and paste’ mechanism (Ding et al., 2005; Kaji et al., 2009). The piggyBac-based reprogramming is reported to have 0.02% to 0.05% reprogramming efficiency (Kaji et al., 2009; Woltjen et al., 2009; Tsukiyama et al., 2014). The iPSC colonies were observed at 14 to 25 days after reprogramming transfection and all colonies were completely free from transgenes (Kaji et al., 2009; Woltjen et al., 2009). However, excision efficiency was low and residual sequences of transgenes may result in integration mutagenesis (Stadtfeld and Hochedlinger, 2010; Narsinh et al., 2011b).

2.3.3.3 Nonviral Nonintegration

While some groups have concentrated on the generation of iPSC by perfecting the viral vector technique, others have focused on developing safer nonviral nonintegrating reprogramming methods by means of avoidance of

temporary or permanent genomic modification (Kim et al., 2009; Narsinh et al., 2010; Miyoshi et al., 2011). The nonviral nonintegrating methods including proteins, episomal vector, minicircle DNA vector, mRNA and microRNAs have been used to reprogramme various cell types (Kim et al., 2009; Yu et al., 2009; Jia et al., 2010; Warren et al., 2010; Lin et al., 2011). Despite of its safer values toward therapeutic purposes, these methods often have extremely low reprogramming efficiency than the viral integration techniques due to transient delivery of reprogramming factors (Kim et al., 2009; Narsinh et al., 2011a; Miyoshi et al., 2011).

Kim and co-worker have successfully produced iPSCs from human fibroblasts by direct delivery of reprogramming proteins fused with a cell-penetrating polyarginine peptide (Kim et al., 2009). The use of cell-penetrating polyarginine peptide overcomes the limitation of macromolecules crossing the cellular membrane which usually has high proportion of basic amino acids, allowing generation of hiPSCs free of viral vector (Ziegler et al., 2005; El-Sayed et al., 2009; Kim et al., 2009). Nevertheless, this protein deliver method is hampered by the need of repetitive treatments and relative low reprogramming efficiency, which approximately reported at 0.001% (Kim et al., 2009).

Nonintegrating episomal vectors have also been used to transfect human somatic cells (Yu et al., 2009; Yu et al., 2011; Hu and Slukvin, 2013). The vectors are mixture of three plasmids expressing seven factors include *OCT3/4*, *SOX2*, *c-MYC*, *KLF4*, *NANOG*, *LIN28*, SV40 large T antigen (*SVLT*),

and Epstein-Barr nuclear antigen-1 (*EBNA1*) (Yu et al., 2009; Yu et al., 2011; Hu and Slukvin, 2013). The method is relied on absolute balanced expression levels of these factors during reprogramming process (Yu et al., 2009). Repeated transient transfection of these vectors resulted in production of transgene-free iPSCs and it is similar to hESCs in proliferative and developmental potential (Yu et al., 2009; Yu et al., 2011; Hu and Slukvin, 2013). Reprogramming efficiency of this approach remained extremely low with three to six colonies per 10^6 input cells (Yu et al., 2009).

A minicircle DNA vector containing a cassette of reprogramming factors (*OCT3/4*, *SOX2*, *NANOG* and *LIN28*) and a reporter green fluorescent protein (*GFP*) has been constructed for reprogramming purpose (Jia et al., 2010). Minicircles are unique and different from plasmids as they consist of eukaryotic expression cassettes, and lack of both antibiotic resistance gene and bacteria origin of replication (Huang et al., 2009; Jia et al., 2010; Kay et al., 2010). These features have been significantly enhanced and provided more consistent transgene expression than plasmids (Huang et al., 2009; Kay et al., 2010). However, the reprogramming efficiency remained low, at 0.005% (Narsinh et al., 2011a).

Warren and co-workers (2010) reported an efficient reprogramming method using combination of modified synthetic mRNAs encoding *OCT3/4*, *SOX2*, *KLF4* and *c-MYC*. This mRNA-based reprogramming yielded efficiency of 1.4% and iPSC colonies were formed at day 17 post-transfection (Warren et al., 2010). Translation of functional reprogramming proteins taken place within

several hours has greatly contributed 36-fold improvement in reprogramming efficiency (Warren et al., 2010; Mandal and Rossi, 2013). The mRNA-based reprogramming is tedious as it requires repeated transfection (Mandal and Rossi, 2013). Furthermore, insertion of synthetic mRNAs could provoke immune response of host cells, leading to massive cell death (Mandal and Rossi, 2013).

The regulatory role of microRNAs during cellular development and differentiation are well characterised (Lee et al., 1993; Ruvkun, 2001). Recent studies reported that specific miRNAs are highly expressed in hESCs and miRNAs-mediated gene regulation played critical role in maintaining pluripotency (Houbaviy et al., 2003; Judson et al., 2009). Certain miRNAs have showed to promote generation of iPSCs, and induced trans-differentiation through activation of lineage-specific transcription factors (Anokye-Danso et al., 2012). miRNA clusters such as miR-290-295 and miR-302-367 are known to enhance reprogramming process (Anokye-Danso et al., 2011; Lin et al., 2008; Lin et al., 2011; Miyoshi et al., 2011).

2.3.3.4 Alternative Approach for Reprogramming

Apart from abovementioned reprogramming methods, small molecule compounds that exhibit the effects of transcription factors have been widely used for reprogramming (Narsinh et al., 2011a; Feltes and Bonatto, 2013; Jung et al., 2014). As shown in Table 2.1, small molecule compounds can be divided into two groups which are synthetic compounds and natural compounds (Jung

et al., 2014). These small molecules showed to regulate various pathways crucial in somatic reprogramming (Jung et al., 2014). Synthetic compounds such as Valproic acid, Butyrate, Parnate, Thiazovivin, PD0325901, CHIR990221, SB431542, A-83-01 and PS48 have been identified to improve reprogramming efficiency (Marson et al., 2008; Lin et al., 2009; Narsinh et al., 2011a). On the other hand, natural compound including Vitamin C has also been identified to enhance reprogramming efficiency (Cai et al., 2010; Esteban et al., 2010). Furthermore, the used of small molecule compounds could possibly avoid integration of viral genome, that may cause to tumour formation (Narsinh et al., 2011a; Jung et al., 2014).

Valproic acid (VPA), a histone deacetylase inhibitor, is an acidic chemical compound used to treat epilepsy, bipolar disorder and prevention of migraine headache (Narsinh et al., 2011a). Histone deacetylase inhibitor showed to promote chromatin relaxation and the binding of transcription factors to DNA (Rybouchkin et al., 2006). The used of VPA coupled with Yamanaka's factor has been shown to improve the reprogramming efficiency by 100 folds compared to the use of Yamanaka's factor alone (Huangfu et al., 2008a). VPA has also been shown to enable expression of relevant stem cell transcription factors for iPSC reprogramming in the absence of *c-MYC* or *KLF4* (Huangfu et al., 2008b; Lyssiotis et al., 2009). Even though VPA could be used to replace both *KLF4* and *c-MYC* in somatic reprogramming, the efficiency was significantly reduced by half (Huangfu et al., 2008b).

CHIR99021, a glycogen synthase kinase-3(GSK3) inhibitor, has been used to enhance iPSC induction by activation of Wnt signaling pathway (Marson et al., 2008). Reprogramming efficiency at 0.2% to 0.4% was reported when CHIR99021 was used with three transcription factors (*OCT3/4*, *SOX2* and *KLF4*) (Li, W et al., 2009). CHIR99021 is often used with Parnate as combination of both small molecules provides synergistic effect in promoting cellular reprogramming (Li, W et al., 2009). Parnate is lysine-specific demethylase 1 that commonly used for depression treatment (Mimasu et al., 2008). Parnate has also been identified as an epigenetic regulator due to its ability to inhibit histone H3K4 demethylation (Mimasu et al., 2008). Reprogramming efficiency using both CHIR99021 and Parnate was reported at 0.002% with the presence of only two transcription factors (*OCT3/4* and *KLF4*) (Li, W et al., 2009; Hanna et al., 2010).

A mixture of chemical compound consists of SB431542, PD0325901 and Thiazovivin which have the properties to inhibit TGF-beta, MEK and Rho signalling pathway, respectively, has been shown to work synergically with reprogramming factors to generate iPSCs from human fibroblasts (Lin et al., 2009; Maherali and Hochedlinger, 2009). A 100 folds increment of reprogramming efficiency was reported (Lin et al., 2009; Maherali and Hochedlinger, 2009). With that, the authors proposed that addition of these small molecules enhance reprogramming efficiency, perhaps by accelerating the kinetics of reprogramming via mesenchymal-epithelial transition (MET) (Lin et al., 2009). MET is a physiological process occurs frequently during embryogenesis, whereby motile mesenchymal cells are transdifferentiate into

polarised epithelial cells (Davies, 1996). Addition of Thiazovivin alone appears to promote better cell survival during reprogramming (Xu et al., 2010). On the other hand, PD0325901 is believed to be crucial for maintaining pluripotency by blocking stem cell differentiation (Ying et al., 2008).

A cocktail containing Butyrate (a histone deacetylase inhibitor), A-83-01 (an inhibitor of TGF-beta kinase/activin receptor) and PS48 (an activator of phosphoinositide-dependent kinase-1, PDK1) has been demonstrated to promote reprogramming process with only the use of *OCT3/4* transcription factor and yielded 0.004% reprogramming efficiency (Zhu et al., 2010). The compounds were found to be involved in signalling pathways that affecting reprogramming process such as MET and glycolysis (Zhu et al., 2010). For example, PS48 exerted its effect at the early phase of reprogramming in order to promote glycolysis, a process to produce energy, whereby this process highly required for successful reprogramming (Zhu et al., 2010). On the other hand, A-83-01 promotes MET and Butyrate facilitates the binding of transcription factors to DNA (Lin and Wu, 2015).

Natural compound such as Vitamin C has been reported to enhance reprogramming process with three (O, S and K) or four factors (O, S, K and M) (Cai et al., 2010; Esteban et al., 2010). Vitamin C treatment showed to reduce expression of intracellular p53 and reactive oxygen species, in which both factors are known as the roadblock in reprogramming process (Esteban et al., 2010). When Vitamin C was used in conjunction with VPA, reprogramming efficiency was reported at 7.06% (Esteban et al., 2010). Nevertheless, the role

of vitamin C as a cofactor for many important enzymes could promote undesired epigenetic modifications in reprogramming (Narsinh et al., 2011a).

Table 2.1: Compounds that modulate stem cell fate and reprogramming. Adopted from Zhang, Y et al., 2012.

	Compound name	Identity	Function	References
Synthetic compounds	Valproic acid	HDAC inhibitor	Promotes MEF reprogramming efficiency, and enables OCT3/4 and SOX2 mediated reprogramming of human fibroblasts.	(Huangfu et al., 2008a)
	Butyrate	HDAC inhibitor	Facilitates OCT3/4 only mediated reprogramming when combined with A-83-01 and PS48.	(Zhu et al., 2010)
	Parnate	LSD1 inhibitor	Enables reprogramming of human keratinocytes mediated by OCT3/4 and KLF4.	(Li, W et al., 2009; Hanna et al., 2010)
	PD0325901	MEK inhibitor	Blocks differentiation pathway of ESCs and supports self-renewal; Facilitates rapid and efficient generation of fully reprogrammed human iPSCs.	(Ying et al., 2008) (Lin et al., 2009)
	Thiazovivin	ROCK inhibitor	Improves survival of hESCs upon dissociation; Facilitates rapid and efficient generation of fully reprogrammed human iPSCs.	(Xu et al., 2010) (Lin et al., 2009)
	CHIR99021	G3K3 inhibitor	Enables OCT3/4 and KLF4 mediated reprogramming of MEFs or human primary keratinocytes with Parnate.	(Li, W et al., 2009; Hanna et al., 2010)
	SB431542	ALK4, ALK5, ALK7 inhibitor	Facilitates rapid and efficient generation of fully reprogrammed human iPSCs;	(Lin et al., 2009)
	A-83-01	ALK4, ALK5, ALK7 inhibitor	Enables OCT3/4 mediated reprogramming when combined with Butyrate /PS48.	(Zhu et al., 2010)
	PS48	PDK1 activator	Enables OCT3/4 mediated reprogramming with A-83-01 and Butyrate.	(Zhu et al., 2010)
Natural compound	Vitamin C	Antioxidant	Facilitates rapid and efficient generation of fully reprogrammed human iPSCs	(Cai et al., 2010; Esteban et al., 2010)

Notice that in this table, reprogramming refers to iPSC-transcription factor-mediated reprogramming (OCT4, SOX2, KLF4 and c-MYC).

HDAC, histone deacetylase; LSD1, lysine-specific demethylase; MEK, MAPK kinase; G3K3, glycogen synthase kinase; ALK4, ACVR1B; ALK5, TGFBR1; ALK7, ACVR1C; PDK1, phosphoinositide-dependent kinase 1; ROCK, Rho-associated-coiled-containing protein kinase; MEF, mouse embryonic fibroblasts; ESC, embryonic stem cell; iPSCs, induced pluripotent stem cells.

2.3.4 Pluripotency Characterisation Assays

According to International Stem Cell Banking Initiative (ISCBI), pluripotency properties of newly developed ESCs or iPSCs line can be verified by several characterisation assays including detection of pluripotency markers, three germ layers differentiation assays and karyotype analysis (Crook et al., 2010).

2.3.4.1 Detection of Pluripotency Markers Expression

Pluripotency markers are the molecules that can affect the stemness properties and self-renewal of pluripotent stem cells (Zhao et al., 2012). A wide range of markers have been identified to be indicative of undifferentiated pluripotent stem cells, including alkaline phosphatase (ALP), OCT3/4, SOX2, NANOG, GABRB3, LEFTY, DNMT3B, ESG1, TRA-1-81, SSEA4 and many more (Zhao et al., 2012). Different approaches have been used to detect the presence of pluripotency markers, for example detection of mRNA levels can be done using polymerase chain reaction (PCR) method (Zhao et al., 2012). Methods such as western blot, immunofluorescence staining and flow cytometry methods have been used to detect protein expression of pluripotency markers (Zhao et al., 2012).

Alkaline phosphatase (ALP) is a hydrolase enzyme which is expressed throughout the body (Singh et al., 2012). There are different ALP isozymes such as intestinal isozyme, tissue-nonspecific isozyme and placental isozyme

(Singh et al, 2012). Of these ALP isozymes, the placental isozyme has found to be overexpressed in undifferentiated pluripotent stem cells, such as embryonic germ cells (EG) and embryonic stem cells (ESCs) (Andrews et al., 1984; Shambloott et al., 1998; Thomson et al., 1998; Pera et al., 2000; Takahashi et al., 2007). ALP positive colonies indicate pluripotency of cells and it is commonly used as an indicator to represent successful reprogrammed cells at early stage of reprogramming (Palmqvist et al., 2005; Gonzalez et al., 2011). Disadvantage of this measure is unable to distinguish between undifferentiated and early differentiating cells, thus required additional markers such as OCT3/4, SOX2 and NANOG, or differentiation assay to confirm pluripotency of the cells (Ramirez et al., 2011).

In addition to the expression of ALP, pluripotency markers including LEFTY, GABRB3, NANOG, TRA-1-60, SSEA4, DNMT3B and ESG1 can be used to define pluripotency properties of stem cells (Tanabe et al., 2013; Feng et al., 2013; Calloni et al., 2013). LEFTY is belongs to transforming growth factor (TGF)- β family members and expressed thoroughly in undifferentiated embryonic stem cells, blastocyst and inner cell mass (Adjaye et al., 2005; Seuntjens et al., 2009). Expression of LEFTY is controlled by transcription factors complex composed of OCT3/4, SOX2 and KLF4 (Nakatake et al., 2006). Deletion of LEFTY in mouse embryonic stem cells showed enhanced differentiation potential, indicated that its expression is a marker of stemness (Park et al., 2013). NANOG is a well-known transcription factor associated with stem cell properties of pluripotency and self-renewal (Pan and Thomson, 2007). NANOG was found to be regulated by OCT3/4/SOX2 motif upstream

of the promoter (Pan and Thomson, 2007). Overexpression of NANOG promotes self-renewal without the presence of feeder layer by inhibition of differentiation pathway (Pan and Thomson, 2007).

ESG1, also named developmental pluripotency-associated (DPPA) genes, is an RNA binding domain with wide range of RNA target (Tanaka et al., 2006). ESG1 is expressed thoroughly in early embryos, germ cells, ESCs, embryonic germ cells and multipotent germline stem cells (Tanaka et al., 2006). Deletion of ESG1 in pluripotent stem cells showed no effect in their pluripotency properties (Zhao et al., 2012). On the other hand, GABRB3 encodes a multisubunit of chloride channel which has functional role during preimplantation stage (DeLorey et al., 1998). Homozygous knockout of GABRB3 in mouse led to high mortality rate with survival animals were found to share several behavioral and physiological abnormalities (DeLorey et al., 1998). TRA-1-81 is a keratin sulfate antigen which widely expressed in pluripotent stem cell surface (Schopperle and DeWolf, 2007). Expression of TRA-1-81 is lost during stem cell differentiation and thus it is often used to indicate pluripotency properties of cells (Pera et al., 2000).

SSEA4 is a carbohydrate-associated molecule which has regulatory role in cell surface interactions during cell development (Zhao et al., 2012). SSEA4 is overexpressed in undifferentiated pluripotent stem cells, human embryonic germ cells and human teratocarcinoma stem cells (Zhao et al., 2012). Expression of SSEA4 is tightly controlled during preimplantation of embryo (Truong et al., 2011). However, deletion of SSEA4 in pluripotent stem cells

caused no changes of their stemness properties (Truong et al., 2011). For DNMT3B, it is a DNA methyltransferase crucial for regulating embryogenesis (Okano et al., 1999). DNMT3B is widely expressed in inner cell mass, epiblast and embryonic ectoderm (Watanabe et al., 2002). Expression of DNMT3B has been used to identify pluripotent stem cells (Wakao et al., 2012).

2.3.4.2 Three Germ Layers Differentiation Assays

The ability to differentiate into any cell types from three germ layers (mesoderm, ectoderm and endoderm) is the hallmark of pluripotent stem cells (Marti et al., 2013). This capability can be assessed through either *in vitro* or *in vivo* differentiation assays (Marti et al., 2013). For the *in vitro* differentiation test, colonies of pluripotent stem cells are first cultured in suspension without anti-differentiation factors in order to allow spontaneous formation of aggregates called embryoid bodies (EBs) (Marti et al., 2013). EBs recapitulate many aspects of cellular differentiation during early embryonic development and thus should consist of different cell types derived from three germ layers (Kurosawa, 2007; Marti et al., 2013). On the other hand, pluripotent stem cells can be cultured in lineage-specific growth factors containing medium that favor differentiation toward a specific cell type/lineage (Marti et al., 2013).

In vivo differentiation method usually accompanies by teratoma formation by injecting pluripotent stem cells into severe combined immunodeficient (SCID) mice (Gutierrez-Aranda et al., 2010). The injected pluripotent stem cells proliferate and ultimately differentiate into cell types

derived from three embryo germ layers (Marti et al., 2013). *In vivo* differentiation is different from *in vitro* differentiation as it provides information of cell behavior in live tissues (Müller et al., 2011). Nevertheless, the necessity of applying an *in vivo* test is highly debatable due to inconsistency of methodology (Buta et al., 2013). For example, differences in injection site, cell culture conditioned and number of injected cells may cause variation of results (Buta et al., 2013). Furthermore, *in vivo* differentiation has been limited due to it requires the use of experimental animals (Buta et al., 2013). In this context, performing an *in vitro* differentiation assay is strongly recommended (Buta et al., 2013).

2.3.4.3 Karyotype Analysis

Karyotype analysis is an important technique which is commonly used to evaluate genomic integrity of ESCs and newly created iPSC line (Marti et al., 2013). Basically, the cells are arrested in the metaphase stage of cell division followed by Giemsa staining (Marti et al., 2013). Karyotype of the cells is then observed under microscope (Marti et al., 2013). Differences in sizes of chromosomes, position of centromeres, basic number of chromosomes, number and position of satellites and banding patterns of cells have been compared (King et al., 2006). Alternatively, spectra karyotyping can be performed on the basis of molecular cytogenetic characteristics to improve the resolution of the Giemsa staining (Schröck et al., 1996). Chromosome-specific DNA probes are labeled with different fluorophores, which are specific for each pair of

chromosome (Marti et al., 2013). The unique coloured chromosomes are then visualised and compared (Marti et al., 2013).

CHAPTER 3

MATERIALS AND METHODS

In overall, transfection of Phoenix cells was optimised using recombinant plasmid encoding green fluorescent protein (GFP) followed by optimisation of infection protocol on parental AML-M5 cells using retrovirus harbouring GFP. Generation of AML-M5-derived iPSCs was carried out using optimised transfection and infection protocols with retroviruses harbouring O, S, K and M. The AML-M5-derived iPSCs was then selected and expanded individually for pluripotency characterisation assays including detection of pluripotency markers on AML-M5-derived iPSCs using reverse transcription-PCR (RT-PCR), immunofluorescence staining, flow cytometry and *in vitro* three germ layers differentiation assays. The AML-M5-derived iPSCs were also subjected to verification assays including detection of monocyte-specific markers using flow cytometry and detection of leukaemia-associated MLL-AF9 using reverse transcription-PCR (RT-PCR). Numerical data were statistical analysed using SPSS. Parental AML-M5 cells, human adipose-derived mesencymal stem cell (hAd-MSC) and hESCs were cultured throughout the study. The overall study was summarised in Figure 3.1.

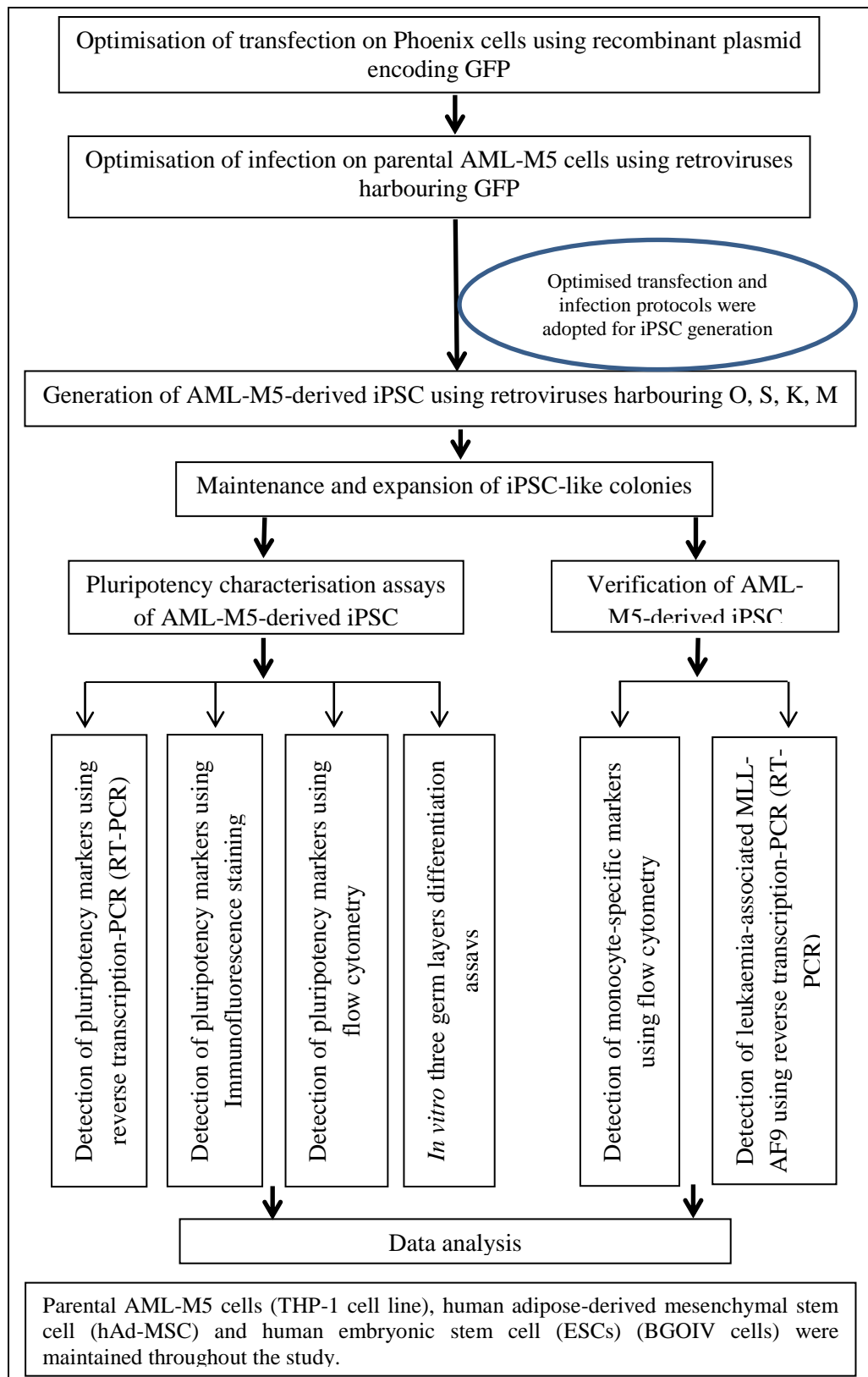


Figure 3.1: Flow chart of this study. The study was started with transfection optimisation of Phoenix cells using recombinant plasmid GFP followed by infection optimisation of parental AML-M5 cells using retroviruses harbouring GFP. Optimised transfection and infection protocols were used to generate AML-M5-derived iPSCs using retroviruses harbouring O, S, K and M. The AML-M5-derived iPSCs were maintained and individually picked, and subjected to pluripotency characterisation assays and verification assays. All the numerical data were subjected to statistical analysis. Parental AML-M5 cells and hESCs were used as control, whereas, hAd-MSC was used as feeder cell and control.

3.1 Cell Culture

3.1.1 Maintenance and Subculture of AML-M5 Leukaemia Cells

The AML-M5 cells (THP-1 cell line) were purchased from ATCC (USA). The cell line was cultured and maintained according to recommended procedure. In brief, parental AML-M5 cells were grown as suspension form and maintained in 37 °C, 5% carbon dioxide (CO₂), 95% humidifying air incubator with complete RPMI 1640 medium (Gibco Invitrogen, USA) supplemented with 10% fetal bovine serum (Gibco Invitrogen, USA), 50 U/ml penicillin and 50 mg/ml streptomycin (Gibco Invitrogen, USA). The cells were grown until 70% to 90% confluent before subculture.

To subculture, the cells were collected and centrifuged to remove supernatant. Next, 5 ml of complete RPMI 1640 medium was added. The cells were subculture at 1:5 split ratios.

To cryopreserve, the cell pellet was resuspended in freezing medium (90% fetal bovine serum and 10% DMSO) at cell concentration about 1×10^6 viable cells/vial. The viable cells were then transferred into a sterile cryovial (Nunc, USA) and stored in CoolCell® Alcohol-Free Cell Freezing Containers (Biocision, USA) and subsequently placed overnight at -80 °C prior to store into liquid nitrogen for long term storage.

3.1.2 Maintenance, Subculture and Inactivation of Feeder Cells

3.1.2.1 Maintenance and Subculture of Feeder Cells

The human adipose-derived mesenchymal stem cell (hAd-MSC) (passage 0) was kindly provided by Cryocord Sdn. Bhd with consent of material transfer agreements (MTA). The hAd-MSC was grown as adherent form and maintained in 37 °C, 5% carbon dioxide (CO₂), 5% oxygen (O₂) incubator with complete DMEM/F12 medium (Gibco Invitrogen, USA) supplemented with 10% fetal bovine serum (Gibco Invitrogen, USA), 50 U/ml penicillin and 50 mg/ml streptomycin (Gibco Invitrogen, USA), 5 ng/ml basic fibroblast growth factor (Invitrogen Cooperation, USA). The cells were grown until 70% to 90% confluent prior to subculture.

To subculture, the cells were washed with 1 X PBS (MP Biomedical, USA) and then 0.05% trypsin-EDTA (Gibco Invitrogen, USA) was added. The cells were incubated at 37 °C, 5% carbon dioxide (CO₂), 95% humidifying air incubator for five minutes or until the cells detached from the flask with the aid of gentle tapping. Subsequently, 2 X volume of complete DMEM/F12 medium (with serum) was added (4 ml of complete medium was added when 2 ml of trypsin-EDTA was used). The trypsinised cells were washed once in 10 ml DMEM/F12 medium before being used for subculture with 1:5 split ratios.

To cryopreserve, the cell pellet was resuspended in freezing medium (90% fetal bovine serum and 10% DMSO (Sigma, USA) at concentration about

1 x 10⁶ viable cells/vial. The viable cells were then transferred into a sterile cryovial (Nunc, USA) and stored in CoolCell® Alcohol-Free Cell Freezing Containers (Biocision, USA) and subsequently placed overnight at -80 °C prior to place into liquid nitrogen for long term storage.

3.1.2.2 Inactivation of Feeder Cells

The hAd-MSC was used as a feeder cells in this study. For that purpose, the cells were treated with 10 ug/ml of mitomycin C (Calbiochem, USA) at 37 °C, 5% carbon dioxide (CO₂), 95% humidifying air incubator for three hours to inactivate them. After that, the cells were washed three times in 1 X PBS. Cells were harvested using 0.05% trypsin-EDTA and seeded onto a 0.1% gelatine-coated well with density of 2 x 10⁵ cells/well. Balance of inactivated cells was cryopreserved with density of 1 x 10⁶ cells/vial in liquid nitrogen for future use.

3.1.3 Maintenance and Subculture of Human Embryonic Stem Cells (hESCs)

The hESC, BGOIV, was purchased from ATCC (USA). BGOIV was grown in feeder free condition as adherent colony. The cells were maintained in 37 °C, 5% carbon dioxide (CO₂), 95% humidifying air incubator with mTeSR™1 medium (STEMCELL™ Technologies, Canada) supplemented with 50 U/ml penicillin and 50 mg/ml streptomycin (Gibco Invitrogen, USA). The cells were subcultured before the colonies begin to touch.

To subculture, Geltrex® LDEV-Free hESC-qualified Reduced Growth Factor Basement Membrane Matrix (Gibco, USA) was pre-coated on 35 mm culture dish and was incubated at 37 °C, 5% CO₂, 95% humidifying air incubator for one hour before use. Coating medium was removed and mTeSR™1 medium was added prior to use. The cell colonies were harvested through mechanical micro-dissection into small pieces or enzymatic digestion using Dispase II (Invitrogen Cooperation, USA). Small pieces of colonies were carefully collected and washed with mTeSR™1 medium. Subsequently, the cell pellet was re-suspended in mTeSR™1 medium and plated in matrix-coated dish at 1:3 split ratios.

To cryopreserve, the cell pellet from 35 mm culture dish (SPL, USA) was resuspended in Synth-a-Freeze® Cryopreservation Medium (Gibco, USA). Cells were then transferred into a sterile cryovial (Nunc, USA) and stored in CoolCell® Alcohol-Free Cell Freezing Containers (Biocision, USA) and subsequently kept overnight at -80 °C prior to placing in liquid nitrogen for long term storage.

3.1.4 Maintenance and Subculture of Phoenix Packaging Cell Line

Phoenix cells were kindly provided by Dr. Kenneth, Raj [Health Protection Agency (HPA), UK]. Phoenix-ampho cells are 293T-based cell line that has been transformed with adenovirus E1a and carried a T antigen co-selected with neomycin (Cornetta et al., 2005). Phoenix cells stably produce

gag-pol and envelope protein that are essential for amphotropic helper-free viruses production.

Phoenix cells were maintained as adherent culture at 37 °C, 5% carbon dioxide (CO₂), 95% humidifying air incubator with complete DMEM high glucose medium (Gibco Invitrogen, USA) supplemented with 10% fetal bovine serum (Gibco Invitrogen, USA), 50 U/ml penicillin and 50 mg/ml streptomycin (Gibco Invitrogen, USA). The cells were grown until 70% to 90% confluent prior to subculture.

To subculture, cells were washed with 1 X PBS (MP Biomedical, USA) and then 0.05% trypsin-EDTA (Gibco Invitrogen, USA) was added. The cells were incubated at 37 °C, 5% carbon dioxide (CO₂), 95% humidifying air incubator for 5 minutes or until the cells detached from the flask with gentle tapping. Subsequently, 2 X volume of complete DMEM high glucose medium (with serum) was added (e.g. 4 ml of complete medium was added when 2 ml of trypsin-EDTA was used). The trypsinised cells were washed once in 10 ml DMEM high glucose medium before being used for subculture at 1:5 split ratios.

To cryopreserve, the cell pellet was re-suspended in freezing medium consisting of 50% complete DMEM high glucose medium, 40% fetal bovine serum, 10 % DMSO (Sigma, USA) with cells at concentration about 1×10^6 viable cells/vial. The viable cells were then transferred into a sterile cryovial (Nunc, USA) and stored in CoolCell® Alcohol-Free Cell Freezing Containers

(Biocision, USA) and subsequently incubated overnight at -80 °C prior to being placed in liquid nitrogen for long term storage.

3.2 Preparation of Recombinant Plasmids

Transformed *E. coli* encoding with human pMX-GFP (G), pMXs-hOCT3/4 (O), pMXs-hSOX2 (S), pMXs-hKLF4 (K), pMXs-hc-MYC (M) plasmids in glycerol stock were kindly provided by Dr Sugii, Shigeki [A* STAR, Singapore Bioimaging Consortium (SBIC)]. All transformed *E. coli* were encoded with ampicillin resistant gene as a selection marker.

3.2.1 Expansion of Transformed *E. coli*

One loop of transformed *E. coli* in glycerol stock was obtained and streaked on Luria-Bertani agar supplemented with 2 µg/ml of ampicillin (Sigma, USA). The plate was sealed and incubated at 37 °C for 16 hours. Then, a single bacteria colony was isolated and transferred into 10 ml LB broth supplemented with 2 µg/ml of ampicillin. Subsequently, the bacteria culture was grown at shaking incubator at 37 °C, 300 rpm for 16 hours. The bacteria culture was ready for plasmid isolation.

3.2.2 Isolation of Recombinant Plasmids

To purify the plasmid DNA, Hybrid-QTM Plasmid Rapidprep Mini Kit (GeneAll Biotechnology, Korea) was used according to the manufacturer's

protocol. Briefly, 1.5 ml bacterial culture was pelleted by centrifugation at 13000 x g for one minute. Pellet was lysed in 170 µl of S1 buffer. Then, 170 µl of S2 buffer was added and the tube was inverted repeatedly for three to four times. A total of 250 µl of G3 buffer was added and the tube was inverted for four to five times to precipitate protein in the mixture. Subsequently, the mixture with protein precipitate was transferred to column stack. The column stack was centrifuged at 13000 x g for 30 seconds. Then, the upper filter unit and flow through were discarded. Next, the column was washed with 500 µl of AW buffer and followed by 700 µl of PW buffer. For each washing step, the column was centrifuged at 13000 x g for 30 seconds and the flow through was discarded. The column was then centrifuged at 13000 x g for an additional one minute to remove residual washing buffer. The column was transferred to a new 1.5 ml tube and 50 µl of EB buffer was added to the column and was left to stand at room temperature for one minute prior to centrifuge at 13000 x g for one minute to elute the plasmid. Before storage at -20 °C, the purity and quantity of the extracted plasmids were determined using NanoPhotometer (Implen, Germany). Plasmid with good purity was estimated by the ratio of absorbance reading of 260:280 and should have a range between 1.8 to 2.0.

3.2.3 Verification of Recombinant Plasmids

Identity of the plasmid was reconfirmed by using restriction enzyme digestion. Restricted enzyme used for each plasmid and their expected product size were shown in Table 3.1. Briefly, 1 µg of plasmid DNA was mixed with 1 X RE buffer and 10 U/µl of restriction enzyme and total volume was brought

up to 20 μ l using double distilled water. The mixture was then incubated at 37 $^{\circ}$ C for three hours. Identity of digested plasmid was determined using gel electrophoresis. Two visible bands at respective product sizes (as shown in Table 3.1) were expected on the stained gel. After restriction enzyme digestion, 10 μ l of each reaction mixture was mixed with 1 x loading dye and loaded onto 1% pre-stained agarose gel containing in 1 X TAE buffer. Digested plasmids were electrophoresed on the gel together with KAPA universal ladder (KAPA Biosystems, South Africa) at 60 Volts, 400 mA for one hour. The gel was visualised and image was captured using Advance Gel Imaging System (UVP, USA).

Table 3.1: Restriction enzymes and their expected product sizes for different recombinant plasmids used in the study.

Recombinant Plasmid	Restriction enzyme Used	Expected product sizes
pMXs-hOCT3/4	EcoRI (Thermo Scientific, USA)	1100 bp, 4600 bp
pMXs-hSOX2	NotI (Thermo Scientific, USA)	1060 bp, 4500 bp
pMXs-KLF4	NotI (Thermo Scientific, USA)	1620 bp, 4500 bp
pMXs-hc-MYC	NotI (Thermo Scientific, USA)	1520 bp, 4500 bp

3.3 Transfection and Infection Optimisation

3.3.1 Transfection Optimisation of Phoenix Cells Using Recombinant Plasmid GFP

Phoenix-ampho cells were transfected with recombinant plasmids using calcium phosphate method (Swift et al., 1999). Recombinant plasmid encoding green fluorescence protein (GFP) was used as reporter gene to determine transfection efficiency. Two 35 mm culture dishes of Phoenix cells were

prepared, one was grown until 50-60% confluent (approximately 1.8×10^6 cells) and another was at 70-80% confluent (approximately 2.2×10^6 cells).

Prior to transfection, 2 ml of complete DMEM/high glucose medium (Gibco Invitrogen, USA) supplemented with 10% fetal bovine serum (Gibco Invitrogen, USA), 50 U/ml penicillin and 50 mg/ml streptomycin (Gibco Invitrogen, USA) were added to the cell culture. Transfection cocktail (for each 35 mm culture dish) was prepared as follow including Mixture A: 3.3 or 6.6 μg of pMXs plasmid and 2.5 M CaCl_2 , whereas, Mixture B: 2 X HEPES-Buffer Saline (HBS) (this buffer consists of 50 mM HEPES, 10 mM KCl, 12 mM Dextrose, 280 mM NaCl and 1.5 mM Na_2HPO_4 ; Calbiochem, USA). Mixture A was added into Mixture B drop by drop with the aid of gentle vortex. Immediately, Mixture A & B were added to the cells in 35mm dish in drop by drop manner. The transfection cocktail was left on the cells at 37 $^\circ\text{C}$, 5% CO_2 and 95% humidifying air incubator for 24 hours. After that, the cells were washed, and medium was replaced. The medium was changed every 24 hours. At 24, 48 and 72 hours post-transfection, pseudo-green signal of GFP-transfected cells was observed and captured using Axio Observer A1 with ZEN 2011 lite software (Carl Ziess, USA).

3.3.2 Infection of Parental Cells Using Retrovirus Harboring GFP

Recombinant retrovirus supernatants from Section 3.3.1 were used to infect parental AML-M5 cells (THP-1 cell line) via spinfection method (Berggren et al., 2012). Briefly, medium containing retroviruses was collected

and filtered through 0.2 µm syringe filter (Merck Milipore, USA)) prior being used directly to infect parental cells or kept at -80 °C for no more than two weeks. Two ml of virus supernatant was used to infect 1×10^5 parental AML-M5 cells in each well of 6-well plate. Parental AML-M5 cells were cultured in minimum volume of RPMI medium supplemented with 10% FBS and 1% Penicilin and Streptomycin (Gibco Invirtogen, USA) before addition of virus supernatant and 8 µg/mL of Polybrene (Merk Milipore, USA), a cationic polymer used to increase efficiency of retrovirus infection. The cell-virus mixture was centrifuged at $1000 \times g$ for one hour at 32 °C and subsequently incubated at 37 °C, 5% CO₂ and 95% humidifying air incubator for 23 hours. On the following day, the existing medium on the cells was removed and replaced with complete RPMI 1640 medium to recover the infected AML-M5 cells. At 24, 48 and 72 hours post-transfection, psedo-green signal of infected AML-M5 cells was observed and captured using Axio Observer A1 with ZEN 2011 lite software (Carl Zeiss, USA).

3.4 Generation of AML-M5-Induced Pluripotent Stem Cell (AML-M5-derived iPSCs)

As shown in Section 3.3.1 and 3.3.2, optimum Phoenix cell transfection and parental AML-M5 cells infection were obtained, accordingly. Phoenix cell transfection was repeated at 70-80% cell confluency using 6.6 µg of O, S, K, M and GFP recombinant plasmids isolated from Section 3.2.2. Briefly, five 35 mm culture dishes containing 2.2×10^6 Phoenix cells each were prepared. Each culture dish was transfected with O, S, K, M and GFP recombinant plasmids, respectively, using calcium phosphate transfection protocol highlighted in

Section 3.3.1. Retrovirus supernatant was collected at 72 hours post-transfection and filtered through 0.2 µm syringe filter prior to being used to directly infect the parental AML-M5 cells.

Two sets of parental AML-M5 cells infection were prepared: 1) parental AML-M5 cells infected with pooled O, S, K and M, and 2) parental AML-M5 cells infected with GFP (reporter of infection efficiency). Virus supernatants harbouring O, S, K and M were pooled and 2 ml of the pooled virus supernatant was used to infect 1×10^5 parental AML-M5 cells using Spinfection method highlighted in Section 3.3.2. Two days post-infection, infected AML-M5 cells were plated on feeder cells and maintained in complete DMEM/F12 medium supplemented with 20% knockout serum replacement (KOSR) (Gibco Invitrogen, USA), 10 ng/ml basic fibroblast growth factor (Miltenyi, USA), 1mM L-glutamine (Gibco, USA), 100 µM nonessential amino acids (Gibco Invitrogen, USA), 100 µM beta-mercaptoethanol (Calbiochem, USA), 50 U/ml penicillin and 50 mg/ml streptomycin (Gibco Invitrogen, USA), and complete RPMI 1640 medium supplemented with 10% fetal bovine serum (Gibco Invitrogen, USA), 50 U/ml penicillin and 50 mg/ml streptomycin (Gibco Invitrogen, USA) at ratio of 1:4. Complete RPMI 1640 medium (medium used to culture parental AML-M5 cells) was gradually replaced by complete DMEM/F12 medium supplemented with 20% knockout serum replacement (KOSR), 10 ng/ml basic fibroblast growth factor, 1mM L-glutamine, 100 µM nonessential amino acids, 100 µM beta-mercaptoethanol, 50 U/ml penicillin and 50 mg/ml streptomycin (medium used to culture AML-M5-derived iPSCs) in next three days. Between day two to day 14, the infected

AML-M5 cells were incubated in hypoxia condition (5% O₂) and 1 mM of Valproic acid (VPA) (STEMCELL™ Technologies, Canada), a histone deacetylase inhibitor, was added into the culture. At Day 15 and onwards, infected AML-M5 cells were incubated at 37 °C, 5% carbon dioxide (CO₂), 95% humidifying air incubator. Infected AML-M5 cells were maintained in culture and fresh medium was changed daily for up to 40 days. Distinct colonies with packed and visible edge were expected to show from day 14 onwards and each colony was picked and expanded individually for further characterisation assays.

3.4.1 Maintenance and Subculture of AML-M5-derived Induced Pluripotent Stem Cell (AML-M5-derived iPSCs)

The AML-M5-derived iPSCs were maintained as adherent colonies using feeder and feeder-free culture method under different circumstances. The cells were maintained in 37 °C, 5% carbon dioxide (CO₂), 95% humidifying air incubator for both the culture system.

In feeder culture system, AML-M5-derived iPSCs were maintained on feeder cells (hAd-MSC) with complete DMEM/F12 medium (Gibco Invitrogen, USA) supplemented with 20% knockout serum replacement (KOSR) (Gibco Invitrogen, USA), 10 ng/ml basic fibroblast growth factor (Miltenyi, USA), 1mM L-glutamine (Gibco, USA), 100 µM nonessential amino acids (Gibco Invitrogen, USA), 100 µM beta-mercaptoethanol (Calbiochem, USA), 50 U/ml penicillin and 50 mg/ml streptomycin (Gibco Invitrogen, USA). The cells were subcultured before the colonies begin to

touch in both the culture system. To subculture, inactivated feeder cells were seeded on 0.1% gelatine-coated culture dish and incubated at 37 °C with 5% CO₂ overnight before use. The cell colonies were harvested through mechanical micro-dissection into small pieces. Small pieces of colonies were carefully collected and washed with complete DMEM/F12 medium supplemented with 20% knockout serum replacement (KOSR), 10 ng/ml basic fibroblast growth factor, 1mM L-glutamine, 100 µM nonessential amino acids, 100 µM beta-mercaptoethanol, 50 U/ml penicillin and 50 mg/ml streptomycin. Subsequently, the cell pellet was resuspended in complete DMEM/F12 medium and seeded in new feeder-coated dish at 1:3 split ratios.

On the other hand, prior to three germ layers differentiation assay, AML-M5-derived iPSCs were maintained on feeder-free condition with mTeSRTM1 medium (STEMCELLTM Technologies, Canada) supplemented with 50 U/ml penicillin and 50 mg/ml streptomycin (Gibco Invitrogen, USA) on culture dish pre-coated with Geltrex® LDEV-Free hESC-qualified Reduced Growth Factor Basement Membrane Matrix (Gibco, USA). The cells were subcultured before the colonies begin to touch in both the culture system. To subculture, Geltrex® was pre-coated on culture dish and incubated at 37 °C, With 5% CO₂ in 95% humidifying air incubator for one hour before use. The cell colonies were harvested through mechanical micro-dissection into small pieces. Small pieces of colonies were carefully collected and washed with mTeSRTM1 medium. Subsequently, the cell pellet was resuspended in mTeSRTM1 medium and seeded in matrix-coated dish at 1:3 split ratios.

To cryopreserve, the cell pellet from 35 mm culture dish (SPL, USA) was re-suspended in Synth-a-Freeze® Cryopreservation Medium (Gibco Invitrogen, USA). Cells were then transferred into a sterile cryovial (Nunc, USA) and stored in CoolCell® Alcohol-Free Cell Freezing Containers (Biocision, USA) and subsequently incubated overnight at -80 °C prior to place into liquid nitrogen for long term storage.

3.5 Characterisation of AML-M5-derived iPSCs

3.5.1 Detection of Pluripotency Markers Using Reverse Transcription-Polymerase Chain Reaction (RT-PCR)

3.5.1.1 RNA Extraction

Total RNA from AML-M5-derived iPSCs was extracted using TRizol (Invitrogen Cooperation, USA). One ml of TRizol was added to resuspend cell pellet and allowed to stand at room temperature for five minutes. Cell pellet was shredded by five times passing through a 21 G syringe needle. Next, cell suspension was centrifuged at 12000 rpm at 4 °C for 15 minutes. Carefully, the aqueous phase was transferred to a new 1.5 ml microcentrifuge tube. Then, 0.5 ml isopropanol was added into the aqueous phase and left for 10 minutes at room temperature before centrifugation at 12000 rpm for 15 minutes at 4 °C. At this point, a gel-like transparent pellet was visualised. The supernatant was discarded and the pellet was washed with 1 ml 70% ethanol and followed by 1 ml 95% ethanol. For each washing step, the pellet was centrifuged at 10000 rpm at 4 °C for five minutes. The supernatant was discarded. After washing

with 95% ethanol, cell pellet was air dried at room temperature for 10-20 minutes. Air dried RNA pellet was dissolved in 20 µl of DEPC treated water containing Ribolock RNase Inhibitor (Thermo Scientific, USA). Before storage at -80 °C, the purity and quantity of the extracted plasmids were determined using NanoPhotometer (Implen, Germany) and the purity of RNA was verified by agarose gel electrophoresis. RNA with good purity was estimated by ratio of absorbance reading of 260:280 at range between 1.9 to 2.0. One µl of each RNA sample was loaded onto 1% agarose gel containing in 1 X TAE buffer. RNA was electrophoresed on the gel together with KAPA universal ladder (KAPA Biosystems, South Africa) at 60 Volts, 400 mAmp for one hour. Bands were visualised and image was captured using Advance Gel Imaging System (UVP, USA). The 18S and 28S RNA bands were expected to be seen in intact RNA sample.

3.5.1.2 First Strand cDNA Synthesis

Reverse transcription was carried out using RevertAid Reverse Transcriptase (Thermo Scientific, USA) according to recommended manufacturer protocol. Approximately 1 µg of RNA was added to reaction mixture consisting of 0.5 µg of Oligo (dT)₂₀ primers (Thermo Scientific, USA) and nuclease-free H₂O. The mixture was incubated at 65 °C for five minutes and chilled on ice for five minutes. Then, 200 units of RevertAid Reverse Transcriptase (Thermo Scientific, USA), 20 units of Ribolock RNase Inhibitor (Thermo Scientific, USA) and 2 µl of 10mM dNTPs were added to the mixture before incubation at 42 °C for one hour followed by 70 °C for 10 minutes.

Generated cDNA was either use directly for detection of pluripotency-associated genes or store at -80 °C for future use.

3.5.1.3 *GAPDH*

PCR was performed using DreamTaq DNA Polymerase (Thermo Scientific, USA). *GAPDH* gene was used as a housekeeping gene. Highly purified salt-free primers for *GAPDH* (IDT, Singapore): forward primer, 5' AGGGCTGCTTTTAACTCTGGT 3'; reverse primer, 5' CCCCACTTGATTTTGGAGGGA 3' (Zhang, X et al., 2013) were used to amplify a 206 bp PCR product. A reaction with 20 µl in total volume was prepared with the following components: 2 µl of 10 X DreamTaq Buffer with 20 mM MgCl₂, 0.4 µl of 10 mM dNTPs (Thermo Scientific, USA), 0.4 µl each of 10 µM forward and reverse primers, 0.5 U DreamTaq DNA Polymerase, 25 ng of cDNA and ddH₂O. PCR was performed using the following PCR program on Veriti 96 well Thermal Cycler (Applied Biosystems, USA): initial denaturation at 95 °C for two minutes; followed by 35 cycles of denaturation at 95 °C for 30 seconds, annealing at 58 °C for 30 seconds, extension at 72 °C for 30 seconds; and final extension at 72 °C for two minutes.

After PCR, 10 µl of each reaction mixture was mixed with 1 X loading dye and loaded onto 1.5% pre-stained agarose gel containing in 1 X TAE buffer. PCR mixture was electrophoresed on the gel together with GeneRuler 100 bp DNA Ladder (Thermo Scientific, USA) at 60 Volts, 400 mAmp for one

hour. The gel was visualised and image was captured using Advance Gel Imaging System (UVP, USA).

3.5.1.4 *OCT3/4*

PCR was performed using DreamTaq DNA Polymerase (Thermo Scientific, USA). Highly purified salt-free primers for *OCT3/4* (IDT, Singapore): forward primer, 5' GACAGGGGGAGGGGAGGAGCTAGG 3'; reverse primer, 5' CTTCCCTCCAACCAGTTGCCCAAAC 3' (Takahashi et al., 2007) were used to amplify a 144 bp PCR product. A reaction with 20 µl in total volume was prepared with the following components: 2 µl of 10 X DreamTaq Buffer with 20 mM MgCl₂, 0.4 µl of 10 mM dNTPs (Thermo Scientific, USA), 0.8 µl each of 10 µM forward and reverse primers, 0.5 U DreamTaq DNA Polymerase, 25 ng of cDNA and ddH₂O. PCR was performed using the following PCR program on Veriti 96 well Thermal Cycler (Applied Biosystems, USA): initial denaturation at 95 °C for two minutes; followed by 35 cycles of denaturation at 95 °C for 30 seconds, annealing at 65 °C for 30 seconds, extension at 72 °C for 30 seconds; and final extension at 72 °C for two minutes. After PCR, 10 µl of each reaction mixture was mixed with 1 X loading dye and loaded onto 1.5% pre-stained agarose gel containing in 1 X TAE buffer. PCR mixture was electrophoresed on the gel together with GeneRuler 100 bp DNA Ladder (Thermo Scientific, USA) at 60 Volts, 400 mA for one hour. The gel was visualised and image was captured using Advance Gel Imaging System (UVP, USA).

3.5.1.5 *SOX2*

PCR was performed using DreamTaq DNA Polymerase (Thermo Scientific, USA). Highly purified salt-free primers for *SOX2* (IDT, Singapore): forward primer, 5' GGGAAATGGGAGGGGTGCAAAAGAGG 3'; reverse primer, 5' TTGCGTGAGTGTGGATGGGATTGGTG 3' (Takahashi et al., 2007) were used to amplify a 151 bp PCR product. A reaction with 20 µl in total volume was prepared with the following components: 2 µl of 10 X DreamTaq Buffer with 20 mM MgCl₂, 0.4 µl of 10 mM dNTPs (Thermo Scientific, USA), 0.4 µl each of 10 µM forward and reverse primers, 0.5 U DreamTaq DNA Polymerase, 25 ng of cDNA and ddH₂O. PCR was performed using the following PCR program on Veriti 96 well Thermal Cycler (Applied Biosystems, USA): initial denaturation at 95 °C for two minutes; followed by 35 cycles of denaturation at 95 °C for 30 seconds, annealing at 68 °C for 30 seconds, extension at 72 °C for 30 seconds; and final extension at 72 °C for two minutes. After PCR, 10 µl of each reaction mixture was mixed with 1 X loading dye and loaded onto 1.5% pre-stained agarose gel containing in 1 X TAE buffer. PCR mixture was electrophoresed on the gel together with GeneRuler 100 bp DNA Ladder (Thermo Scientific, USA) at 60 Volts, 400 mA for one hour. The gel was visualised and image was using Advance Gel Imaging System (UVP, USA).

3.5.1.6 *GABRB*

PCR was performed using DreamTaq DNA Polymerase (Thermo Scientific, USA). Highly purified salt-free primers for *GABRB* (IDT, Singapore): forward primer, 5' CCTTGCCCAAATCCCCTATGTCAAAGC 3'; reverse primer, 5' GTATCGCCAATGCCGCCTGAGACCTC 3' (Takahashi et al., 2007) were used to amplify a 277 bp PCR product. A reaction with 20 µl in total volume was prepared with the following components: 2 µl of 10 X DreamTaq Buffer with 20 mM MgCl₂, 0.4 µl of 10 mM dNTPs (Thermo Scientific, USA), 0.3 µl each of 10 µM forward and reverse primers, 0.5 U DreamTaq DNA Polymerase, 25 ng of cDNA and ddH₂O. PCR was performed using the following PCR program on Veriti 96 well Thermal Cycler (Applied Biosystems, USA): initial denaturation at 95 °C for two minutes; followed by 35 cycles of denaturation at 95 °C for 30 seconds, annealing at 59 °C for 30 seconds, extension at 72 °C for 30 seconds; and final extension at 72 °C for two minutes. After PCR, 10 µl of each reaction mixture was mixed with 1 X loading dye and loaded onto 1.5% pre-stained agarose gel containing in 1 X TAE buffer. PCR mixture was electrophoresed on the gel together with GeneRuler 100 bp DNA Ladder (Thermo Scientific, USA) at 60 Volts, 400 mAmp for one hour. The gel was visualised and image was captured using Advance Gel Imaging System (UVP, USA).

3.5.1.7 *LEFTY*

PCR was performed using DreamTaq DNA Polymerase (Thermo Scientific, USA). Highly purified salt-free primers for *LEFTY* (IDT, Singapore): forward primer, 5' CTTGGGGACTATGGAGCTCAGGGCGAC 3'; reverse primer, 5' CATGGGCAGCGAGTCAGTCTCCGAGG 3' (Takahashi et al., 2007) were used to amplify a 255 bp PCR product. A reaction with 20 µl in total volume was prepared with the following components: 2 µl of 10 X DreamTaq Buffer with 20 mM MgCl₂, 0.4 µl of 10 mM dNTPs (Thermo Scientific, USA), 0.3 µl each of 10 µM forward and reverse primers, 0.5 U DreamTaq DNA Polymerase, 25 ng of cDNA and ddH₂O. PCR was performed using the following PCR program on Veriti 96 well Thermal Cycler (Applied Biosystems, USA): initial denaturation at 95 °C for two minutes; followed by 35 cycles of denaturation at 95 °C for 30 seconds, annealing at 67 °C for 30 seconds, extension at 72 °C for 30 seconds; and final extension at 72 °C for two minutes. After PCR, 10 µl of each reaction mixture was mixed with 1 X loading dye and loaded onto 1.5% pre-stained agarose gel containing in 1 X TAE buffer. PCR mixture was electrophoresed on the gel together with GeneRuler 100 bp DNA Ladder (Thermo Scientific, USA) at 60 Volts, 400 mA for one hour. The gel was visualised and image was captured using Advance Gel Imaging System (UVP, USA).

3.5.1.8 *DNMT3B*

PCR was performed using DreamTaq DNA Polymerase (Thermo Scientific, USA). Highly purified salt-free primers for *DNMT3B* (IDT, Singapore): forward primer, 5' TGCTGCTCACAGGGCCCGATACTTC 3'; reverse primer, 5' TCCTTTCGAGCTCAGTGCACCACAAAAC 3' (Takahashi et al., 2007) were used to amplify a 242 bp PCR product. A reaction with 20 µl in total volume was prepared with the following components: 2 µl of 10 X DreamTaq Buffer with 20 mM MgCl₂, 0.4 µl of 10 mM dNTPs (Thermo Scientific, USA), 0.6 µl each of 10 µM forward and reverse primers, 0.5 U DreamTaq DNA Polymerase, 25 ng of cDNA and ddH₂O. PCR was performed using the following PCR program on Veriti 96 well Thermal Cycler (Applied Biosystems, USA): initial denaturation at 95 °C for two minutes; followed by 35 cycles of denaturation at 95 °C for 30 seconds, annealing at 63 °C for 30 seconds, extension at 72 °C for 30 seconds; and final extension at 72 °C for two minutes. After PCR, 10 µl of each reaction mixture was mixed with 1 X loading dye and loaded onto 1.5% pre-stained agarose gel containing in 1 X TAE buffer. PCR mixture was electrophoresed on the gel together with GeneRuler 100 bp DNA Ladder (Thermo Scientific, USA) at 60 Volts, 400 mAmp for one hour. The gel was visualised and image was captured using Advance Gel Imaging System (UVP, USA).

3.5.1.9 *ESGI*

PCR was performed using DreamTaq DNA Polymerase (Thermo Scientific, USA). Highly purified salt-free primers for *ESGI* (IDT, Singapore): forward primer, 5' ATATCCCGCCGTGGGTGAAAGTTC3'; reverse primer, 5' ACTCAGCCATGGACTGGAGCATCC 3' (Takahashi et al., 2007) were used to amplify a 243 bp PCR product. A reaction with 20 µl in total volume was prepared with the following components: 2 µl of 10 X DreamTaq Buffer with 20 mM MgCl₂, 0.4 µl of 10 mM dNTPs (Thermo Scientific, USA), 0.6 µl each of 10 µM forward and reverse primers, 0.5 U DreamTaq DNA Polymerase, 25 ng of cDNA and ddH₂O. PCR was performed using the following PCR program on Veriti 96 well Thermal Cycler (Applied Biosystems, USA): initial denaturation at 95 °C for two minutes; followed by 35 cycles of denaturation at 95 °C for 30 seconds, annealing at 63 °C for 30 seconds, extension at 72 °C for 30 seconds; and final extension at 72 °C for two minutes. After PCR, 10 µl of each reaction mixture was mixed with 1 X loading dye and loaded onto 1.5% pre-stained agarose gel containing in 1 X TAE buffer. PCR mixture was electrophoresed on the gel together with GeneRuler 100 bp DNA Ladder (Thermo Scientific, USA) at 60 Volts, 400 mA for one hour. The gel was visualised and image was captured using Advance Gel Imaging System (UVP, USA).

3.5.2 Detection of Pluripotency Markers Using Immunofluorescence Staining

AML-M5-derived iPSCs were maintained on feeder-coated 24-well plate (TPP, USA) and hESCs (BGOIV) were maintained in Geltrex-coated Nunc™ Lab-Tek™ II Chamber Slide™ System (Thermo Scientific, USA). Cell colonies were subjected to immunofluorescence staining before the colonies begin to touch. Fluorochrome-conjugated mouse anti-human antibodies were used such as, FITC-TRA-1-81, FITC-SSEA4, FITC-NANOG, PE-SOX2 and PE-OCT3/4 (all the antibodies were purchased from BD Pharmingen, USA). Prior to fix the cells using 2% paraformaldehyde (PFA) at room temperature for 30 minutes, the cells were washed twice with 1% BSA in PBS (washing buffer). After that, the cells were washed and permeabilised with 1 X Perm/Wash Solution (BD Pharmingen, USA) at room temperature for 45 minutes. Subsequently, antibodies at 1: 50 dilution were added and incubated overnight at 4 °C. On the next day, the cells were washed for two to three times with 1 X Perm/Wash solution before staining with DAPI at room temperature for 30 minutes. Then, the cells were washed and one or two drops of Dako Fluorescence Mounting Medium (Dako, Denmark) were added prior to microscopic analysis. Phase contrast and fluorescent images were capture using Axio Observer A1 with ZEN 2011 lite software fitted with Argon laser and filter sets BP 450/490 and BP 546/12 (Carl Zeiss, USA). All steps described above were performed in the dark or without direct light exposure.

3.5.3 Detection of Pluripotency Markers Using Flow Cytometry

Surface and intracellular marker monoclonal antibodies used were listed in Table 3.2. All antibodies were purchased from BD Pharmingen (USA) except for purified SOX2 (Cell Signaling, USA) and PE-Cy7 against SOX2 (Santa Cruz, USA).

Table 3.2: Monoclonal antibodies used for intracellular and surface staining.

	Markers	Antibodies Used	
		Primary Antibodies	Secondary Antibodies
Intracellular	OCT3/4	Mouse anti-human OCT3/4 PerCP-Cy TM 5.5	-
	SOX2	Mouse anti-human SOX2	Goat anti-mouse PE-Cy TM 7
	NANOG	Rat anti-human NANOG	Goat anti-rat APC-Cy TM 7
Surface	TRA-1-81	Mouse anti-human TRA-1-81 APC	-
	SSEA4	Mouse anti-human SSEA4 PE	-

Notes: PE, Phycoerythrin; FITC, Fluoresceine isothiocyanate; APC, Allophycocyanin; PE-CyTM7, Phycoerythrin- CyTM7; APC-CyTM7, Allophycocyanin- CyTM7; PerCP-CyTM5.5, Peridinin chlorophyll protein- CyTM5.5.

Two 5 ml Falcon tubes (BD Bioscience, USA) were prepared, one for antibodies stained tube and another for negative control. In brief, cells were harvested and resuspended at concentration of 1×10^6 cells/ml in each 5 ml Falcon tube. Cells were incubated with surface antibodies at room temperature for 30 minutes. The cells were then washed with 0.2% BSA in PBS (wash buffer) and followed by fixation using 2% PFA in PBS at room temperature for 30 minutes. Next, cells were washed for three times before permeabilisation with 1 X Perm/Wash Solution at room temperature for 45 minutes.

Subsequently, intracellular antibodies were added into the cells and incubated at room temperature for 30 minutes. Cells were washed and followed by incubation of secondary fluorochrome-conjugated antibodies at room temperature for another 20 minutes. The cells were washed, and resuspended in 800 µl of wash buffer prior to analysis using FACS Canto II flow cytometry with BDFACS DIVA software (BD Bioscience, USA). FACS Canto II flow cytometry is equipped with blue laser (488nm, 20mW solid state) and red laser (633nm, 17mW HeNe) and four multipliers with bandpass filter of 530 nm (FITC), 578 nm (PE), 660 nm (APC), 695 nm (PerCP-CyTM5.5), 785 nm (PE-CyTM7) and 785 nm (APC-CyTM7). A total of 10000 cells were included during data acquisition and analysis. The experiment was repeated with three biological samples. Staining procedures listed above were carried out in dark.

3.5.4 *In Vitro* Three Germ Layers Differentiation

Functional property of stem cells was validated using three germ layers differentiation (for example, mesoderm, ectoderm and endoderm). In this study, directed-differentiation was used.

3.5.4.1 Mesoderm Lineage

In order to determine the ability of AML-M5-derived iPSCs to differentiate into mesoderm lineage, adipogenesis and osteogenesis differentiation assays were performed. hESC and hAd-MSc were used as control for these assay. For adipogenesis differentiation, cells were grown on

matrix-coated 24-well plate until 50% confluent before being cultured on adipogenesis differentiation medium consisting complete DMEM/F12 medium (Gibco Invitrogen, USA) supplemented with 10% fetal bovine serum (Gibco Invitrogen, USA), 50 U/ml penicillin and 50 mg/ml streptomycin (Gibco Invitrogen, USA), 1 mM Glutamax (Gibco Invitrogen, USA), 0.25 mM methylisobutylxanthine (Sigma, USA), 1 μ M dexamethason (Sigma, USA) and 100 μ M indomethacine (Sigma, USA) for three weeks. Medium was replaced every two days. To determine the presence of lipid deposit in adipogenic differentiated cells, Oil Red O staining method was used (Qian et al., 2010). In brief, cells were fixed in 10% formalin at room temperature for 30 minutes. Then, cells were washed once and stained with 60% triethyl phosphate aqueous solution (Nacalai Tesque, Japan). Subsequently, the cells were stained with Oil Red O at room temperature for 15 minutes and followed by washing step with water. After that, the cells were ready for microscopic analysis and phase contrast images were captured using Eclipse Ts 100 with NIS-Elements D software (Nikon, Japan). Lipid droplets were expected to be stained by Oil Red O staining in red colour.

For osteogenesis differentiation, cells were grown on matrix-coated 24-well plate until 50% confluent before being cultured on osteogenesis differentiation medium consisting complete DMEM/F12 medium supplemented with 10% fetal bovine serum, 50 U/ml penicillin and 50 mg/ml streptomycin, 1 mM Glutamax, 50 μ g/ml ascorbate-2-phosphate (Sigma, USA), 10 mM β -glycerophosphate (Sigma, USA) and 100 nM dexamethasone (Sigma, USA) for three weeks. Medium was replaced every two days. To detect the

presence of free calcium compounds in the osteogenic differentiated cells, Alizarin Red staining was carried out (Sidney et al., 2014). Briefly, the cells were fixed in ice cold 70% ethanol at room temperature for one hour. Then, the cells were washed twice with water before staining with Alizarin Red at room temperature for 30 minutes and followed by repeated washing step with water. Finally, water was added into cells to prevent drying and cells were ready for analysis. Phase contrast images were captured using Eclipse Ts 100 with NIS-Elements D software (Nikon, Japan). Calcium deposition was stained red by Alizarin Red.

3.5.4.2 Endoderm Lineage

To determine the capability of AML-M5-derived iPSCs to differentiate into endoderm lineage, endoderm differentiation assay was carried out. hESC was used a positive control. Both the iPSCs and hESCs were grown to form embryoid bodies (EBs) in suspension condition in complete DMEM/F12 medium (Gibco Invitrogen, USA) for five days. The EBs were then transferred into gelatine-coated chamber slide for five days and were culture in complete DMEM/F12 medium (Gibco Invitrogen, USA) supplemented with 10% fetal bovine serum (Gibco Invitrogen, USA) and 50 ng/ml of Activin A (Merck Milipore, USA). The medium was changed every two days. At day five, the cells were ready for immunofluorescence staining to detect the expression of definitive endoderm marker, SOX17. Purified polyclonal goat anti-human SOX17 (R&D Systems, USA) and TRITC-conjugated monoclonal donkey anti-goat (Santa Cruz, USA) were used and the cells were counterstained with

DAPI. Immunofluorescence staining protocol was highlighted in Section 3.5.2. Phase contrast and fluorescent images were capture using Axio Observer A1 with ZEN 2011 lite software fitted with Argon laser and filter set BP 546/12 (Carl Zeiss, USA).

3.5.4.3 Ectoderm Lineage

To determine the capability of AML-M5-derived iPSCs to differentiate into ectoderm lineage, ectoderm differentiation assay was performed. hESC was used as positive control. The cells were grown to form embryoid bodies (EBs) in suspension condition in complete DMEM/F12 medium (Gibco Invitrogen, USA) for five days. The EBs were then transferred into gelatine-coated chamber slide and cultured in complete DMEM/F12 medium (Gibco Invitrogen, USA) supplemented with 10% fetal bovine serum and 100 ng/ml of Noggin (Sigma, USA). The medium was changed every two days. At day five, the cells were ready for immunofluorescence staining to detect the expression of ectoderm specific marker, MAP2. Purified monoclonal mouse anti-human antibodies against MAP2 (Merck Milipore, USA) and FITC-conjugated monoclonal goat anti-mouse (BD Pharmingen, USA) were used. Immunofluorescence staining protocol was highlighted in Section 3.5.2. Phase contrast and fluorescent images were capture using Axio Observer A1 with ZEN 2011 lite software fitted with Argon laser and filter set BP 450/490 (Carl Zeiss, USA).

3.6 Verification of AML-M5-derived iPSCs

3.6.1 Detection of Monocyte-specific Markers Using Flow Cytometry

Surface markers monoclonal antibodies used were listed as follow: PE-conjugated monoclonal antibodies CD11c (BD Pharmingen, USA), purified monoclonal antibodies CD15s (BD Pharmingen, USA), and FITC-conjugated monoclonal antibodies against purified CD15s (BD Pharmingen, USA). Two Falcon tubes were prepared, one for antibodies staining and another for negative control. Briefly, AML-M5-derived iPSCs were harvested and resuspended at concentration of 1×10^6 cells/ml in 5 ml Falcon tube (BD Bioscience, USA). Cells were incubated with surface antibodies at room temperature for 30 minutes. The cells were washed with wash buffer and followed by secondary fluorochrome-conjugated monoclonal antibodies incubation at room temperature for another 20 minutes. The cells were fixed with 2% PFA in BSA and resuspended in 800 μ l of wash buffer prior to analysis using FACS Canto II flow cytometry with BDFACS DIVA software (BD Bioscience, USA). FACS Canto II flow cytometry was equipped with blue laser (488nm, 20mW solid state) and red laser (633nm, 17mW HeNe) and four multipliers with bandpass filter of 530 nm (FITC), 578 nm (PE), 660 nm (APC), 695 nm (PerCP-CyTM5.5), 785 nm (PE-CyTM7) and 785 nm (APC-CyTM7). A total of 10000 cells were included during data acquisition and analysis. The experiment was repeated with three biological samples. Staining procedures listed above were carried out in dark.

3.6.2 Detection of Leukaemia-associated MLL-AF9 Fusion Gene Using Reverse Transcription- Polymerase Chain Reaction (RT-PCR)

RNA was extracted from all AML-M5-derived iPSCs using TRIzol (Invitrogen Cooperation, USA) and the extraction protocol was highlighted in Section 3.5.1.1. Subsequently, RNA was converted to cDNA using RevertAid Reverse Transcriptase (Thermo Scientific, USA) according to the protocol highlighted in Section 3.5.1.2. PCR was performed using DreamTaq DNA Polymerase (Thermo Scientific, USA). Detection of leukaemia-associated *MLL-AF9* fusion gene was carried out using the following primer set (IDT, Singapore): forward primer, 5' GAATCAGGTCCAGAGCAGAG 3'; reverse primer, 5' CCTCAAAGGACCTTGTTGCC 3' (Pession et al., 2003) and a 177 bp PCR product was expected. A reaction with 20 µl in total volume was prepared with the following components: 2 µl of 10 X DreamTaq Buffer with 20 mM MgCl₂, 0.4 µl of 10 mM dNTPs (Thermo Scientific, USA), 0.6 µl each of 10 µM forward and reverse primers, 0.5 U DreamTaq DNA Polymerase, 25 ng of cDNA and ddH₂O. PCR was performed using the following PCR program on Veriti 96 well Thermal Cycler (Applied Biosystems, USA): initial denaturation at 95 °C for two minutes; followed by 35 cycles of denaturation at 95 °C for 30 seconds, annealing at 58 °C for 30 seconds, extension at 72 °C for 30 seconds; and final extension at 72 °C for two minutes. After PCR, 10 µl of each reaction mixture was mixed with 1 X loading dye and loaded onto 1.5% pre-stained agarose gel containing in 1 X TAE buffer. PCR mixture was electrophoresed on the gel together with GeneRuler 100 bp DNA Ladder (Thermo Scientific, USA) at 60 Volts, 400 mAmp for one hour. The gel was

visualised and image was captured using Advance Gel Imaging System (UVP, USA).

3.7 Data Analysis

All the numerical data were tested for statistical significance using Statistical package for Social Sciences (SPSS) version 17. The data were presented as mean \pm standard error of mean for triplicate experimental results. Values were analysed using independent T-test and Mann-Whitney U test. Statistical significance was set at $p < 0.05$.

CHAPTER 4

RESULTS

4.1 Verification of Recombinant Plasmids Using Restriction Enzymes

Identity of recombinant plasmids was verified using restriction enzyme digestion. All the digested recombinant plasmids have expected products sizes as shown in Table 3.1. A faint band was observed in pMXs-hOCT3/4, probably due to insufficient digestion duration of restriction enzyme.

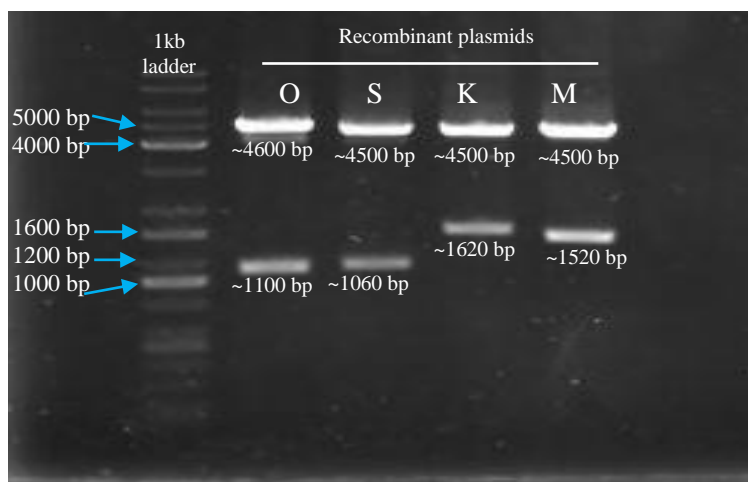


Figure 4.1: Verification of recombinant plasmids using restriction enzyme digestion. Gel image showed the restriction enzyme digestion result of recombinant plasmids pMXs-hOCT3/4 (O), pMXs-hSOX2 (S), pMXs-hKLF4 (K) and pMXs-hc-MYC (M). The 1 kb DNA ladder was used to determine the size of digested products.

4.2 Optimisation of Transfection and Infection Protocols

A control vector encoding green fluorescent protein (GFP) was used to optimise transfection and infection protocols. Efficiency of transfection and infection was estimated by counting percentage of cells with pseudo-green signal using naked eye. Transfection optimisation was carried out by using different Phoenix cells confluency (50-60% and 70-80% confluency), amount of plasmid (3.3 and 6.6 μg) and time to harvest supernatant carrying retroviruses (24, 48 and 72 hours). Phoenix cells are packaging cell line that stably produces gag-pol and envelope protein which are important for production of amphotropic helper-free viruses (Cornetta et al., 2005). Transfection was done using calcium phosphate method (Swift et al., 1999). Infection optimisation was carried out by using 2 ml of supernatant carrying retroviruses to infect 1×10^5 AML-M5 cell line using spinfection method (Berggren et al., 2012).

In Figure 4.2, Phoenix cells at 50-60% cell confluency that were transfected with 3.3 μg pMX-GFP showed approximately 30% efficiency at 24 hours post-transfection, and increased to 40% and 50% at 48 hours and 72 hours post-transfection, respectively. Transfection with 6.6 μg pMX-GFP showed approximately 40% efficiency at 24 hours post-transfection, and increased to 50% and 60% at 48 hours and 72 hours post-transfection, respectively. The virus supernatants at 72 hours post-transfection were collected and used to infect AML-M5 cells. As shown in Figure 4.3, AML-M5 cell line was infected with virus particles produced from 3.3 μg and 6.6 μg

pMX-GFP. Pseudo-green signal were observed at 48 hours post-infection had approximately 10% of infection efficiency. The percentage of cells with pseudo-green signal did not increase but remained at about 10% at 72 hours post-infection, probably due to loss of GFP expression during cell division.

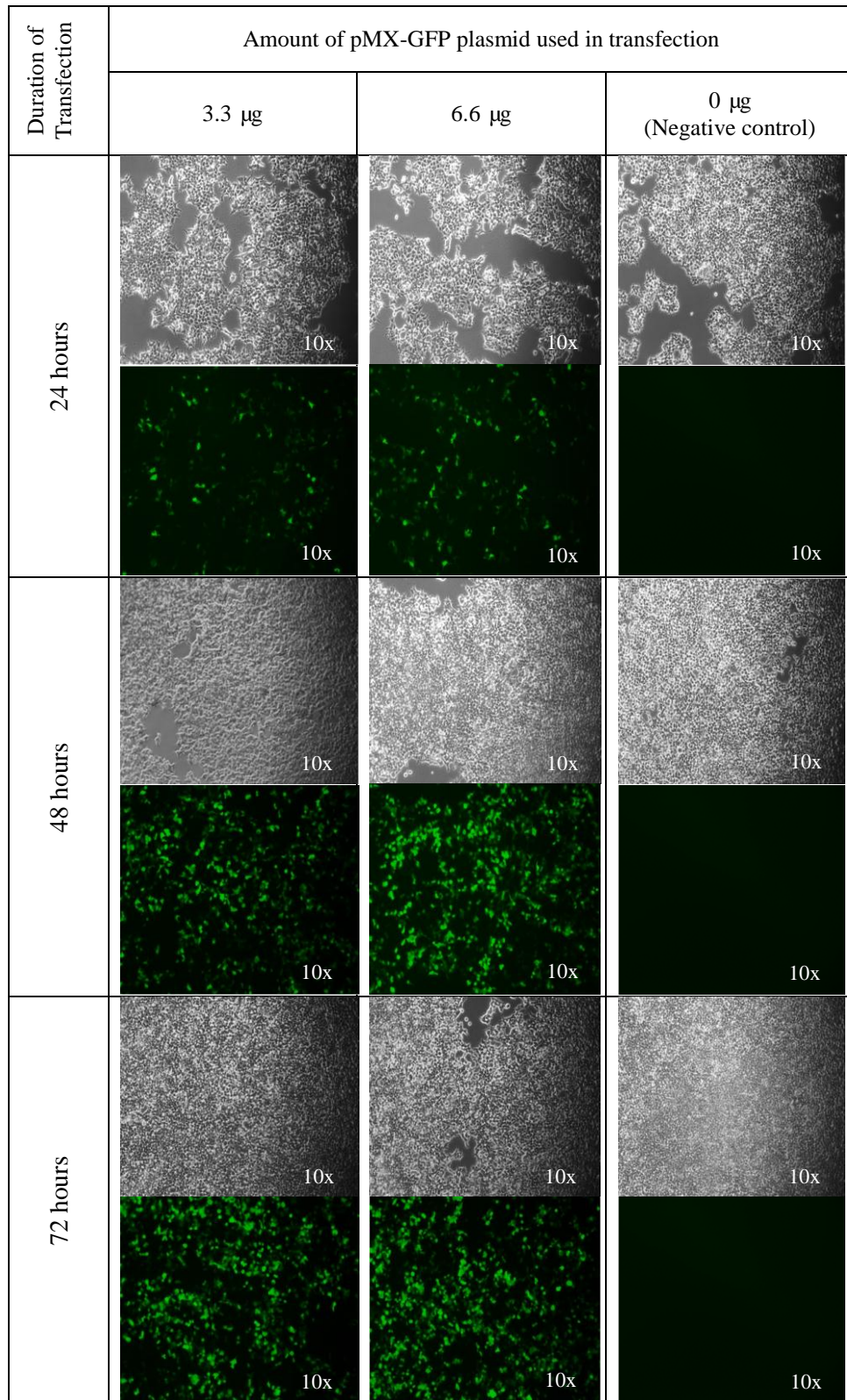


Figure 4.2: Transfection of Phoenix cells with different concentration of pMX-GFP at 50-60% cell confluency. Phase contrast and fluorescent images were captured from transfected Phoenix cells at 24, 48 and 72 hours post-transfection. Pseudo-green indicates GFP-transfected Phoenix cells. For Phoenix cells transfected with 3.3 μ g of pMX-GFP, about 30% of cells with pseudo-green signal were observed at 24 hours post-transfection and reached 50% at 72 hours post-transfection. For Phoenix cells transfected with 6.6 μ g of pMX-GFP, about 40% of cells with pseudo-green signal were observed at 24 hours post-transfection and reached 60% at 72 hours post-transfection. Supernatant carrying retroviruses were collected at 72 hours post-transfection and used for AML-M5 cell line infection.

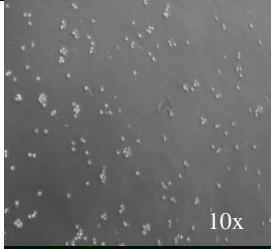
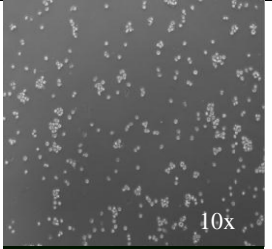
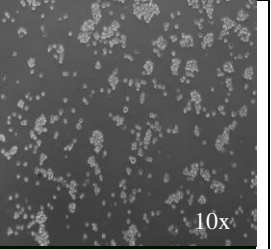
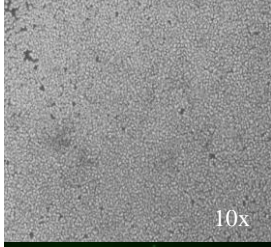
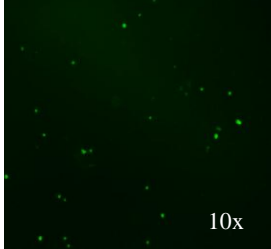
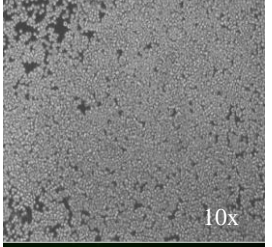
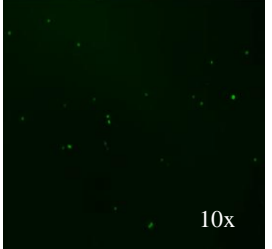
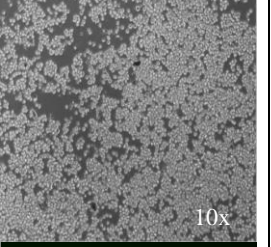
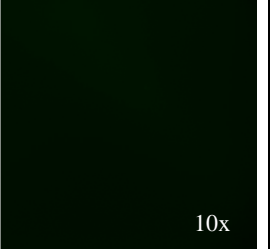
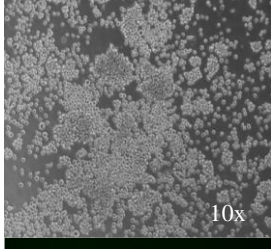
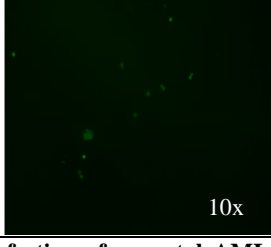
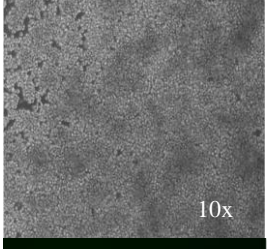
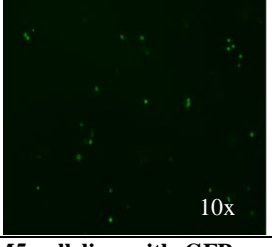
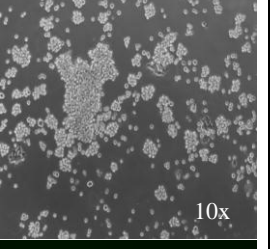
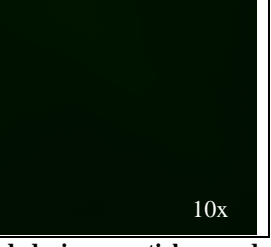
Duration of Transfection	Origin of recombinant retrovirus supernatants used in spinfection method		
	From '3.3 µg of pMX-GFP'	From '6.6 µg of pMX-GFP'	From '0 µg of pMX-GFP'
24 hours	 	 	 
48 hours	 	 	 
72 hours	 	 	 

Figure 4.3: Infection of parental AML-M5 cell line with GFP encoded virus particles produced from 50-60% confluency of Phoenix cells. Phase contrast and fluorescent images were captured from infected AML-M5 cell line at 24, 48, and 72 hours post-infection. Pseudo-green indicates GFP-infected AML-M5 cells. At 48 hours post-infection, approximately 10% of parental AML-M5 cell line infected with virus particles produced from 3.3 µg and 6.6 µg of pMX-GFP exhibited pseudo-green signal. The number of infected AML-M5 cell line with pseudo-green remained the same at 72 hours post-infection.

In Figure 4.4, Phoenix cells at 70-80% cell confluency that were transfected with 3.3 μg pMX-GFP showed approximately 30% efficiency at 24 hours post-transfection, and increased to 50% and 70% at 48 hours and 72 hours post-transfection, respectively. Transfection with 6.6 μg pMX-GFP showed approximately 40% efficiency at 24 hours post-transfection, and increased to 70% and 90% at 48 hours and 72 hours post-transfection, respectively. Supernatant harbouring retroviruses were collected at 72 hours post-transfection and used to infect parental AML-M5 cells.

In Figure 4.5 showed parental AML-M5 cells infected with virus particles produced from 3.3 μg and 6.6 μg pMX-GFP. For parental AML-M5 cells infected with virus particles produced from 3.3 μg pMX-GFP, pseudo-green signal were observed at 48 hours post-infection with infection efficiency at about 10%. Infection efficiency was increased to 15% at 72 hours post-infection. Parental AML-M5 cells infected with virus particles produced from 6.6 μg pMX-GFP showed infection efficiency at 5% at 24 hour post-infection. The efficiency was increased to 10% and 15% at 48 hours and 72 hours post-infection, respectively. Given that pseudo-green signal was detected as early as 24 hours, therefore transfection carried out on 70-80% confluent Phoenix cells with 6.6 μg pMX-GFP was the optimal protocol to generate retrovirus particles.

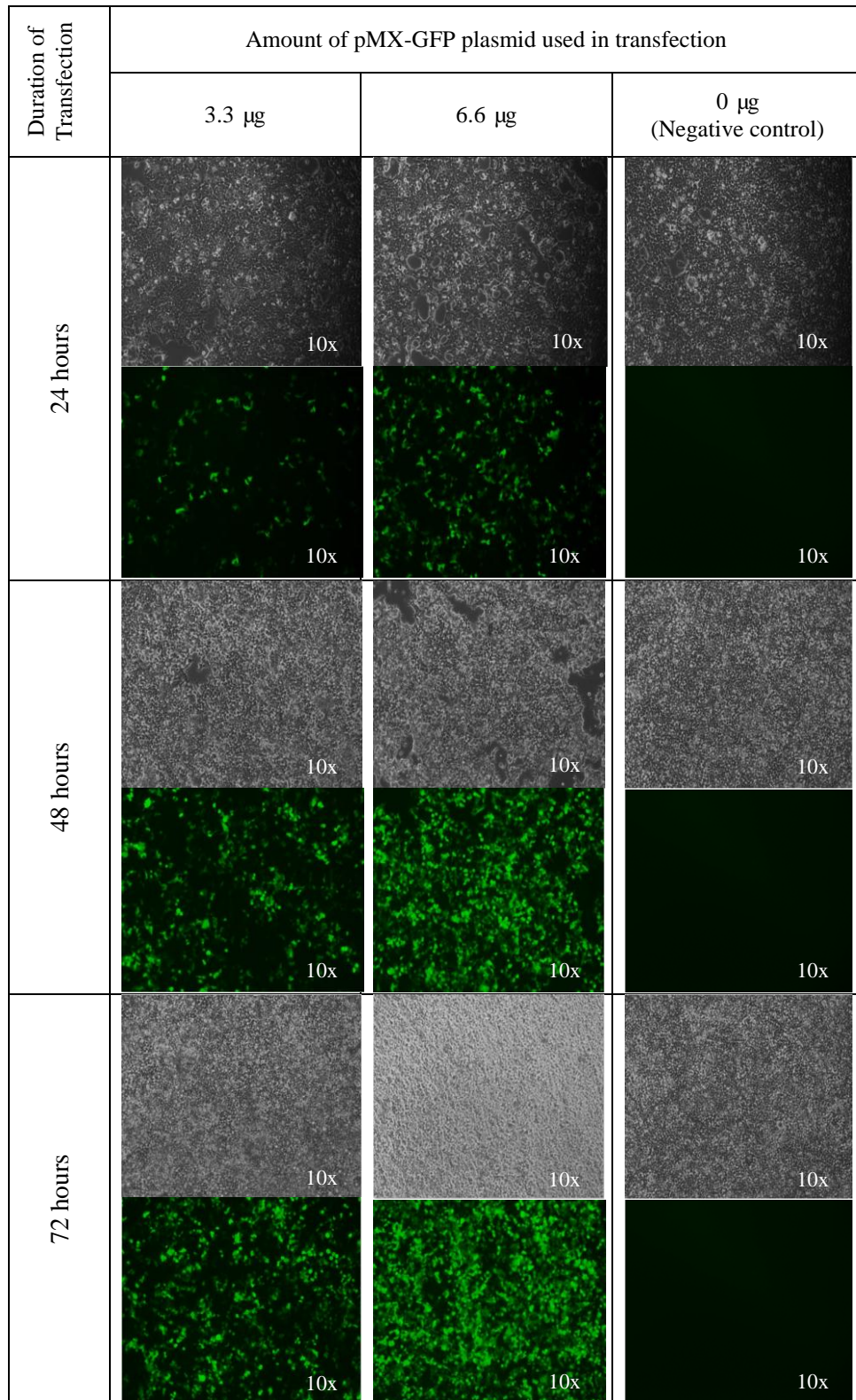


Figure 4.4: Transfection of Phoenix cells with different concentration of pMX-GFP at 70-80% cell confluency. Phase contrast and fluorescent images were captured from transfected Phoenix cells at 24, 48 and 72 hours post-transfection. Pseudo-green indicates GFP-transfected Phoenix cells. For Phoenix cells transfected with 3.3 μg of pMX-GFP, about 30% of cells with pseudo-green signal were observed at 24 hours post-transfection and reached 70% at 72 hours post-transfection. For Phoenix cells transfected with 6.6 μg of pMX-GFP, about 40% of cells with pseudo-green signal were observed at 24 hours post-transfection and reached 90% at 72 hours post-transfection. Supernatant carrying retroviruses were collected a 72 hours post-transfection and used for parental AML-M5 cells infection.

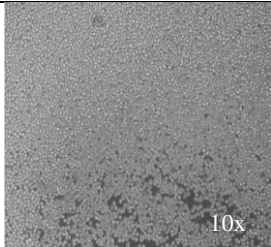
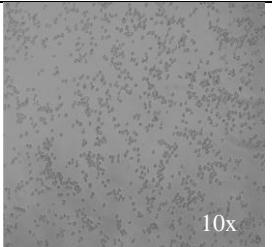
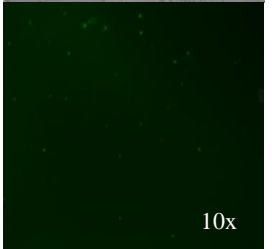
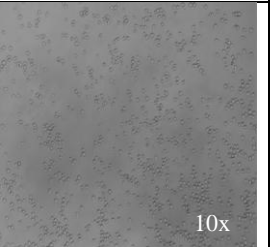
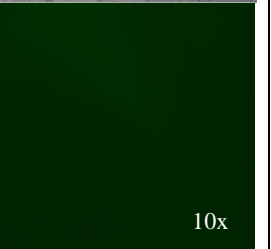
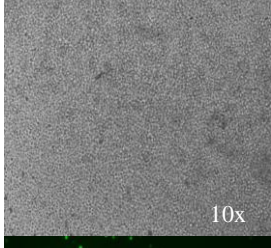
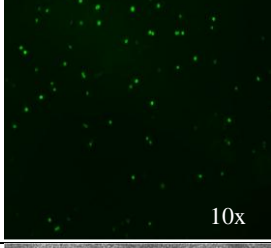
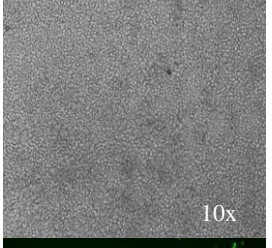
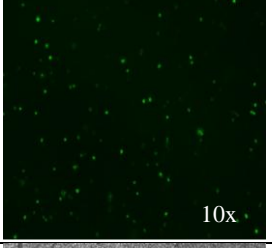
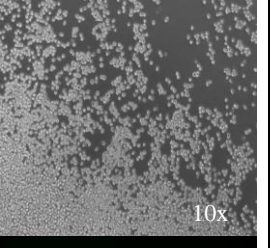
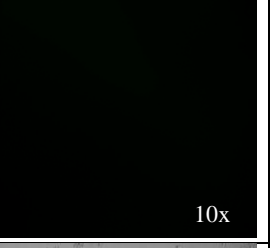
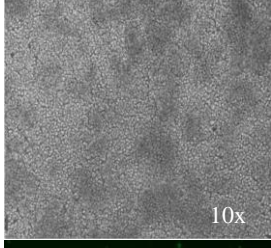
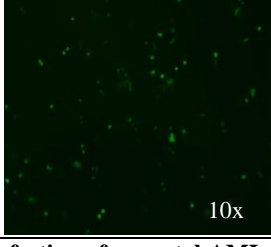
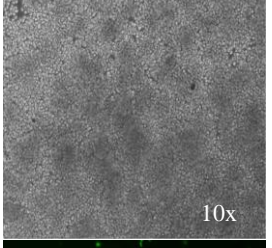
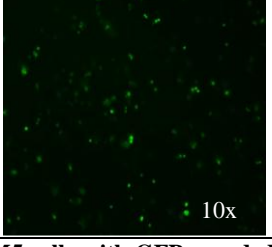
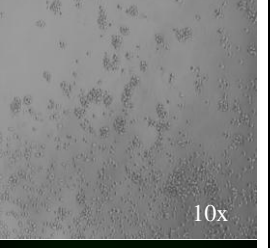
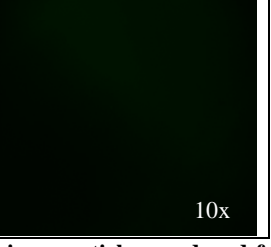
Duration of Transfection	Origin of recombinant retrovirus supernatants used in spinfection method		
	From '3.3 μ g of pMX-GFP'	From '6.6 μ g of pMX-GFP'	From '0 μ g of pMX-GFP''
24 hours	 	 	 
48 hours	 	 	 
72 hours	 	 	 

Figure 4.5: Infection of parental AML-M5 cells with GFP encoded virus particles produced from 70-80% confluency of Phoenix cells. Phase contrast and fluorescent images were capture from infected AML-M5 cell line at 24, 48, and 72 hours post-infection. Pseudo-green indicates GFP-infected AML-M5 cells. AML-M5 cells infected with retroviral produced from 3.3 μ g of pMX-GFP exhibited pseudo-green signal at 10% of efficiency at 48 hours post-infection. For AML-M5 cells infected retroviral produced from 6.6 μ g of pMX-GFP, pseudo-green signal was observed at 24 hours post-infection at 5% infection efficiency.

4.3 Generation of AML-M5-derived iPSCs Using Retrovirus Particles Harboured O, S, K and M

Optimal Phoenix cells transfection protocol carried out on 70-80% cell confluency using 6.6 μg of recombinant plasmids to produce retrovirus particles was repeated using recombinant plasmids O, S, K, M and GFP. In this study, GFP expression was used as a marker for expression of O, S, K and M. Transfection efficiency, was estimated using pseudo-green positive cells by naked eye. Figure 4.6 showed transfection efficiency at 90% after 72 hours of transfection, assuming that same transfection efficiency was achieved for other recombinant plasmids.

Parental AML-M5 cells were infected with pooled virus supernatant that containing O, S, K and M. GFP expression was also used as a marker for expression of O, S, K and M. Number of parental AML-M5 cells with pseudo-green signal (GFP) was used to estimate infection efficiency, as indicated in pseudo-green signal. Figure 4.7 showed approximately 20% of infection efficiency was achieved at 24 hours post-infection.

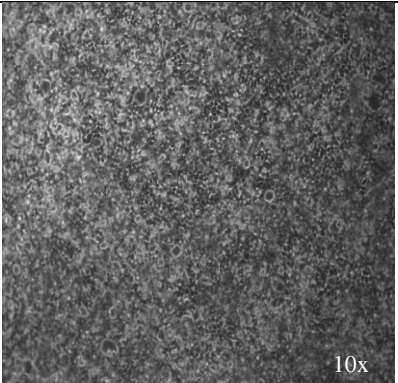
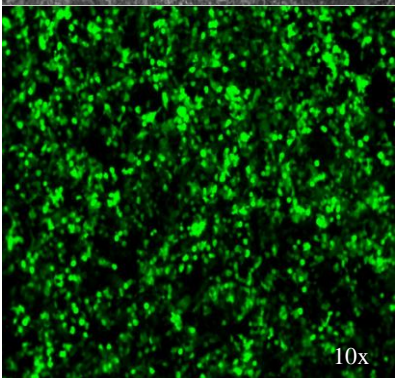
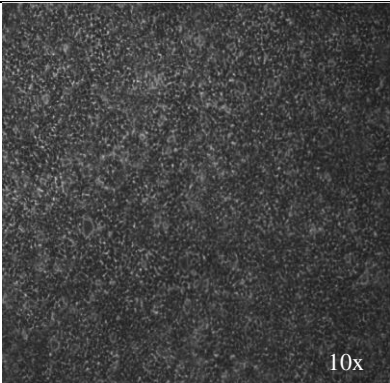
Duration of transfection	Amount of pMX-GFP used in transfection	
	6.6 μ g	Negative
72 hours	 	 

Figure 4.6: Optimal Phoenix cells transfection protocol. Phase contrast and fluorescent images were captured from GFP-transfected Phoenix cells at 72 hours post-infection. Pseudo-green signal was used as a marker for expression of O, S, K and M. Number of pseudo-green positive cells was used to measure transfection efficiency. Approximately 90% of transfection efficiency was observed.

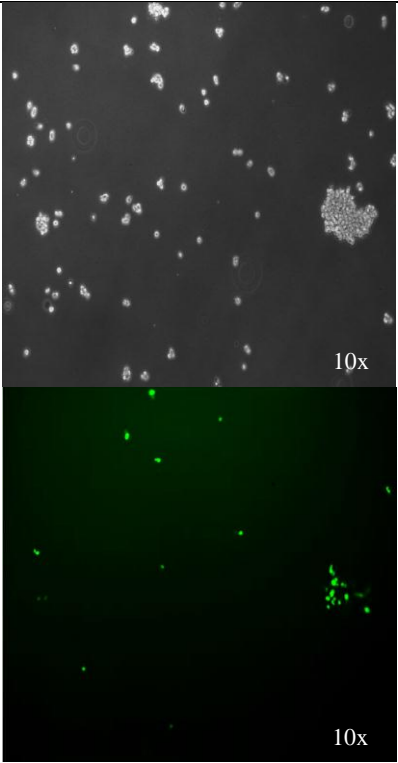
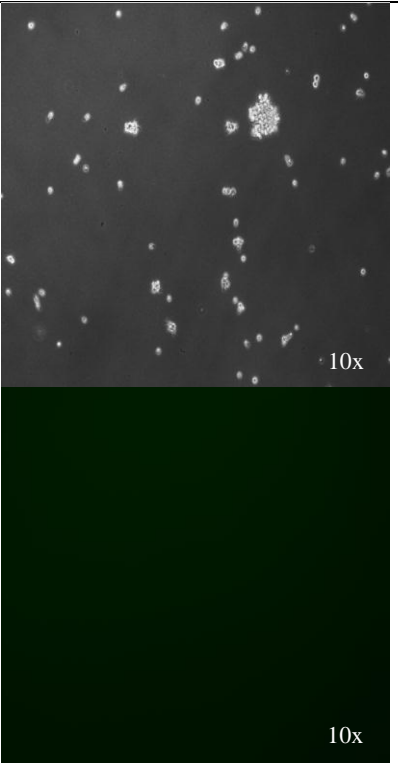
Duration of transfection	Origin of recombinant retroviruses supernatants used in spinfection method	
	From '6.6 µg of pMX-GFP'	From ' 0 µg of pMX-GFP'
24 hours		

Figure 4.7: Optimal parental AML-M5 cells infection protocol. Phase contrast and fluorescence images were captured from infected AML-M5 cells at 24 hours post-infection. Expression of pseudo-green signal was used to represent infection efficiency of O, S, K and M. Approximately 20% of infection efficiency was observed.

4.4 Formation and Maintenance of AML-M5-derived iPSCs

O, S, K, M- infected AML-M5 cells (THP-1 cell line) were maintained on feeder cells (hAd-MSC). Representative result for iPSC formation from infected AML-M5 cells was showed in Figure 4.8. As shown in Figure 4.8a, infected parental AML-M5 cells were cultured in suspension form. Small proportion of infected AML-M5 cells started to attach on feeder cells at Day 2 (Figure 4.8b). Consequently, more and more infected AML-M5 cells were attached. Floating cells were removed (Figure 4.8c). Small packed colonies which are morphologically different from feeder cells (fibroblast-shaped) as well as parental AML-M5 cells (suspension form) were observed from day 14 (refer to Figure 4.8d). iPSC-like colonies were picked from Day 16 to Day 25. iPSC-like colonies were disintegrated after Day 26. Figure 4.9 showed morphology of these iPSC-like colonies was similar to hESC, in which they were tightly packed with well-defined border, meager cytoplasm and large nucleus. The number of colonies was increased over the period of maintenance. This experiment was repeated three times. An average of 20 iPSC-like colonies was formed in individual reprogramming experiments and reprogramming efficiency at approximately 0.02% was achieved. All the iPSC-colonies were individually selected and expanded. Of the 60 colonies/clones isolated, five clones namely as A1, H1, ii-18, ii-19 and ii-22 were susccesfully isolated and selected for further characterisation assays.

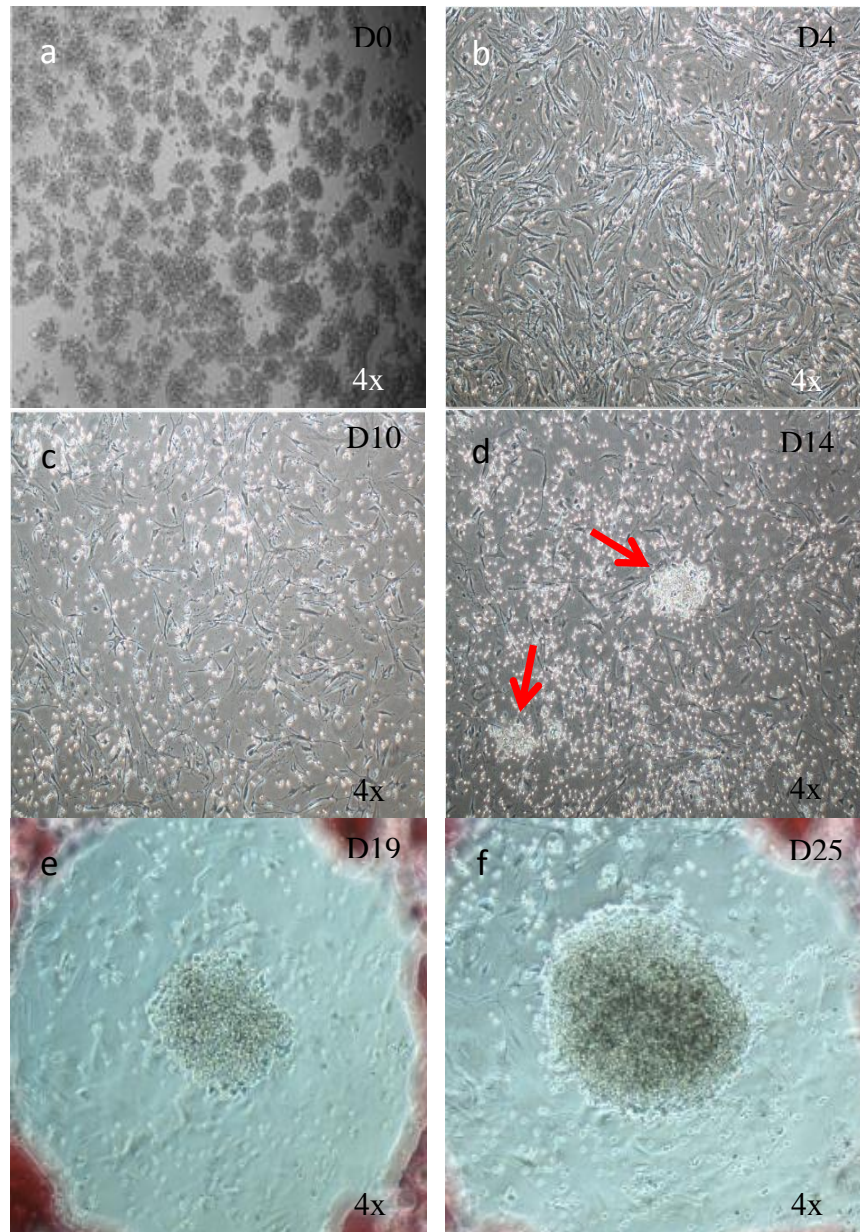


Figure 4.8: Formation of iPSC-like colonies from D0 to D25. Small packed colonies were appeared at Day 14. Size of iPSC-like colonies was getting bigger over the duration of maintenance on feeder cells. iPSC-like colonies were picked between Day 16 to Day 25. (a) Infected AML-M5 cells in suspension. Infected AML-M5 cells on feeder cells at (b) Day 4, (c) Day 10, (d) Day 14, arrows pointed to the distinctive colonies (e) Day 19 and (f) Day 25.

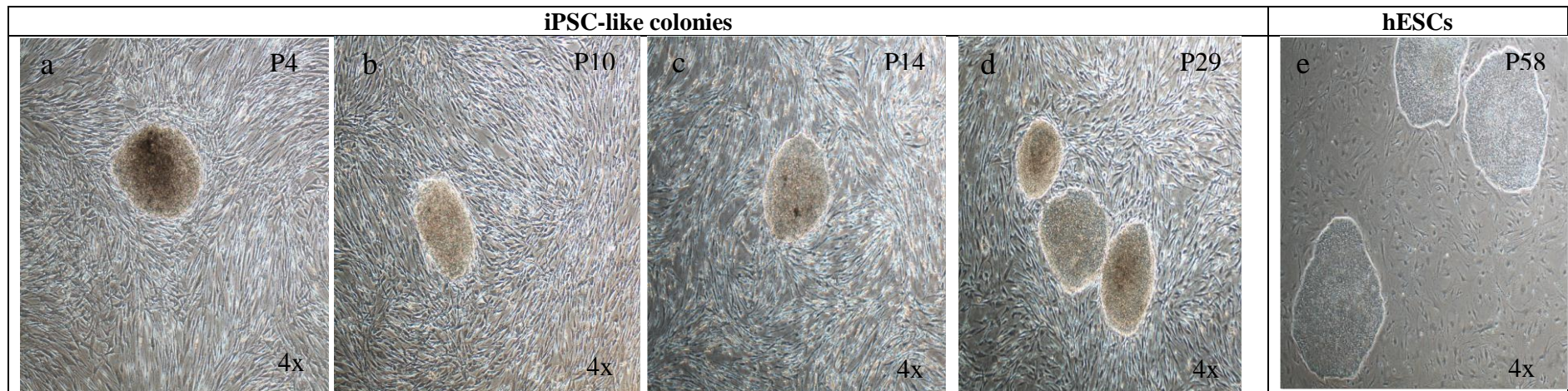


Figure 4.9: Appearance of iPSC-like colonies on feeder cells from Passage 4 to Passage 29. Phase contrast images of iPSC-like colonies were captured. Morphology of iPSC-like colonies were getting similar to hESCs after long term maintenance as they were tightly packed with well-defined border and high proportion of nucleus/cytoplasm. Appearance of iPSC-like colonies on feeder cells at (a) Passage 4, (b) Passage 10, (c) Passage 14 and (d) Passage 29. Appearance of hESCs on feeder cells at (e) Passage 58.

4.5 Pluripotency Characterisation of AML-M5-derived iPSCs

4.5.1 Gene Expression Study of Pluripotency Markers using RT-PCR Method

To characterise pluripotency of the selected iPSC-like clones, gene expression of pluripotency markers was carried on all AML-M5-derived iPSCs clones using RT-PCR. Human ESC (BGOIV) was used as positive control while parental AML-M5 cells (THP-1 cell line) as negative control. Feeder cells (hAd-MSC) were included to rule out the possibility of contamination in PCR. A total of six pluripotency markers were screened in this assay, including *OCT3/4*, *SOX2*, *GABRB*, *LEFTY*, *ESG1* and *DNMT3B*. *GAPDH* was used as housekeeping gene. Table 4.1 shows summary of gene expression of all tested pluripotency markers. Briefly, gene expression of pluripotency markers *GABRB*, *OCT3/4*, *LEFTY* and *SOX2* was detected in all AML-M5-derived iPSC clones, but expression of *DNMT3B* and *ESG1* was not detectable. Feeder cells were found to be expressed *GABRB*, *OCT3/4* and *SOX2*, perhaps due to their stem cell properties. Gene expression of *OCT3/4*, *LEFTY* and *SOX2* was also found in parental AML-M5 cells, probably due the role of these pluripotency markers in tumorigenesis. Gene expression study showed that all AML-M5-derived iPSC clones expressed an additional pluripotency marker *GABRB* compared to parental AML-M5 cells after reprogramming process. Representative gel images of positive result (*GABRB*, *OCT3/4*, *SOX2* and *LEFTY*) were showed in Figure 4.10.

Table 4.1 Comparison of gene expression of pluripotency markers in hESCs, AML-M5-iPSCs, feeder cells and parental AML-M5 cell line.

Cell type Pluripotency markers (amplicon size)	hESCs (BGOIV)	AML-M5-derived iPSC clones					Feeder cells (hAd- MSC)	Parental AML-M5 cells
		A1	H1	ii18	ii19	ii22		
<i>GABRB</i> (277 bp)	√	√	√	√	√	√	√	X
<i>OCT3/4</i> (144 bp)	√	√	√	√	√	√	√	√
<i>LEFTY</i> (255 bp)	√	√	√	√	√	√	X	√
<i>SOX2</i> (151 bp)	√	√	√	√	√	√	√	√
<i>DNMT3B</i> (242 bp)	√	X	X	X	X	X	X	X
<i>ESG1</i> (243 bp)	√	X	X	X	X	X	X	X

Note that √ indicates gene was detected, X indicates gene not detected.

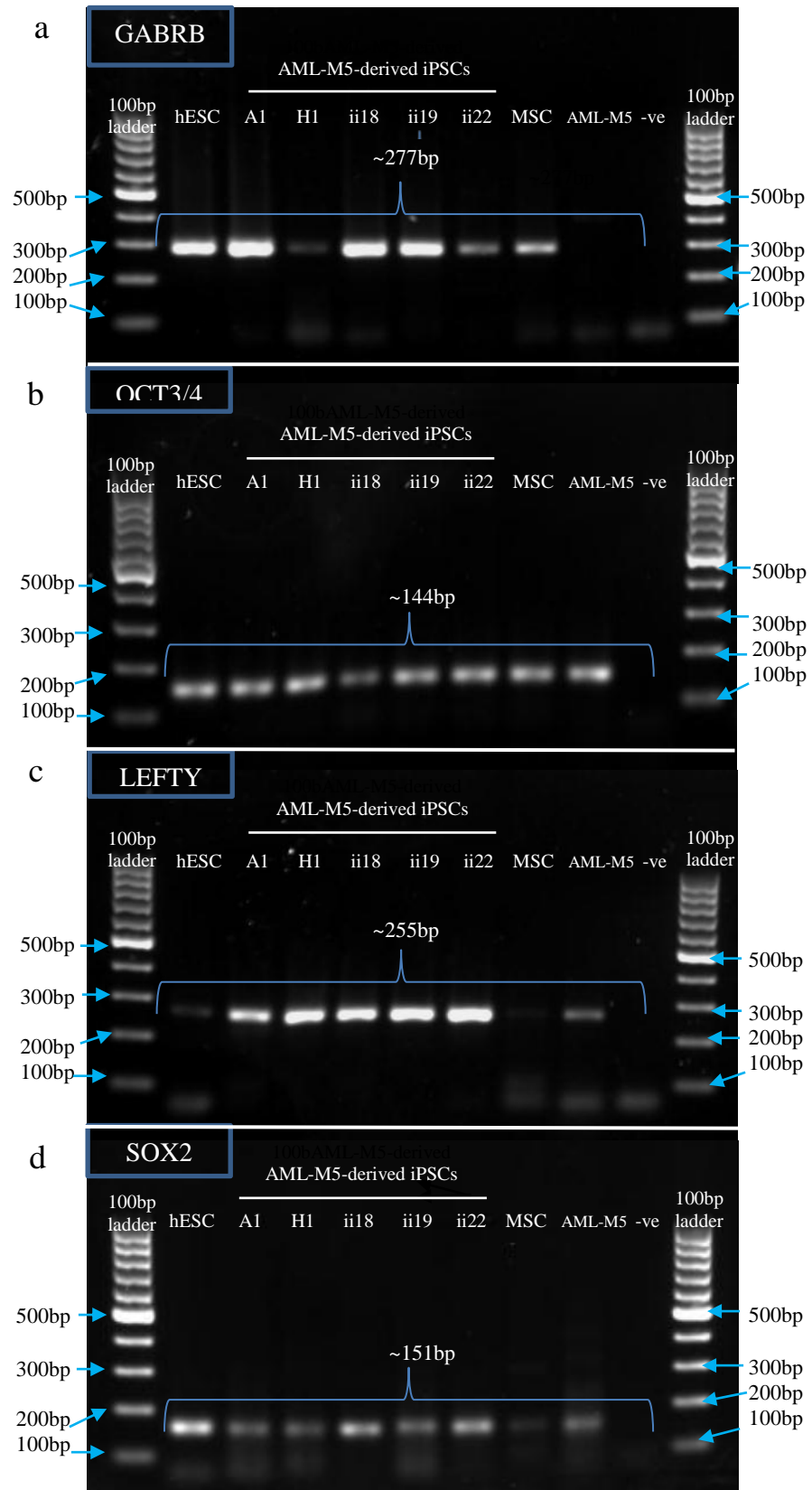


Figure 4.10: Detection of pluripotency markers using RT-PCR on various cells. Gel Images showed gene expression results of (a) *GABRB*, (b) *LEFTY*, (c) *OCT3/4* and (d) *SOX2* in hESC (positive control), AML-M5-derived iPSCs (A1, H1, ii18, ii19 and ii22), hAd-MSC (feeder), AML-M5 cells (parental negative control) and non-template control (-ve). The 100bp DNA ladder was used to determine the size of the PCR product. Expression of *GABRB*, *LEFTY*, *SOX2* and *OCT3/4* was detected in all AML-M5-derived iPSCs clones. Expression of *LEFTY*, *SOX2* and *OCT3/4* were detected in parental AML-M5 cells whereas *GABRB*, *SOX2* and *OCT3/4* were also expressed in feeder cells.

4.5.2 Detection of Pluripotency Markers Using Immunofluorescence Staining

Expression of pluripotency markers were further analysed using immunofluorescence staining. This experiment was carried out on four iPSC clones (A1, H1, ii-19 and ii-22) as clone ii-18 failed to propagate after several passages. Again, at the time of performing immunofluorescence staining, clone H1 had differentiated and could no longer be cultured for further study (Appendix D). Representative results of clone A1 was shown in this study as all these clones showed similar immunofluorescence staining pattern (Figure 4.11-4.15). The staining result of iPSC clones H1, ii-19 and ii-22 was showed in Appendix D. hESCs (BGOIV) were used as positive control and parental AML-M5 cells (THP-1 cell line) used as negative control. AML-M5-derived iPSCs were cultured on feeder cells at the time of staining. A total of five pluripotency genes including intracellular markers (mouse anti-human specific to PE-OCT3/4, PE-SOX2 and FITC-NANOG) and surface markers (mouse anti-human specific to FITC-TRA-1-81 and FITC-SSEA4) were used in this study.

In summary, AML-M5-derived iPSCs (clone A1, ii-19 and ii-22) were positively stained with pluripotency markers OCT3/4, SOX2, NANOG, TRA-1-81 and SSEA4 (refer to Figure 4.11-4.15). These markers were homogenously expressed in AML-M5-derived iPSC colonies. Similar staining pattern was observed in hESCs. On the other hand, approximately 50% of parental AML-M5 cells was positively stained with SOX2 and no positive result for OCT3/4, NANOG, TRA-1-81 and SSEA4 (refer to Figure 4.15).

Feeder cells did not stain with any pluripotency marker (refer to Figure 4.11-4.15). These results indicated AML-M5-derived iPSCs acquired the stemness properties by expressing pluripotency markers OCT3/4, SOX2, NANOG, TRA-1-81 and SSEA4 after reprogramming process.

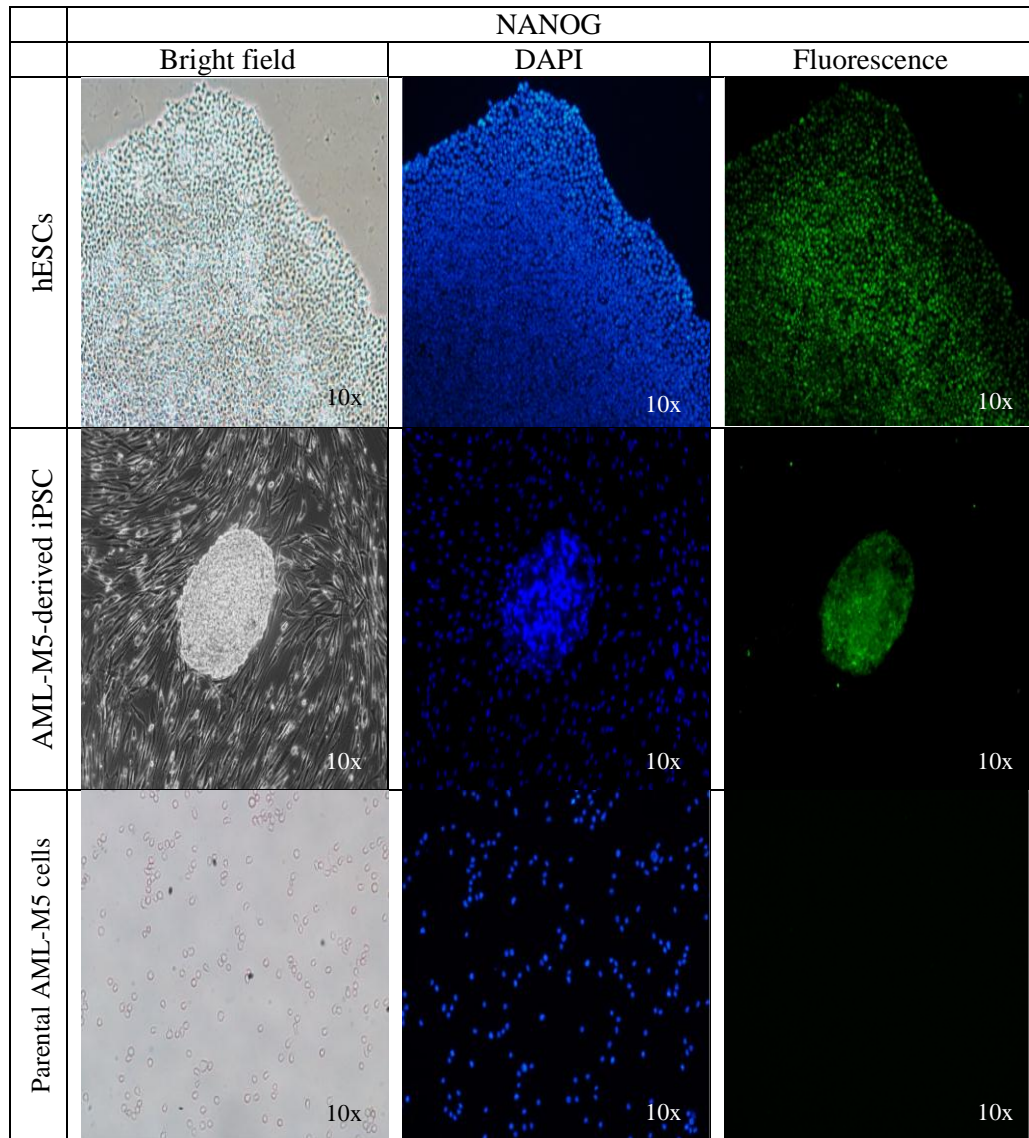


Figure 4.11: Detection of NANOG using immunofluorescence staining. Pseudo-green fluorescence signal indicates positive staining for NANOG marker. NANOG was homogenously expressed in AML-M5-derived iPSCs and hESCs. DAPI was used to indicate the presence of nuclei acid.

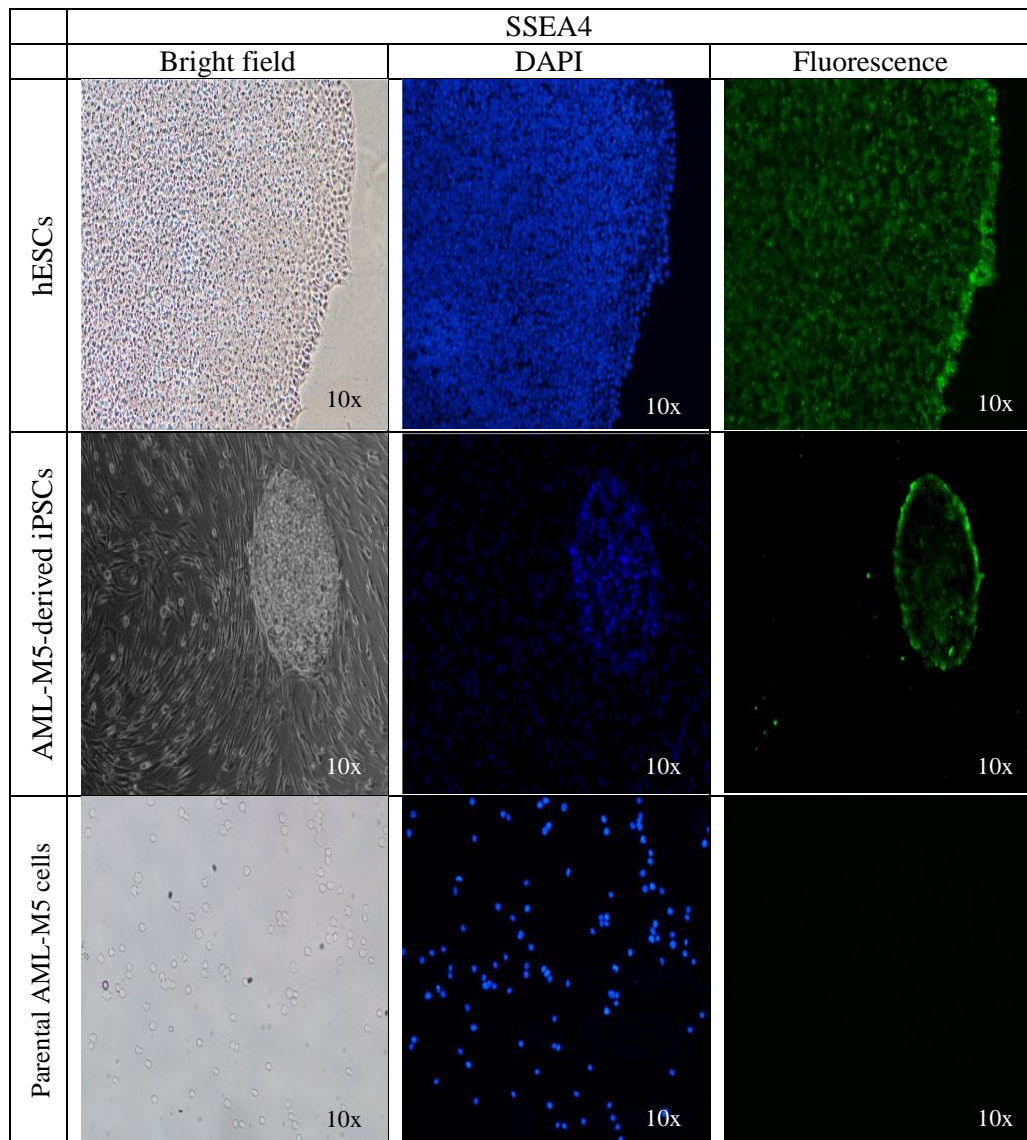


Figure 4.12: Detection of SSEA4 using immunofluorescence staining. Pseudo-green fluorescence signal indicates positive staining for SSEA4 marker. SSEA4 was homogenously expressed in AML-M5-derived iPSCs and hESCs. DAPI was used to indicate the presence of nuclei acid.

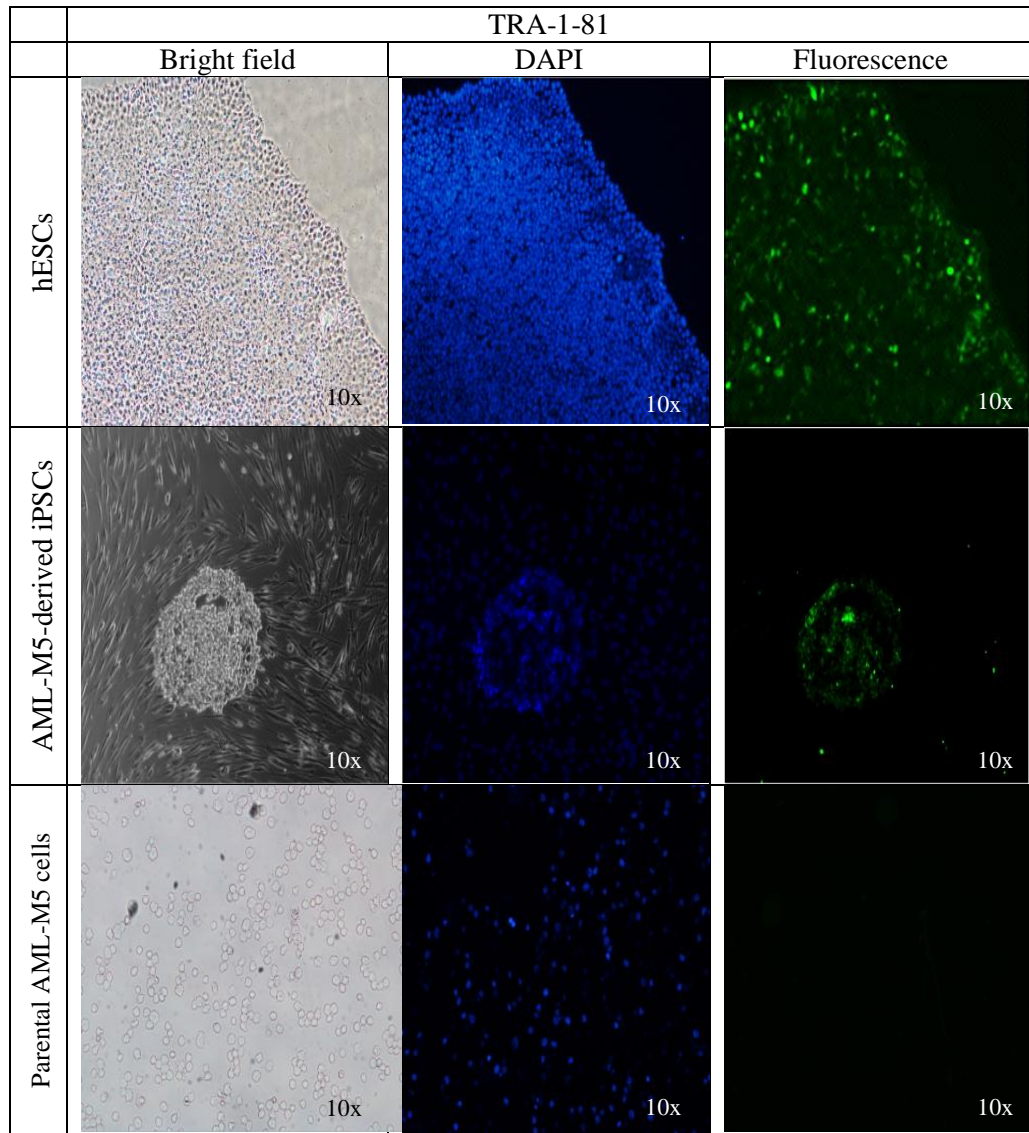


Figure 4.13: Detection of TRA-1-81 using immunofluorescence staining. Pseudo-green fluorescence signal indicates positive staining for TRA-1-81 marker. TRA-1-81 was homogenously expressed in AML-M5-derived iPSCs and hESCs. DAPI was used to indicate the presence of nuclei acid.

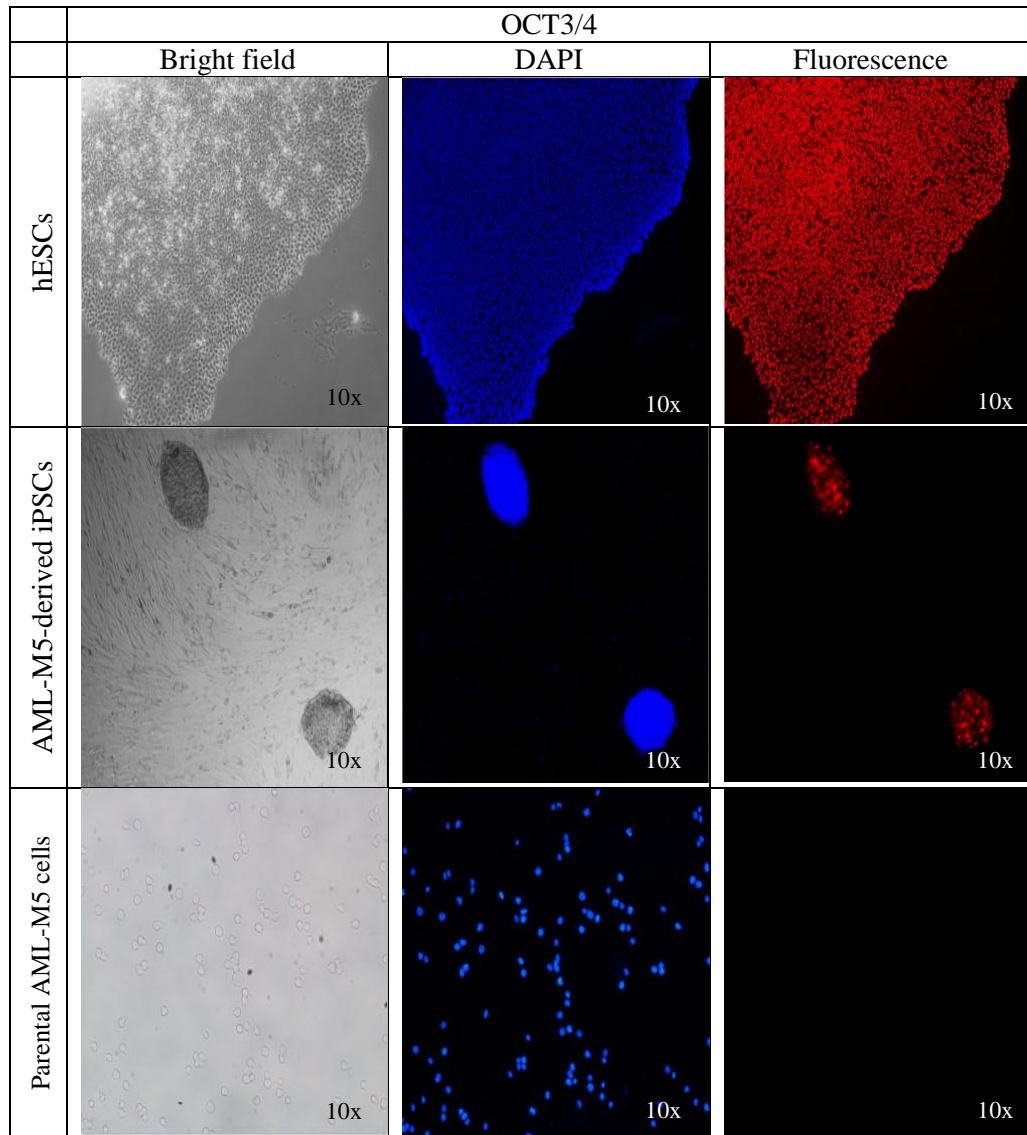


Figure 4.14: Detection of OCT3/4 using immunofluorescence staining. Pseudo-red fluorescence signal indicates positive staining for OCT3/4 marker. OCT3/4 was homogenously expressed in AML-M5-derived iPSCs and hESCs. DAPI was used to indicate the presence of nuclei acid.

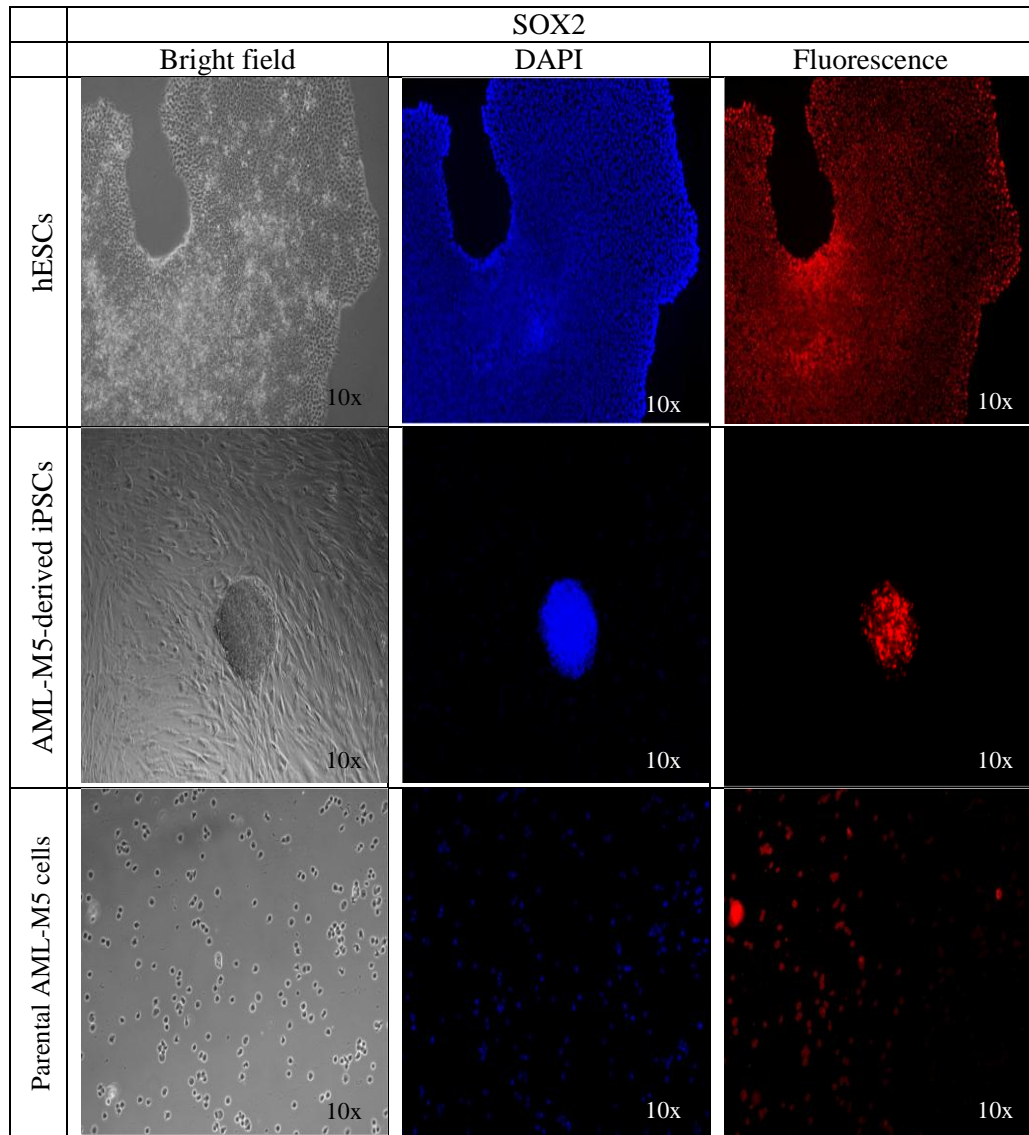


Figure 4.15: Detection of SOX2 using immunofluorescence staining. Pseudo-red fluorescence signal indicates positive staining for SOX2 marker. SOX2 was homogenously expressed in AML-M5-derived iPSCs and hESCs. A small population of parental AML-M5 cells was stained positively with SOX2. DAPI was used to indicate the presence of nuclei acid.

4.5.3 Detection of Pluripotency Markers Using Flow Cytometry Analysis

Flow cytometry analysis was carried out to quantitate the expression of pluripotency markers on AML-M5-derived iPSCs. A total of five pluripotency markers were analysed in this study including NANOG, SSEA4, OCT3/4, SOX2 and TRA-1-81. Human embryonic stem cell (hESC) and parental AML-M5 cells (THP-1 cell line) were used as positive and negative control, respectively. This experiment was repeated using three biological samples which are clone A1, ii-19 and ii-22. These three biological replicates were grouped and used to calculate significance of the expression of pluripotency markers. Figure 4.16 showed representative dot plots of flow cytometry analysis of NANOG, SSEA4, OCT3/4, SOX2 and TRA-1-81 on AML-M5-derived iPSCs, hESCs and parental AML-M5 cells.

As shown in Table 4.2 and Figure 4.17, SSEA4 was expressed at significantly higher level in AML-M5-derived iPSCs ($68.8\% \pm 17.8$) than parental AML-M5 cells ($0.4\% \pm 0.1$) ($p < 0.005$). Expression of TRA-1-81 and OCT3/4 also found to be significantly upregulated ($p < 0.005$) in AML-M5-derived iPSCs (TRA-1-81, $10.5\% \pm 4.7$; OCT3/4, $20.0\% \pm 3.7$) when compared with parental AML-M5 cells (TRA-1-81, $0.6\% \pm 0.2$; OCT3/4, $1.0\% \pm 0.5$). Noted that expression of SOX2 and NANOG was also highly expressed in AML-M5-derived iPSCs with mean expression of $89.6\% \pm 1.5$ and $73.9\% \pm 18.0$, respectively. SOX2 and NANOG were also expressed in parental AML-M5 cells in a relatively high level, with mean expression of $62.0\% \pm 0.5$ and $70.5\% \pm 0.4$, respectively. However, expression of SOX2 was expressed at

significantly higher level in AML-M5-derived iPSCs than parental AML-M5 cells ($p < 0.005$). On the other hand, NANOG was not expressed at significantly higher level in AML-M5-derived iPSCs than parental AML-M5 cells ($p > 0.005$). Thus, of the five pluripotency markers tested, four (SSEA4, TRA-1-81, SOX2 and OCT3/4) were expressed at statistically significantly higher level in AML-M5-derived iPSCs than parental cells.

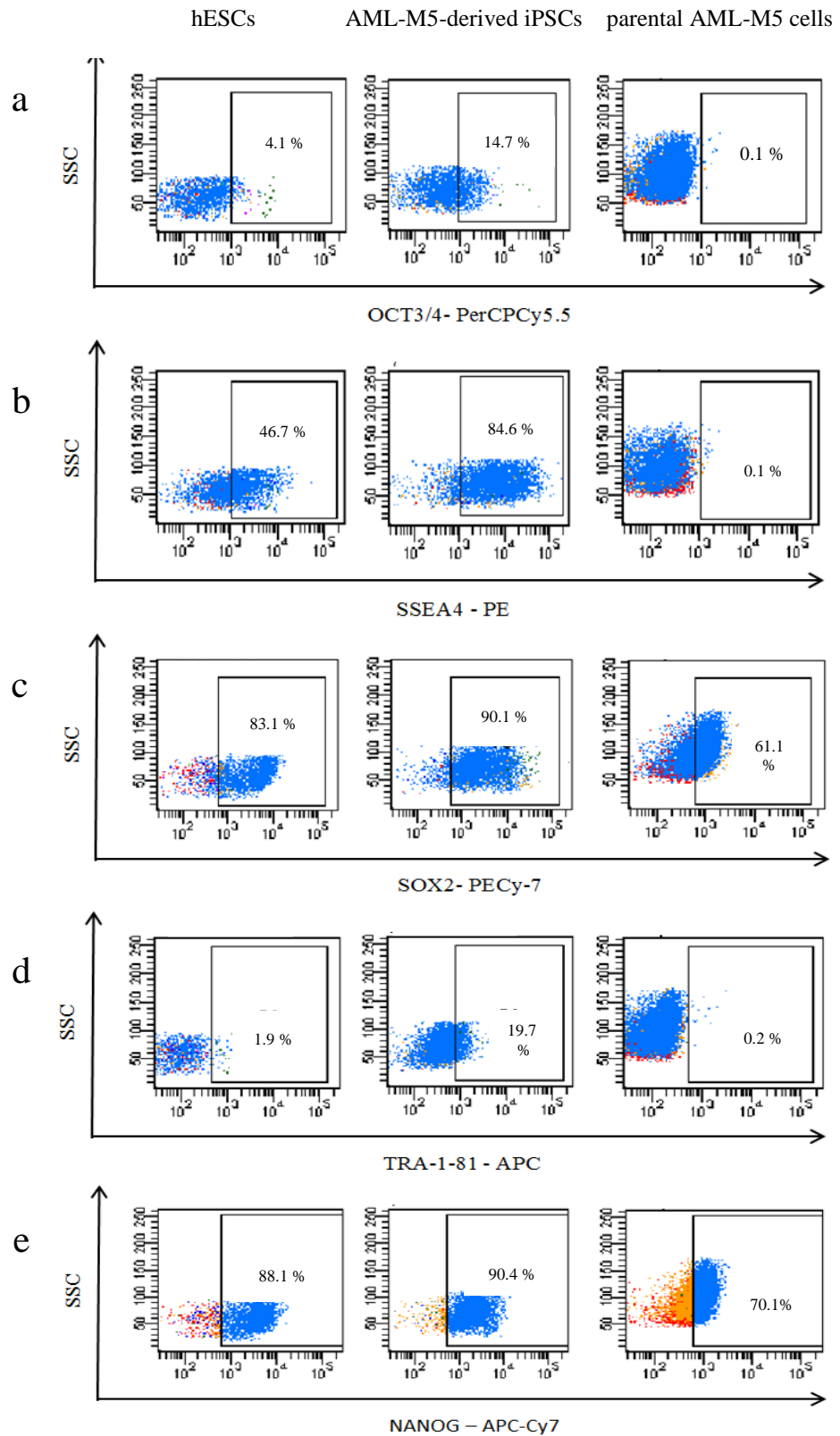


Figure 4.16: Flow cytometry analysis of pluripotency markers on AML-M5-derived iPSCs. Representative dot plots showed the expression of pluripotency markers (a) OCT3/4, (b) SSEA4, (c) SOX2, (d) TRA-1-81, and (e) NANOG on AML-M5-derived iPSCs, hESCs and parental AML-M5 cells. hESCs and parental AML-M5 cells were used as control. Expression of all pluripotency markers was upregulated in AML-M5-derived iPSCs compared to parental AML-M5 cells.

Table 4.2: Comparison of expression of pluripotency markers in AML-M5-derived iPSCs and parental AML-M5 cells.

Sample Pluripotency markers	Parental AML-M5 cells (%), n=3	AML-M5-derived iPSCs (%), n=3	<i>p</i> -value
SSEA4	0.4 ± 0.1	68.8 ± 17.8	0.00*
TRA-1-81	0.6 ± 0.2	10.5 ± 4.7	0.00*
OCT3/4	1.0 ± 0.5	20.0 ± 3.7	0.00*
SOX2	62.0 ± 0.5	89.6 ± 1.5	0.00*
NANOG	70.5 ± 0.4	73.9 ± 18.0	3.00

Note that standard error of mean and *p*-value were obtained using independent T-test and Mann-Whitney U test. **p*-value < 0.05 indicates statistical significance.

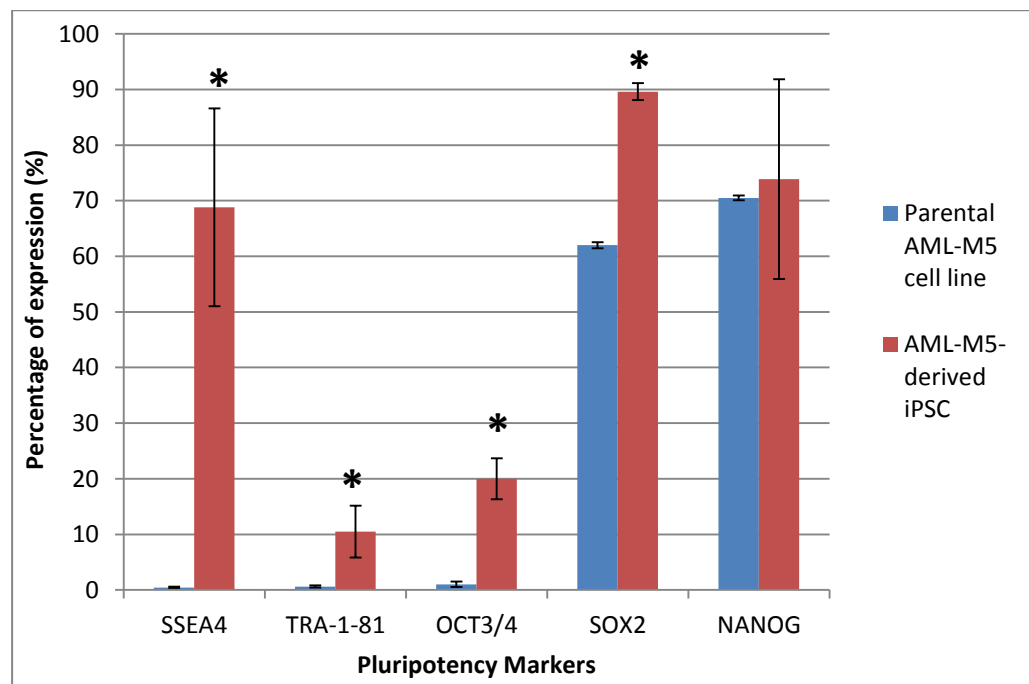


Figure 4.17: Mean expression of pluripotency markers on AML-M5-derived iPSCs and parental AML-M5 cell. Bar chart showed that expression of SSEA4, TRA-1-81, OCT3/4 and SOX2 were significantly increased in AML-M5-derived iPSCs compared to parental AML-M5 cells. * denotes *p*-value < 0.05. Error bars represent standard error of mean (n=3).

4.5.4 *In vitro* Three Germ Layers Differentiation Assays

As demonstrated in Session 4.5.1, 4.5.2 and 4.5.3, pluripotency of AML-M5-derived iPSCs was verified by detection of pluripotency markers in all AML-M5-derived iPSC clones. Next step is to further confirm pluripotency properties of AML-M5-derived iPSCs by *in vitro* three germ layers differentiation, which is capability of AML-M5-derived iPSCs to differentiate into mesoderm, endoderm and ectoderm lineages.

4.5.4.1 Mesoderm Lineage Differentiation

For mesoderm lineage, adipogenesis differentiation and osteogenesis differentiation were carried out on AML-M5-derived iPSC clones (clone A1, ii-19 and ii-22). hESCs and hAd-MSC were used as positive control. Representative result of adipogenesis induction was shown in Figure 4.18. Oil Red O staining was used to detect the presence of oil droplets in the cells, as indicated in red colour staining. In Figure 4.18 showed iPSC-differentiated cells resembled elongated fibroblast shape. Nonetheless, the iPSC-differentiated cells did not form visible oil droplets after 22 days of differentiation induction. Same observation was found in hESCs control. On the other hand, large and visible oil droplets were accumulated in hAd-MSC. Oil droplets in ESC/iPSC-differentiated cells were positively stained by Oil Red O staining, as shown by arrow head (refer to Figure 4.18).

Representative result of osteogenesis differentiation was showed in Figure 4.19. Alizarin Red staining was used to visualise the presence of calcium deposits which were secreted by osteoblasts. Positive staining was indicated as red precipitates. Figure 4.19 showed that red precipitates were observed in all differentiated iPSC, hESCs and hAd-MSc, but more red precipitates were observed in iPSC-differentiated cells compared to ESC/hAd-MSc-differentiated cells.

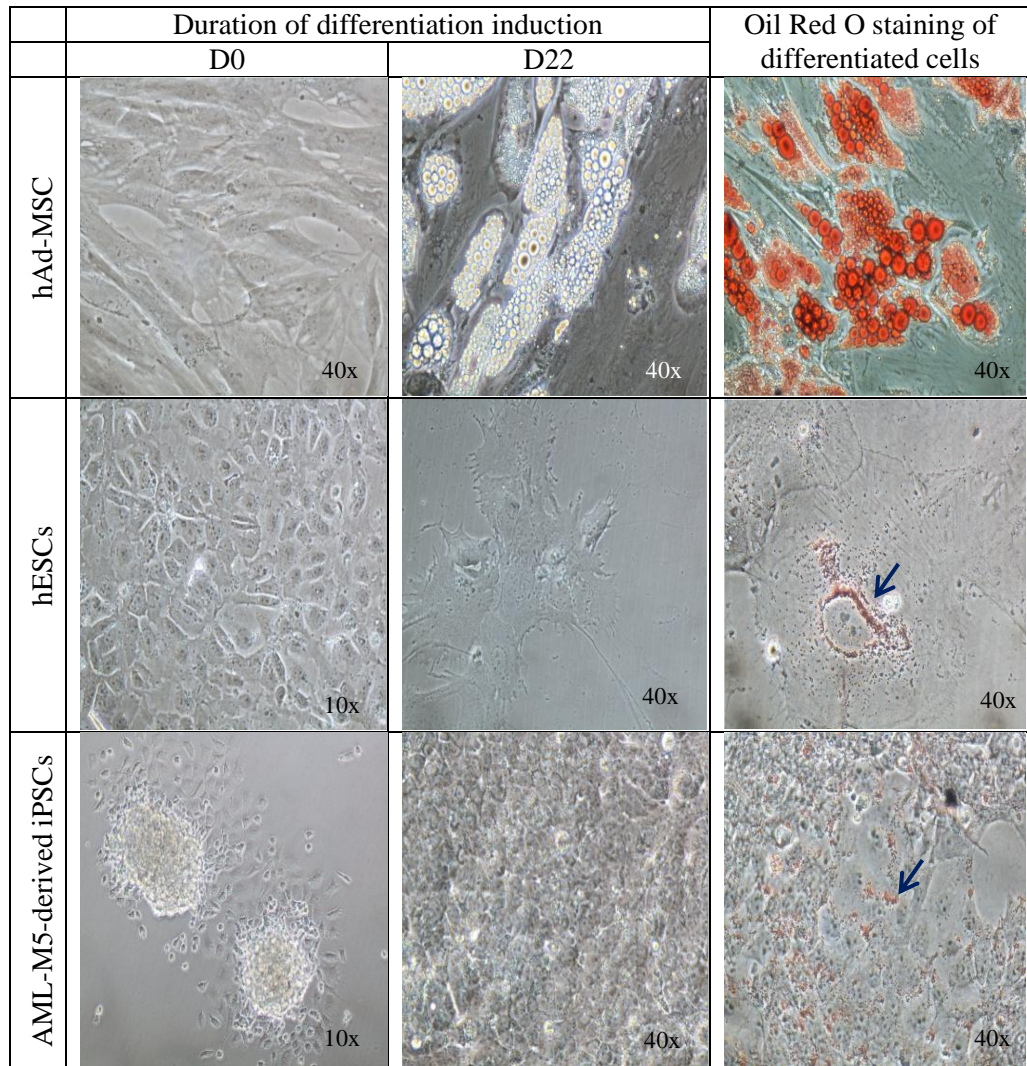


Figure 4.18: Induction of adipogenesis differentiation. Phase contrast images showed morphological changes of hAd-MSC, hESCs and AML-M5-derived iPSCs clone from day 0 (D0) to day 22 (D22). At 22 days post-differentiation, visible oil droplet was not observed in differentiated iPSC and hESCs, but in differentiated hAd-MSC. Presence of oil droplets in differentiated hAd-MSC, hESCs and iPSC clone were stained by Oil Red O staining, as indicated in red colour staining (pointed by arrows).

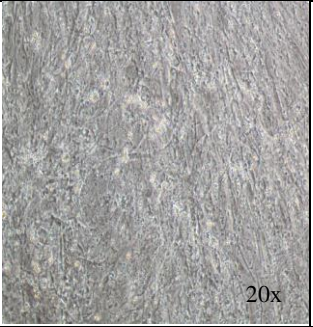
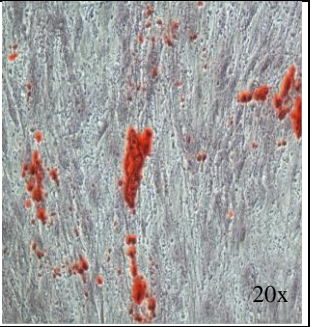
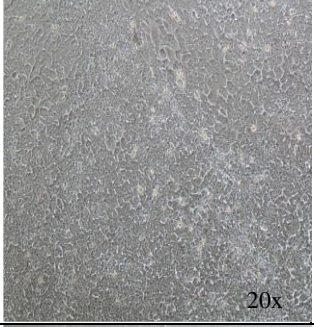
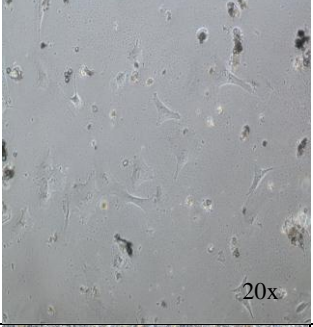
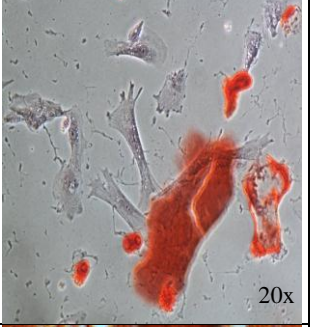
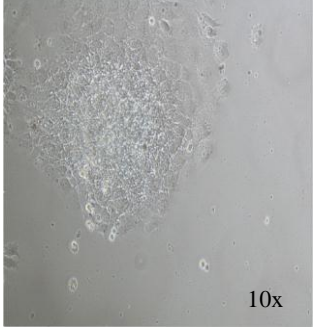
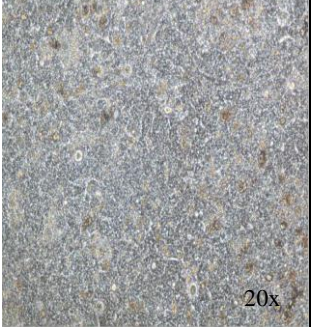
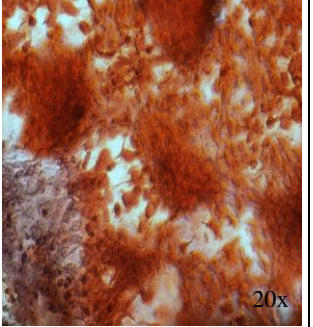
	Duration of differentiation induction		Alizarin Red staining of differentiated cells
	D0	D22	
hAd-MSC			
hESCs			
AML-M5-derived iPSCs			

Figure 4.19: Induction of osteogenesis differentiation. Phase contrast images showed morphological changes of AML-M5-derived iPSCs, hAd-MSC and hESCs from day 0 to day 22. Accumulation of calcium deposits in all differentiated cells were positively stained by Alizarin Red stain, as indicated by the presence of red precipitate.

4.5.4.2 Endoderm Lineage Differentiation

Endoderm lineage differentiation was carried out on iPSC-derived embryoid bodies (iPSC-derived EBs) using Activin A, which is an endoderm lineage specific growth factor. Human embryonic stem cell-derived embryoid bodies (hESC-derived EBs) were used as control. Figure 4.20 showed representative result of Activin A-induced endoderm differentiation. iPSC-derived EBs were adhered to the culture dish, and cell outgrowth was observed on the following day (refer to Figure 4.20). On Day 5 of differentiation induction, cells outgrew from the iPSC colony exhibited endoderm-like morphology which showed high cytoplasm to nucleus content and lost of cell-cell junction (Figure 4.20). Similar observation was seen in human ESC-derived EBs.

Detection of definitive endoderm marker, SOX17 was carried out using immunofluorescence staining. Representative immunofluorescence staining result was shown in Figure 4.21. Positive staining of SOX17 was detected in iPSC-differentiated cells and human ESC-differentiated cells, as shown in pseudo-red signal. Expression of SOX17 was confined in cell outgrowth but not in attached aggregates.

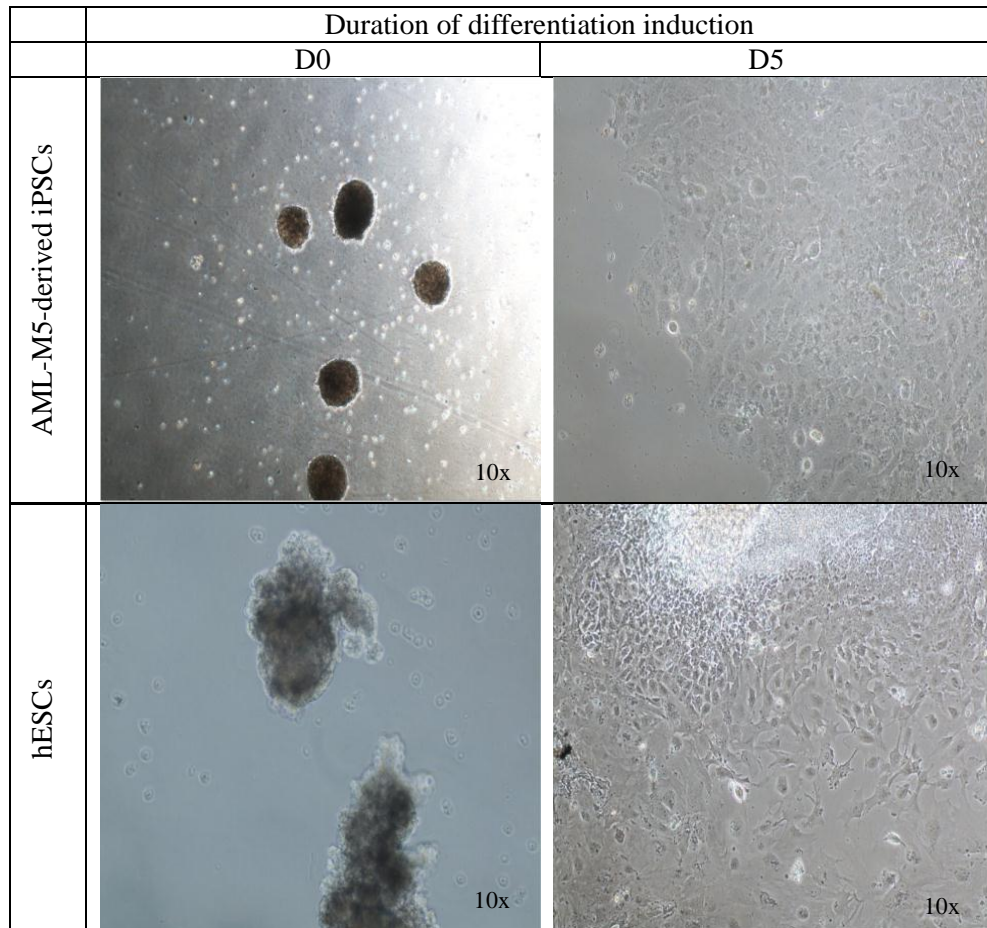


Figure 4.20: Activin A-induced endoderm differentiation. Phase contrast images showed morphological changes of iPSC-derived embryoid bodies (iPSC-derived EBs) and human embryonic stem cell-derived embryoid bodies (hESC-derived EBs) from day zero to day five of differentiation induction. Cell outgrowths were formed from ESC/iPSC-derived EBs.

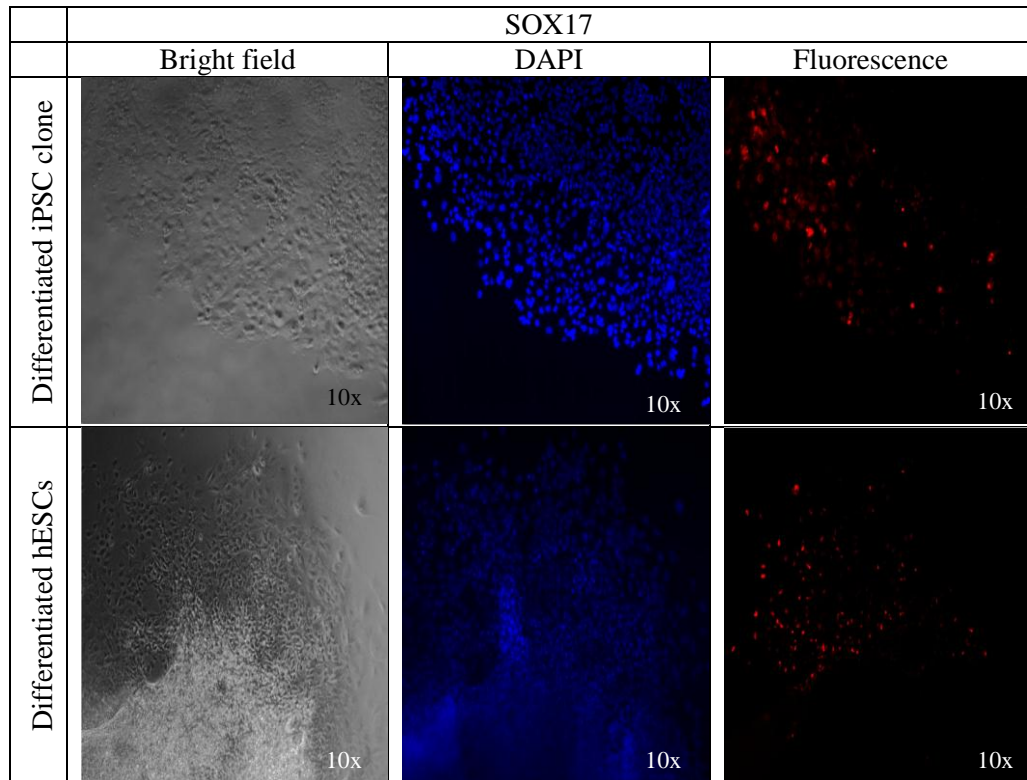


Figure 4.21: Detection of definitive endoderm marker SOX17 using immunofluorescence staining. Phase contrast and fluorescent images were captured from differentiated cells. DAPI was counterstained to indicate the presence of nuclei acid. Pseudo-red fluorescence signal indicated positive staining of SOX17 in differentiated hESCs and differentiated iPSC. Endoderm differentiation was confined in outgrowth region, as indicated by the presence of pseudo-red fluorescence signal.

4.5.4.3 Ectoderm Lineage Differentiation

Ectoderm lineage differentiation was carried out on iPSC-derived EBs using Noggin, which is an ectoderm lineage-specific growth factor. Human ESC-derived EBs were used as control. Representative result of Noggin-induced ectoderm differentiation was shown in Figure 4.22. iPSC-derived EBs were attached to the culture dish and outgrowths were formed. On Day 5 of differentiation induction, the differentiated cells were morphologically varied from AML-M5-derived iPSCs and more resembled primary neurons with elaborate networks (Figure 4.22). Similar observation was seen in ESC-derived EBs.

Detection of ectoderm marker, MAP2 was carried out using immunofluorescence staining. Figure 4.23 showed representative immunofluorescence staining of iPSC. Positive staining of MAP2 was detected in differentiated cells from iPSC and hESCs, as indicated in pseudo-green signal. MAP2 was widely expressed in the cell monolayer. Taken together, iPSC derived from parental AML-M5 cells showed capability to differentiate into three germ layers (which are mesoderm, endoderm and ectoderm), further confirming the pluripotency of iPSC.

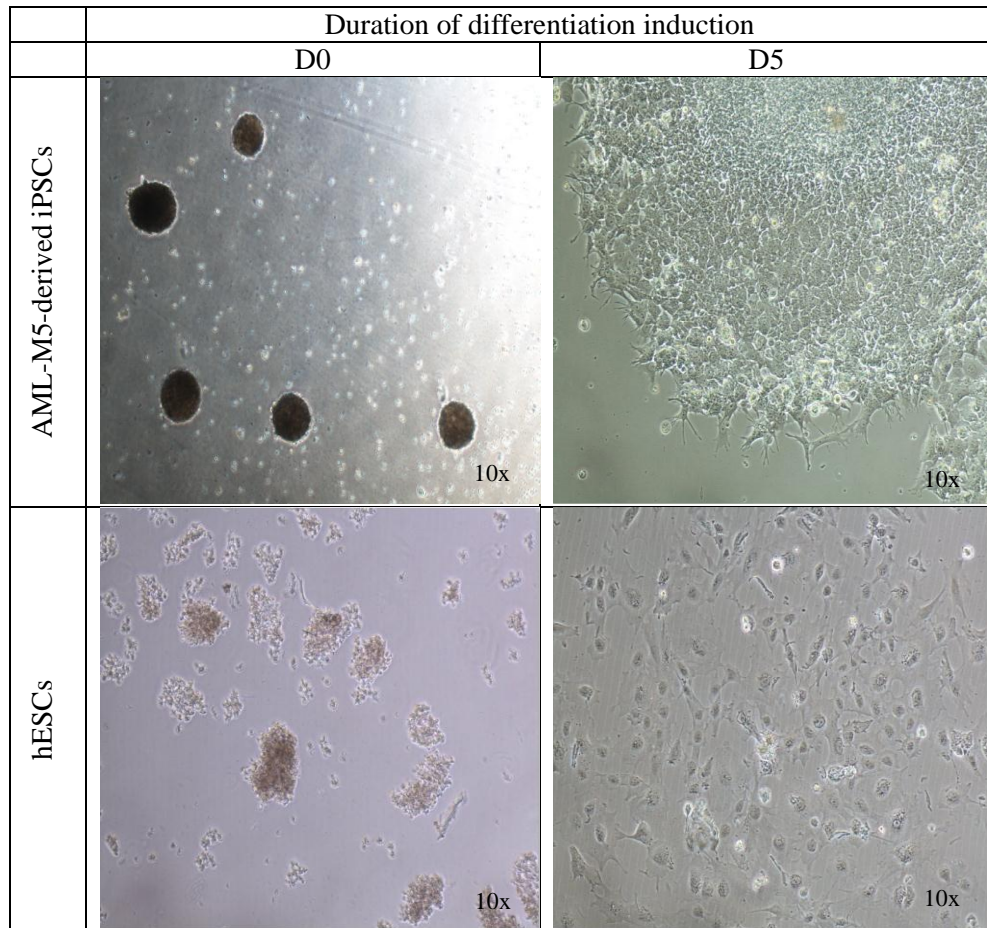


Figure 4.22: Noggin-induced endoderm differentiation. Phase contrast images showed morphological changes of iPSC-derived EBs and human ESC-derived EBs from day zero to day five of differentiation induction. Cell outgrowths were formed from ESC/iPSC-derived EBs.

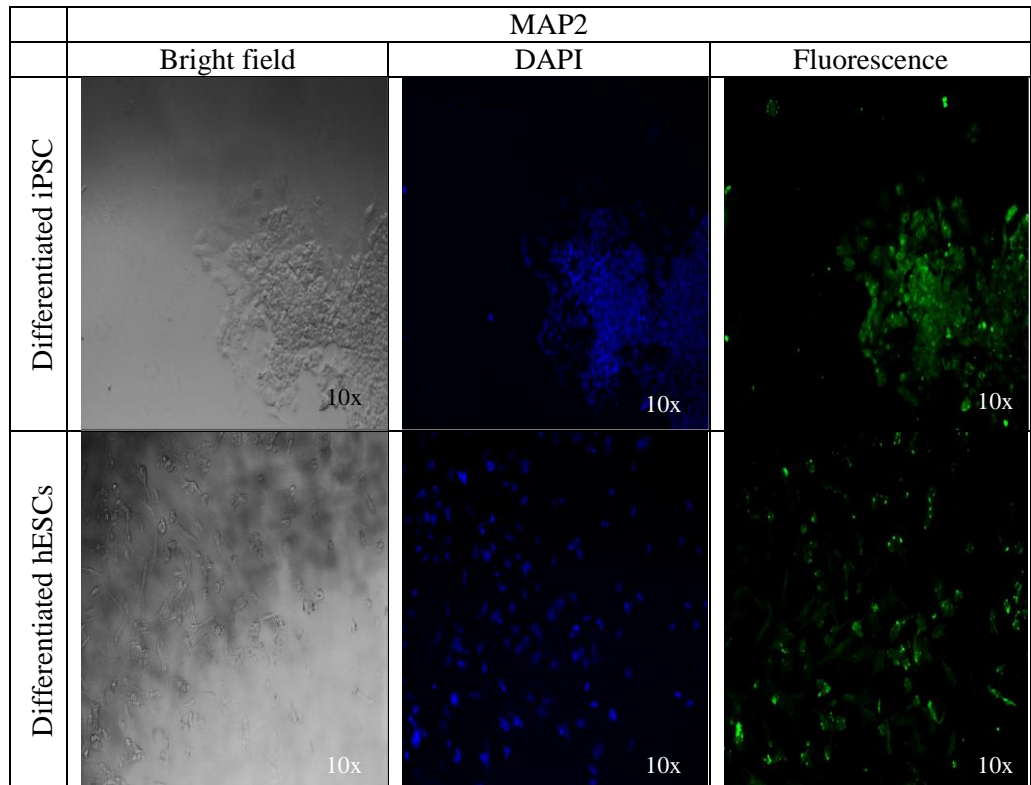


Figure 4.23: Detection of ectoderm marker MAP2 using immunofluorescence staining. Phase contrast and fluorescent images were captured from differentiated cells. DAPI was counterstained to indicate the presence of nuclei acid. Pseudo-green fluorescence signal indicated positive staining of MAP2 in differentiated iPSC and differentiated hESCs. MAP2 was widely expressed in cell monolayer for both differentiated cells, as indicated by the presence of pseudo-green fluorescence signal.

4.6 Verification of AML-M5-derived iPSCs

4.6.1 Detection of Monocyte-specific Markers Using Immunophenotyping

Once the expression of pluripotency markers and differentiation ability of AML-M5-derived iPSCs were confirmed, next step is to further verify the changes of cellular state between iPSC and their parental AML-M5 cells (THP-1 cell line). Monocytic markers including CD11c and CD15s, which are the specific markers found in differentiated monocytic cells were used in this study. Detection of monocytic markers was carried out on all AML-M5-derived iPSCs and parental AML-M5 cells line using immunophenotyping in order to access the relative changes of these markers. As demonstrated in Figure 4.24, representative histograms obtained from flow cytometry profile showed expression of CD15s and CD11c was downregulated in AML-M5-derived iPSCs when compared with parental AML-M5 cells.

Table 4.3 and Figure 4.25 showed that expression of CD15s was significantly downregulated in AML-M5-derived iPSCs when compared with parental AML-M5 cells ($p < 0.05$), with mean expression at $14.8\% \pm 4.7$ and $98.4\% \pm 0.7$, respectively. Similar result was also found in expression of CD11c in AML-M5-derived iPSCs when compared with parental AML-M5 cells ($p < 0.05$), whereby mean expression of CD11c was $1.36\% \pm 0.0$ and $79.2\% \pm 0.5$, respectively. Expression of both monocytic-specific markers CD15s and CD11c was downregulated in AML-M5-derived iPSCs, indicating that AML-M5-derived iPSCs have different cell identity from parental cell line.

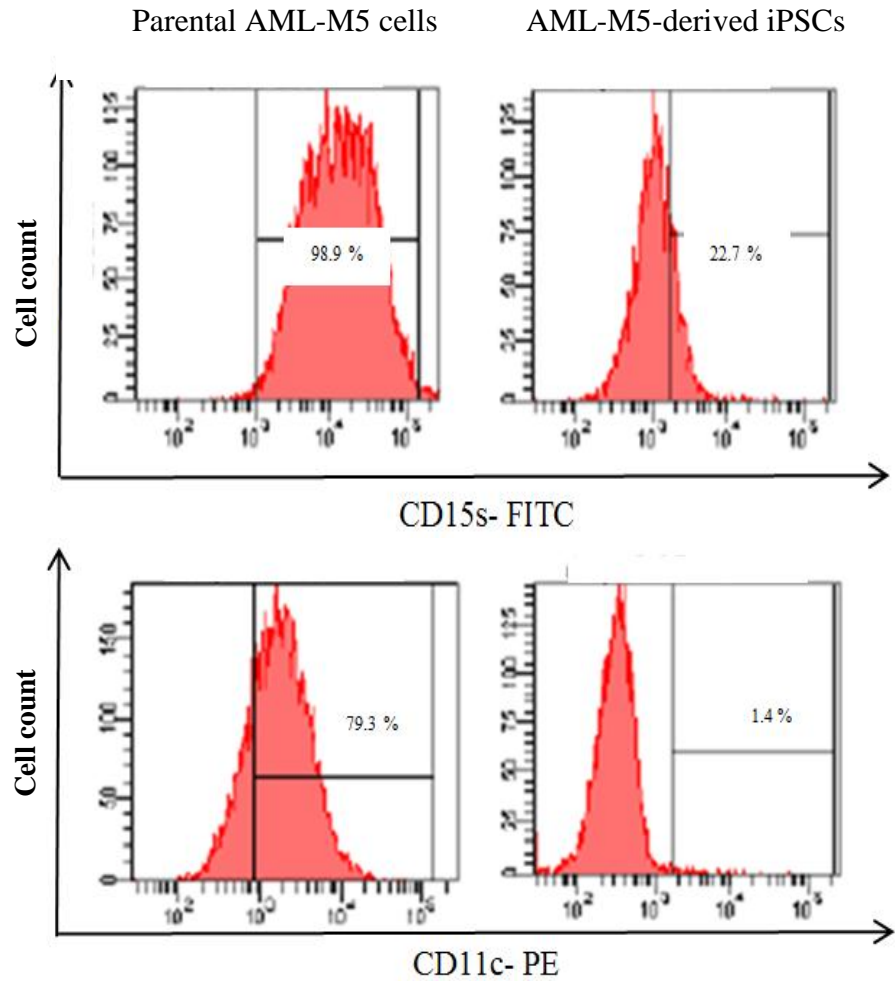


Figure 4.24: Flow cytometry analysis of monocytic-specific markers on AML-M5-derived iPSCs and parental AML-M5 cell. Histograms showed expression of monocytic-specific markers CD15s and CD11c on parental AML-M5 cells was recorded at 98.9% and 79.3%, respectively. On the other hand, expression of monocytic-specific markers CD15s and CD11c on AML-M5-derived iPSCs was noted at 22.7% and 1.4%, respectively. Results demonstrated that these monocytic-specific markers were downregulated in AML-M5-derived iPSCs compared to parental AML-M5 cells.

Table 4.3: Comparison of expression of monocytic-specific markers in AML-M5-derived iPSCs and parental AML-M5 cells.

Sample Monocytic marker	Parental AML-M5 cells (%), n=3	AML-M5-derived iPSCs (%), n=3	<i>p</i> -value
CD15s	98.4 ± 0.7	14.8 ± 4.7	0.00*
CD11c	79.2 ± 0.5	1.36 ± 0.0	0.00*

Note that standard error of mean and *p*-value were obtained using independent T-test and Mann-Whitney U test. **p*-value <0.05 indicates statistical significance.

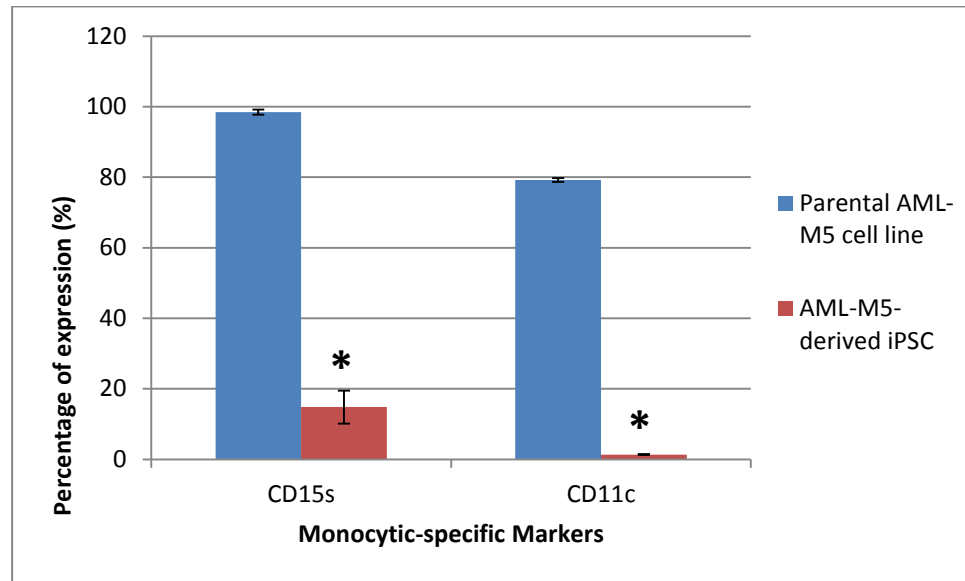


Figure 4.25: Mean expression of monocytic-specific markers on AML-M5-derived iPSCs and parental AML-M5 cells. Bar chart showed that expression of CD15s and CD11c was significantly decreased in AML-M5-derived iPSCs compared to parental AML-M5 cells (* *p*<0.05). Error bars represent standard error of mean (n=3).

4.6.2 Detection of MLL-AF9 Fusion Gene

In order to verify the cell line –specific origin of each generated iPSC clone, RT-PCR was used to detect the presence of leukaemia specific gene mutation *MLL-AF9* (Pession et al., 2003). Parental AML-M5 cells (THP-1 cell line) were used as positive control while peripheral blood mononuclear cells (PBMC) were used as negative control in this assay. Feeder cells were included to exclude the possibility of contamination. GAPDH was used as housekeeping gene. Amplicon at approximately size of 177 bp was observed in all AML-M5-derived iPSC clones and parental AML-M5 cells, indicating both the parental AML-M5 cells and AML-M5-derived iPSC clones share the same genetic makeup (refer to Figure 4.26).

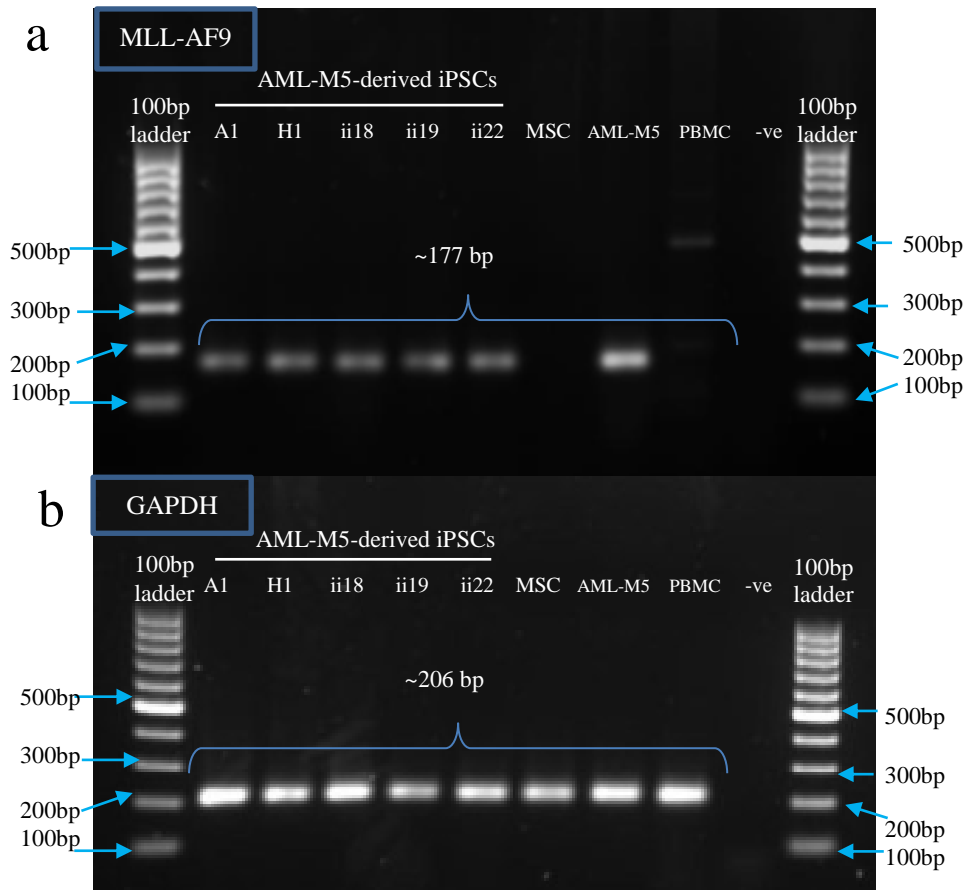


Figure 4.26: Detection of leukaemia-specific mutation *MLL-AF9* using PCR. Gel image showed the RT-PCR result of (a) *MLL-AF9* fusion gene and (b) GAPDH in AML-M5-derived iPSC clones (A1, H1, ii18, ii19 and ii22), hAd-MSC (feeder cell), AML-M5 cells (parental positive control), and PBMC (negative control). Both the parental AML-M5 cells and AML-M5-derived iPSC clones expressed an amplicon at size of approximately at 177 bp. The 100bp DNA ladder was used to determine the size of the PCR product.

CHAPTER 5

DISCUSSION

5.1 Generation of AML-M5-derived iPSCs

THP-1 cell line, which are derived from a 2-year old patient with AML-M5 were used as a starting material in this study (Tsuchiya et al., 1980). Prognosis of AML-M5 is often bad due to the involvement of chromosomal abnormalities, *MLL-AF9* fusion gene (McCormack et al., 2008). Presently, the cellular mechanism involved with *MLL-AF9* is poorly understood (McCormack et al., 2008). Hence, development of a disease model is necessary for unravelling pathogenesis of AML-M5, and eventually this model can be used for drug discovery. In this study, a disease model of AML-M5 (THP-1 cell line) was generated using iPSC technique. This technique was first introduced by Professor Yamanaka and his co-worker, to revert somatic cells into pluripotent state using the four transcription factors (Takahashi and Yamanaka, 2006).

In our study, cellular reprogramming was carried out using retrovirus method carrying OSKM. There is a rational for using integration retrovirus method in this study. First of all, retrovirus method is the most established method among the reprogramming methods (Takahashi and Yamanaka, 2006; Okita et al., 2007; Takahashi et al., 2007). Generation of iPSCs using

retrovirus method has been reported for many cell types including fibroblasts, neural stem cells, liver cells, blood cells, mesenchymal stem cells, and amniotic cells (Robinton & Daley, 2012; Takahashi, et al., 2007). This method also reported with higher reprogramming efficiency compared to other methods such as protein delivery method and mRNA method (Takahashi, et al., 2007). These features make retroviruses an attractive candidate for iPSC production especially those cell types that never been reprogrammed.

Using the combination of OSKM factors in iPSC generation is highly debatable. The expression of OSKM is well associated with tumours development (Ohnishi et al., 2014). Injection of OSKM-derived iPSCs into mice eventually leads to neoplastic development (Takahashi and Yamanaka, 2006). In particular, elevated expression of *OCT3/4* causes epithelial cell dysplasia (Semi et al., 2012). Overexpression of *SOX2* causes formation of polyps and mucinous colon carcinomas, aberrant expression of *KLF4* is associated with breast cancer (Foster et al., 2005; Park, E.T et al., 2008). *c-MYC* is associated with almost 70% of human cancers (Semi et al., 2012). iPSCs that are generated using retroviruses with OSKM factors may hamper cell therapy for human diseases due to high risk of the integration of virus genome, and failed to silence the exogenous OSKM factors (Lewinski et al., 2006). Despite the fact that there are some disadvantages of using retrovirus method and OSKM factors, this method was used in this study because the priority of our study is to generate a disease model from AML-M5 to elucidate pathogenesis of AML-M5.

In this study, we used human adipose-derived mesenchymal stem cell (hAd-MSC) as feeder cell to support the growth of AML-M5-derived iPSCs. hAd-MSC is derived from embryonic mesoderm lineage and it is one of the multipotent stem cells which has the ability to differentiate into tissues of bone, cartilage, muscle and fat (Zuk et al., 2002; Krampera et al., 2007). Like pluripotent stem cells, hAd-MSC is self-renewal (Hass et al., 2011). In most study, xeno-origin feeder such as mouse embryonic fibroblasts (MEFs) was used in maintaining hESCs and iPSCs culture (Takahashi et al., 2007; Zhang, Y et al., 2012). However, the use of xeno-origin feeder has been associated with risk of pathogen contaminations, thus, limiting the application of iPSCs in clinical setting such as regenerative medicine (Takahashi et al., 2009; Amit et al., 2003; Richards et al., 2002). To overcome this problem, numerous human primary cells such as neonatal foreskin fibroblasts, adult fallopian tube epithelial cells, amniotic mesenchymal stem cells and hESC-derived fibroblast cells have been used as a substitution of feeder to support the growth of hESCs and iPSCs (Takahashi et al., 2009; Amit et al., 2003; Hovatta et al., 2003; Cheng et al., 2003). The hAd-MSC was chosen for our study because it is abundant and accessible as it can be retrieved from the waste of liposuction (Rehman et al., 2004). The hAd-MSC has better proliferation potential comparing to other human primary cells mentioned above (Rehman et al., 2004). Similar to xeno-origin feeder, hAd-MSC was also found to provide various growth factors and cytokines including bFGF and transforming growth factor-beta (TGF- β) that are crucial for maintenance of stem cell properties (Montes et al., 2009).

In this study, we used Phoenix cells to produce recombinant retrovirus. Phoenix cell is a packaging cell line containing retroviral *gag/pol* and *env* genes that facilitate the production of pseudotype 4070A Amphotropic virus (Cornetta et al., 2005). Higher transfection efficiency can be achieved using Phoenix cells compared to other packing cell line (Seo et al., 2013). This is because only plasmid of interested are added during transfection (Seo et al., 2013). Transfection efficiency is also influenced by various factors such as confluency of packaging cell line, quality and quantity of plasmid DNA (Kheyroodin and Ghazvinian, 2012).

Optimal transfection protocol was attained with 6.6 μg recombinant plasmid and 70-80% confluent of Phoenix cells at the time of transfection (Figure 4.4). Many studies have demonstrated 70-80% confluency of Phoenix cells was needed for optimal transfection protocol (Shahjahan Miah and Campbell, 2010; Polak et al., 2012). Confluency of Phoenix cells must be at optimal level, as too few cells lead to the culture growing slowly because lack of cell-to-cell contact; whereas too many cells results in contact inhibition, and thus preventing uptake of foreign DNA (Anson, 2004). Recombinant plasmid at 6.6 μg was found to give the highest transfection efficiency (Figure 4.4). Nevertheless, the amount of plasmid used in this study is relatively high as compared to the other studies (Swift et al., 1999; Saida et al., 2006; Li et al., 2008). Generally, increasing the quantity of transfected plasmid may not yield better transfection efficiency. The reason is because of an increase in the number of plasmid delivered per cells will eventually leads to cell toxicity (Saida et al., 2006).

In this study, retroviral vector was used as a tool to deliver genes of interest into AML-M5 cells (THP-1 cell line) because this vector allows stable expression of exogenous genes and have wide range of host tropism (Osten et al., 2007). Retrovirus vector has several drawbacks such as slow diffusion of virus to the target cells and rapid decay of virus (Andreadis et al., 2000). To overcome these, we have optimised the retrovirus infection method by using spinfection method (centrifuged at 32 °C) and addition of polybrene, a cationic polymer, at the time of infection (Davis et al., 2002; Berggren et al., 2012).

As demonstrated in Figure 4.3 and 4.5, infection efficiency was first observed at 24 hours at 5% and achieved highest infection efficiency at approximately 20% at 72 hours. Treatment with polybrene has been shown to improve transduction by enhancing receptor-independent virus adsorption on host cell's membrane (Davis et al., 2002). Given that parental AML-M5 cells (THP-1 cell line) were grown as suspension cells, the adsorption of virus to cell membrane may be interrupted by rapid movement of parental AML-M5 cells in culture, suggesting that addition of polybrene in this study may not be sufficient. Therefore, spinfection method was used to improve retrovirus infection efficiency by allowing virus particles to have close contact with the host cells (Berggren et al., 2012). In addition, Spinfection method was carried out with centrifugation at 32 °C which is an optimal temperature for retroviruses survival and thus preventing rapid decay of viruses (Forestell et al., 1995).

5.2 Characterisation of AML-M5-derived iPSCs

In this study, an average of 20 iPSC-like colonies per 10^5 input cells was isolated and reprogramming efficiency at approximately 0.02% was achieved. However, previous study demonstrated that reprogramming under hypoxic condition and combined with valproic acid (VPA) increased reprogramming efficiency to 200 folds in mouse cells (or 2.28%) (Yoshida et al., 2009). VPA is known as a reprogramming enhancer as it improves reprogramming efficiency to 100 folds (Huangfu et al., 2008a). On the other hand, low oxygen environment (5% O_2) prevents differentiation of hESCs (Ezashi et al., 2005). Low reprogramming efficiency may be due to cell type that was used in this study. Most of the reprogramming experiments were carried out using healthy somatic cells, whereas AML-M5 cells, a leukaemia cells that carried abnormal phenotypes with one or more aberrant genetic lesions was used in our study. The aberrant genetic lesion in AML-M5 cells may acts as reprogramming roadblock and contributes to low reprogramming efficiency (Yamanaka, 2012). Consistent with previous studies, although iPSC have been successfully derived from AML-M5 cells, reprogramming efficiency was low.

Distinct iPSC-like colonies were successfully isolated from Day 16 to Day 25 post-infection, suggested that it is possible to derive iPSC from AML-M5 cells. These iPSC-like colonies were notably different from the parental AML-M5 cells and feeder cells but indistinguishable from hESC as they have high ratio of nucleus to cytoplasm, large nucleus, tightly packed, formed round

colonies with border-defined edges (Figure 4.9; Thomson et al., 1998). Besides morphologically similar to typical hESC, iPSC-like colonies (AML-M5-derived iPSCs) were able to grow indefinitely (> Passage 25) without differentiation. AML-M5-derived iPSCs also required similar culture conditions used for the maintenance of pluripotent stem cells. These include dependency of feeder cells and requirement of basic fibroblast growth factors (bFGF) (Bendall et al., 2007). Feeder cells are important to support pluripotency and undifferentiated state of pluripotent stem cells (for example hESCs and iPSC) by providing adhesion molecules, extracellular matrix components and signalling molecules (Takahashi et al., 2007; Desai et al., 2015). bFGF also plays essential role in regulating stem cell renewal (Coutu and Galipeau, 2011). Removal of both feeder cells and bFGF leads to stem cell differentiation (Coutu and Galipeau, 2011).

Of note, AML-M5-derived iPSCs formed multilayer by stacking on top of each other at early passages and the colonies tend to dissociate (< Passage 4) (Figure 4.9). However, prolonged maintenance of AML-M5-derived iPSCs in culture condition mimicking stem cell niche showed significantly improvement in their morphology as they were more similar to bona fide hESCs whereby has flatter, tightly packed but do not override each other (Figure 4.9; Thomson et al., 1998). This finding presuming that the *in vitro* culture mimics to stem cell niche could promote pluripotent characteristic of AML-M5-derived iPSCs. Stem cell niche refers to a microenvironment where pluripotent stem cells were found (Lane et al., 2014). The stem cell niche consists of feeder cells and various factors such as extracellular matrix components, growth factors,

oxygen tension, pH, metabolites and so on (Mohyeldin et al., 2010; Van Der Sanden et al., 2010). This specific microenvironment maintains stem cells in a quiescent state that is resistant to differentiation via cell-cell interactions between stem cell, as well as interaction between stem cells and niche molecules (Li and Xie, 2005). Of note, stem cell niches generated stem cell population as niche save stem cells from depletion by replenishing stem cell population from stem cell-initiating colonies (Scadden, 2006).

In summary, a total of nine pluripotency markers (OCT3/4, SOX2, NANOG, GABRB, LEFTY, TRA-1-81, SSEA4, DNMT3B and ESG1) were used to investigate the expression of pluripotency markers at both mRNA and protein levels. These markers have been commonly used to characterise pluripotent stem cells in other reprogramming experiments (Takahashi and Yamanaka, 2006; Masaki et al., 2008; Choi et al., 2011; Liu et al., 2013). Gene expression study (at mRNA level) showed that the AML-M5-derived iPSC clones expressed pluripotency markers such as *GABRB*, *OCT3/4*, *LEFTY* and *SOX2* at the level similar to or higher than in the human ESC line (refer to Table 4.1 and Figure 4.10). On the other hand, all AML-M5-derived iPSCs clones and parental AML-M5 cells did not express DNMT3B and ESG1 (refer to Table 4.1 and Figure 4.10).

In the protein expression study using immunofluorescence staining, expression pattern of pluripotency markers NANOG, SOX2, OCT3/4, SSEA4 and TRA-1-81 on AML-M5-derived iPSCs was obtained (Figure 4.11-4.15). Subsequently, immunophenotyping using flow cytometry was carried out to

quantitate the expression of the selected pluripotency markers such as SOX2, OCT3/4, NANOG, TRA-1-81 and SSEA4 (Figure 4.16, 4.17, Table 4.2). SOX2 ($89.6\% \pm 1.5$), OCT3/4 ($20.0\% \pm 3.7$), TRA-1-81 ($10.5\% \pm 4.7$) and SSEA4 ($68.8\% \pm 17.8$) were expressed at significantly higher levels in AML-M5-derived iPSCs than parental AML-M5 cells (Figure 4.17, Table 4.2). These results provide evidence that AML-M5-derived iPSCs acquired pluripotency state. OCT3/4 and SOX2 are key transcription factors in determining pluripotency (Rizzino, 2013). Expression of NANOG has shown to be essential in maintaining self-renewal and repression of differentiation signalling pathway in hESCs (Niwa et al., 2000; Pan et al., 2006). Accordingly, OCT4, SOX2 and NANOG help to maintain pluripotency in hESCs through formation of a complex regulatory feedback loop that regulate each other (Rodda et al., 2005). Recent study reported that NANOG, OCT3/4 and FOXD3 form a negative feedback loop to maintain the expression of OCT3/4 at a steady level in order to prevent differentiation process (Pan et al., 2006).

We noticed that feeder cell (hAd-MSC) used in this study have positive expression of pluripotency markers such as *GABRB*, *OCT3/4* and *SOX2* at mRNA level (Table 4.1). It is well-known that hAd-MSC has multipotency and limited differentiation capability as well as self-renewal. These properties may confer the presence of pluripotency markers (Krampera et al., 2007; Hass et al., 2011). Eventhough these markers are detectable at mRNA level, there are absent in protein level (refer to Figure 4.11-4.15). Similar expression pattern was also observed in parental AML-M5 cells, in which pluripotency markers including OCT3/4, SOX2 and LEFTY were found to be expressed at mRNA

level but only SOX2 was positively detected at protein level (Figure 4.11-4.15; Table 4.1). These results showed that pluripotency markers with detectable mRNA level may not be found in immunofluorescence staining. mRNA level expression may not a good indicator to predict protein expression (Vogel and Marcotte, 2012). Variation in protein abundances in mammalian cells are primarily determined by regulation of post-transcription, translation and protein degradation (Vogel and Marcotte, 2012). Protein expression levels are influenced by post-transcriptional regulation at mRNA level (Vogel et al., 2010). If an 'off' signal is given during the post-transcriptional process, proteins expression will be suppressed, and vice versa (Vogel et al., 2010). Furthermore, it has been shown that proteins that are involved in chromatin organization and transcriptional regulation tend to be degraded rapidly due to its specific biological function, for example OCT3/4 (Schwanhäusser et al., 2011).

Notably, the expression of *OCT3/4*, *LEFTY* and *SOX2* was also found in parental AML-M5 cells at mRNA level. Besides, high expression of NANOG (70.1%) and SOX2 (61.1%) of parental AML-M5 cells was found in flow cytometry analysis. It is well known that OCT3/4, NANOG and SOX2 are involved in maintaining pluripotency, and play an essential role in self-renewal (Masui et al., 2007; Wang et al., 2008). Self-renewal is a process by which a cell gives rise to indefinitely of identical cells, which is also the property of cancer cells (He et al., 2009). This is not surprising as many ESC markers are also found in cancer cells because self-renewal is a hallmark shared by stem cells and cancer cells (Hanahan and Weinberg, 2011).

According to Table 4.1, *OCT3/4* and *SOX2* were found endogenously expressed in the parental AML-M5 cells. Hence, we speculate that it may not be necessary to include *OCT3/4* or *SOX2* to reprogramme AML-M5 cells. Some studies have reported that those cell types with endogenous expression of reprogramming factors (either *OCT3/4* or *SOX2*) were able to reprogramme without the need of exogenous *SOX2*, or reprogramming process could be done by using exogenous *OCT3/4* alone (Eminli et al., 2008; Kim et al., 2008; Maherali and Hochedlinger, 2008; Li et al., 2009). Gene expression of *SOX2* and *OCT3/4* must be tightly controlled at equivalent levels for optimal reprogramming process. Several studies have demonstrated that the ratio of *SOX2* and *OCT3/4* influence both the reprogramming efficiency and their quality (Papapetrou et al., 2009; Yamaguchi et al., 2011; Carey et al., 2011). In particular, approximately three folds increase of *OCT3/4* level would slightly enhance reprogramming efficiency, whereas, decrease *OCT3/4* level would reduce reprogramming efficiency (Papapetrou et al., 2009). On the other hand, overexpression of *SOX2* levels decreased the reprogramming efficiency and resulted in production of partial reprogrammed cells (Yamaguchi et al., 2011).

In our study, directed differentiation method was carried out to detect the pluripotent state of the iPSC clones. For that, AML-M5-derived iPSCs were exposed in controlled culture conditions involving specific growth factors that promote differentiation (Murnmery et al., 2012). Directed differentiation method has advantage over spontaneous differentiation method because the latter method may be impaired by partial differentiation of pluripotent stem cells (Murnmery et al., 2012). Our study demonstrated that AML-M5-derived

iPSCs were able to undergo cellular differentiation as the cells changed from less specialised type to a more specialised type which is from high proportion of nucleus/cytoplasm, tightly packed colonies to fibroblast-like shape, large cytoplasm and less cell-to-cell contact (Figure 4.9, 4.18, 4.19, 4.20 and 4.22). Successful adipogenic differentiation was indicated by the formation of lipid vacuoles within the cytoplasm which can be visualised using Oil Red O stain (Figure 4.18) (Zhang et al., 2012a). On the other hand, osteogenic differentiation was indicated by detection of extracellular calcium deposit secreted by osteoblasts which was visualised by Alizarin Red stain (Figure 4.19) (Zhang et al., 2012a). Taken together, AML-M5-derived iPSCs were able to differentiate into cell types of mesodermal lineage, such as osteoblasts and adipocytes (Figure 4.18 and 4.19).

A definitive endoderm marker SOX17 was positively detected in differentiated AML-M5-derived iPSCs after Activin A-induced endoderm differentiation (Figure 4.20). Activin A, which belongs to the transforming growth factor beta superfamily, has been shown to induce pluripotent stem cells into definitive endoderm cells (Sulzbacher et al., 2009; Zhang et al., 2012b). Presence of SOX17 is associated with definitive endoderm lineage (Lee and Chung, 2011). Besides, positive MAP2 staining was observed in differentiated AML-M5-derived iPSCs after Noggin-induced ectoderm differentiation (Figure 4.22). Noggin is a polypeptide molecule that plays important role in neural development during embryogenesis, and this molecule has been used for differentiation induction in iPSC (Lim et al., 2000; Takahashi et al., 2007; Zhang et al., 2012b). MAP2 is associated with differentiating

neurons, which is a cell type derived from ectoderm lineage (Schulz et al., 2003).

We observed that AML-M5-derived iPSCs were more ready to generate osteocytes (indicated as positive staining by Alizarin Red) than adipocytes (Figure 4.18 and 4.19). Previous study demonstrated that different lines of pluripotent stem cells may be prone to differentiate into a particular lineage (Cohen and Melton, 2011). Variation in culture condition may contribute to some extent of the differentiation bias (Cahan and Daley, 2013). Recently, a study reported that epigenetic make up of cell line underpin their tendencies of differentiation (Cahan and Daley, 2013).

In our study, immunophenotyping result showed that the CD15s and CD11c were significantly downregulated in AML-M5-derived iPSCs ($14.8\% \pm 4.7$, and $1.36\% \pm 0.0$ respectively) compared to parental AML-M5 cells ($98.4\% \pm 0.7$, and $79.2\% \pm 0.5$ respectively) (Figure 4.25). Downregulation of both monocytic markers CD15s and CD11c indicated AML-M5-derived iPSCs had achieved primitive level compared to parental AML-M5 cells, perhaps acquiring pluripotent properties. CD15s is expressed widely on mature blood cells such as neutrophils, basophils, granulocytes, monocytes, NK cells and T cells (Washington State University, 2008). This marker also expressed in myelomonocytic leukaemia cells (Washington State University, 2008). On the other hand, CD11c is a myeloid marker that commonly found in monocyte-derived dendritic cells (Qu et al., 2014). CD11c has been used to identify myelomonocytic leukaemia cells (Sojitra et al., 2013). Both markers are

associated with terminally differentiated monocytic cells.

Of note, *MLL-AF9* fusion oncogene was retained in all AML-M5-derived iPSCs after the reprogramming process (Figure 4.26). Our result was consistent with other study that no loss of genetic/chromosomal abnormalities was observed in reprogrammed AML-M5-derived iPSCs. Parental AML-M5 cells exhibited *MLL-AF9* fusion gene, a commonly observed chromosomal abnormality of AML-M5 (Chandra et al., 2010). Formation of *MLL-AF9* is the result of translocation t(9;11)(p22;q23) (Corral et al., 1996). *MLL-AF9* is also believed to be driven by epigenetic dysregulation (Neff and Armstrong, 2013). It is well-known that reprogramming is a process where the reprogrammed cells erasing the original cellular identity while acquiring pluripotency properties (Hochedlinger and Plath, 2009; Semi et al., 2012). However, the present study confirms the findings of others that reprogramming has no deletion effect on genetic/chromosomal abnormalities in cancer cells (Semi et al., 2012). For instant, chronic myeloid leukaemia (CML)-derived iPSC was found to be expressed BCR-ABL fusion protein which also found in parental CML cells (Kumano et al., 2012).

It is noted that the expression level of *MLL-AF9* fusion oncogene declined in AML-M5-derived iPSC clones compared to parental AML-M5 cells (Figure 4.26), suggesting a possibility of reduction of oncogenic properties in reprogrammed cells. Similar expression pattern of oncogene was also observed in reprogramming experiment conducted using osteosarcomas, lung cancer and gastrointestinal cancer (Miyoshi et al., 2010; Mahalingam et

al., 2012; Zhang et al., 2012a). These experiments showed the evidences that reprogrammed cancer cells mimic embryonic stem cells from the aspect of pluripotency markers expression and differentiation capability (Miyoshi et al., 2010; Mahalingam et al., 2012; Zhang et al., 2012a). Nonetheless, a remarkable decreased of oncogenes expression was observed in reprogrammed cancer cells compared to their parental cancer cells (Miyoshi et al., 2010; Mahalingam et al., 2012; Zhang et al., 2012a). Indeed, the reprogrammed cancer cells became less proliferative or aggressive, showing that direct reprogramming may result in loss of tumorigenicity (Zhang et al., 2012a). Previous study concluded that direct reprogramming can alter epigenetic changes of the cancer cells (Zhang et al., 2012a). As such, epigenetics changes are believed to be pertinent the reduction of oncogenes seen in other related studies.

CHAPTER 6

CONCLUSION

6.1 Conclusion

In conclusion, AML-M5 cells carrying *MLL-AF9* fusion gene can be reprogrammed with four transcription factors (OSKM). AML-M5-derived iPSCs were morphologically similar to typical hESCs as they have tightly packed colonies with defined margin and large proportion of nucleus to cytoplasm. AML-M5-derived iPSCs acquired pluripotent characteristics by expressing pluripotency markers and able to differentiate into three germ layers. Expression of monocytic-specific markers was downregulated in AML-M5-derived iPSCs. *MLL-AF9* fusion gene was retained in this AML-M5-derived iPSCs.

6.2 Limitations of the study

Viral genome integration and low reprogramming efficiency were the concerns in this study. The use of retroviruses may increase risk of viral genomic integration into host genome and impede the use of iPSC in clinical applications (Hottam and Ellis, 2008; Yu et al., 2009; Si-Tayeb et al., 2010). Thus, non-viral nonintegration reprogramming methods such as using microRNA, minicircle DNA vector, mRNA and protein can be adopted for iPSC generation (Kim et al., 2009; Yu et al., 2009; Jia et al., 2010; Warren et al., 2010; Lin et al., 2011). Low reprogramming efficiency (0.002%) was reported in this study. This may be due to their abnormal genetic status as parental AML-M5 cells are cancer cells with multiple genetic lesions (Yamanaka, 2012). To overcome this problem, reprogramming enhancers such as Vitamin C, Thiazovivin, PD0325901 and Parnate can be used during reprogramming process (Lin et al., 2009; Cai et al., 2010; Hanna et al., 2010; Xu et al., 2010).

Pluripotency markers including GABRB, OCT3/4 and SOX2 are found to be expressed in feeder cell (hAd-MSC) at mRNA level (Table 4.1). This may indicate certain extent of interference of human-origin hAd-MSC in pluripotency characterisation assay, at least at mRNA level. Precautionary step can be adopted to overcome the undesirable contamination from feeder cells. For example, cell sorting method could be imposed at the time of harvesting AML-M5-derived iPSCs for RNA extraction (Basu et al., 2010). Cell sorting is a technique to isolate cells according to their cell properties such as surface antigens (Basu et al., 2010; Foo, 2013). This method has been commonly used to separate different cell types from heterogeneous cell mixture including

organs and tissues (Basu et al., 2010; Foo, 2013). With this technique, feeder cells can be completely removed and ruled out the possibility of contamination.

Though the MLL-AF9 fusion oncogene was retained, there is a possibility that AML-M5-derived iPSCs have reduced oncogenic properties compared to parental AML-M5 cells. Perhaps the reduction of tumorigenic properties in reprogrammed cancer cells affects sensitivity towards chemotherapy (Kumano et al., 2012). More assays are needed to ensure the cancer properties of the reprogrammed cells prior to use as a disease model. Assays including DNA methylation analysis and whole-transcriptome sequencing which allow closer look at post-transcriptional modifications, gene fusion, changes in gene expression and gene regulation (Miyoshi et al., 2012; Zhang et al., 2012a; Liu et al., 2013).

6.3 Future Studies

Since the AML-M5-derived iPSCs were able to recapitulate cancer phenotypes through expression of MLL-AF9 fusion protein, it is expected to offer a novel opportunity to establish disease models *in vitro*. For example, CML-derived iPSC that consistently expressed BCR-ABL fusion protein was used as a disease model to investigate the response of cancer cells to therapeutic agent, imatinib (Kumano et al., 2012). This model provided precious opportunity to understand cancer cell behaviour and ultimately contributed to the discovery of effective therapeutic strategies such potential drug and gene therapy. In recent years, iPSC technique may in fact used to cure inheritance diseases. A proof-of principle experiment demonstrated a successful cure of sickle cell anaemia was reported by corrected defect sickle globin gene (Hanna et al., 2007). Another example was the use of haemophilia-derived iPSC in the correction of disease genotypes whereby the corrected cells regained their function in blood clotting mechanism (Xu et al., 2009). Development of a disease model using the AML-M5-derived iPSCs to recapitulate disease phenotype of AML-M5 may help to elucidate AML-M5 pathogenesis, the correction of *MLL-AF9* mutation in AML-M5 may be achievable in future and aid in identification of novel therapeutic approaches such as targeted drug therapy.

REFERENCES

- Aasen, T., 2008. Efficient and rapid generation of induced pluripotent stem cells from human keratinocytes. *Nature Biotechnology*, 26, pp. 1276-1284.
- Abbott, B.L. et al., 2003. Clinical significance of central nervous system involvement at diagnosis of pediatric acute myeloid leukemia: a single institution's experience. *Leukemia*, 17, pp. 2090-2096.
- Adjaye, J. et al., 2005. Primary differentiation in the human blastocyst: comparative molecular portraits of inner cell mass and trophectoderm cells. *Stem Cells*, 23(10), pp. 1514-1525.
- Amit, M. et al., 2003. Human feeder layers for human embryonic stem cells. *Biology of Reproduction*, 68(6), pp. 2150-2156.
- Andreadis, S. et al., 2000. Toward a more accurate quantitation of the activity of recombinant retroviruses: alternatives to titer and multiplicity of infection. *Journal of Virology*, 74(3), pp. 1258-1266.
- Andrews, P.W., Meyer, L.J., Bednarz, K.L. and Harris, H., 1984. Two monoclonal antibodies recognizing determinants on human embryonal carcinoma cells react specifically with the liver isozyme of human alkaline phosphatase. *Hybridoma*, 3, pp. 33-39.
- Ankye-Danso, F., Snitow, M. and Morrisey, E.E., 2012. How microRNAs facilitate reprogramming to pluripotency. *Journal of Cell Science*, 125, pp. 1-9.
- Anokye-Danso, F. et al., 2011. Highly efficient miRNA-mediated reprogramming of mouse and human somatic cells to pluripotency. *Cell Stem Cell*, 8, pp. 376-388.
- Anson, D.S., 2004. The use of retroviral vectors for gene therapy-what are the risks? A review of retroviral pathogenesis and its relevance to retroviral vector-mediated gene delivery. *Genetic Vaccines and Therapy*, 2, pp. 1-9.
- Avilion, A.A. et al., 2003. Multipotent cell lineages in early mouse development depend on SOX2 function. *Genes and Development*, 17, pp. 126-140.
- Ayton, P.M. and Clearly, M.L., 2001. Molecular mechanisms of leukemogenesis mediated by MLL fusion proteins. *Oncogene*, 20, pp. 5695-5707.
- Baldwin, A., 2009. Morality and human embryo research. Introduction to the talking point on morality and human embryo research. *EMBO reports*, 10(4), pp. 299-300.

- Balgobind, B.V. et al., 2011. Integrative analysis of type-I and type-II aberration underscores the genetic heterogeneity of pediatric acute myeloid leukemia. *Haematologica*, 96(10), pp. 1478-1487.
- Barrett, A.J. and Battiwalla, M., 2010. Relapse after allogeneic stem cell transplantation. *Expert Review of Hematology*, 3(4), pp. 429-441.
- Basu, S., Campbell, H.M., Dittel, B.N. and Ray, A. 2010. Purification of specific cell population by fluorescence activated cell sorting (FACS). *Journal of Visualized Experiments*, (41), pp. 1546-1549.
- Ben-Nun, I.F. et al., 2011. Induced pluripotent stem cells from highly endangered species. *Nature Methods*, 8, pp. 829-831.
- Bendall, S.C. et al., 2007. IGF and FGF cooperatively establish the regulatory stem cell niche of pluripotent human cells in vitro. *Nature*, 448(7157), pp. 1015-1021.
- Berggren, W.T., Lutz, M., and Modesto, V., 2012. General Spinection Protocol. In: StemBook, (ed.). *The Stem Cell Research Community*. California: StemBook, pp. 1-3.
- Bertani, S., Sauer, S., Bolotin, E. and Sauer, F., 2011. The noncoding RNA mistral activates Hoxa6 and Hoxa7 expression and stem cell differentiation by recruiting MLL1 to chromatin. *Molecular Cell*, 43, pp. 1040-1046.
- Bisschop, M.M. et al., 2001. Extramedullary infiltrates at diagnosis have no prognostic significance in children with acute myeloid leukaemia. *Leukemia*, 15, pp. 46-49.
- Bloomfield, C.D. and Brunning, R. D., 1985. The revised French-American-British classification of acute myeloid leukemia: is new better? *Annals of Internal Medicine*, 103, pp. 614-616.
- Boyer, L.A. et al., 2005. Core transcriptional regulator circuitry in human embryonic stem cells. *Cell*, 122, pp.947-956.
- Bruno, B. et al., 2007. A comparison of allografting with autografting for newly diagnosed myeloma. *The New England Journal of Medicine*, 356, pp. 1110-1120.
- Bruce, S.J. et al., 2007. Dynamic transcription programs during ES cell differentiation towards mesoderm in serum versus serum-free BMP4 culture. *BMC Genomics*, 8, pp. 365-390.
- Buta, C. et al., 2013. Reconsidering pluripotency tests: Do we still need teratoma assays? *Stem Cell Research*, 11(1), pp. 552-562.

- Cahan, P. and Daley, G.Q., 2013. Origins and implications of pluripotent stem cell variability and heterogeneity. *Nature Reviews Molecular Cell Biology*, 14, pp. 357-368.
- Cai, J. et al., 2010. Generation of human induced pluripotent stem cells from umbilical cord matrix and amniotic membrane mesenchymal cells. *Journal of Biology Chemistry*, 285, pp. 11227-11234.
- Calloni, R., Alicia Aparicio Cordero, E., Antonio Pegas Henriques, J. and Bonatto, D., 2013. Reviewing and Updating the Major Molecular Markers for Stem Cells. *Stem Cells and Development*, 22(9), pp. 1455-1476.
- Carette, J.E. et al., 2010. Generation of iPSCs from cultured human maglinant cells. *Blood*, 115, pp. 4039-4042.
- Carey, B.W. et al., 2009. Reprogramming of murine and human somatic cells using a single polycistronic vector. *Proceedings of the National Academy of Sciences*, 106, pp. 157-162.
- Carey, B.W. et al., 2011. Reprogramming factor stoichiometry influences the epigenetic state and biological properties of induced pluripotent stem cells. *Cell Stem Cell*, 9, pp. 588-598.
- Chandra, P. et al., 2010. Acute myeloid leukemia with t(9;11)(p21-22;q23). *American Journal of Clinical Pathology*, 133, pp. 686-693.
- Chapman-Smith, A. and Whitelaw, M., 2006. Novel DNA binding by a basic helix-loop-helix protein. *The Journal of Biological Chemistry*, 281(18), pp. 12535-12545.
- Chauhan, P.S. et al., 2013. Mutation of NPM1 and FLT3 genes in acute myeloid leukemia and their association with clinical immunophenotypic features. *Disease Markers*, 35(5), pp. 581-588.
- Chen, L. et al., 2013. Abrogation of MLL-AF10 and CALM-AF10-mediated transformation through genetic inactivation or pharmacological inhibition of the H3K79 methyltransferase Dot1l. *Leukemia*, 27(4), pp. 813-822.
- Cheng, L., Hammond, H., Ye, Z., Zhan, X. and Dravid, G., 2003. Human adult marrow cells support prolonged expansion of human embryonic stem cells in culture. *Stem Cell*, 21(2), pp. 131-142.
- Cheng, J. and Sakamoto, K.M., 2005. Topics in pediatric leukemia- Acute myeloid leukemia. *Medscape General Medicine*, 7(1), pp. 20-25.
- Chin, M.H. et al., 2009. Induced pluripotent stem cells and embryonic stem cells are distinguished by gene expression signatures. *Cell Stem Cell*, 5, pp. 111-123.

- Choi, S. M. et al., 2011. Reprogramming of EBV-immortalized B-lymphocyte cell lines into induced pluripotent stem cells. *Blood*, 118, pp. 1801-1805.
- Chun, Y.S., Chaudhari, P. and Jang, Y.Y., 2010. Applications of patient-specific induced pluripotent stem cells; focused on disease modeling, drug screening and therapeutic potentials for liver disease. *International Journal of Biological Science*, 6(7), pp. 796-805.
- Cohen, D.E. and Melton, D., 2011. Turning straw into gold: directing cell fate for regenerative medicine. *Nature Reviews Genetics*, 12, pp. 243-252.
- Collina, E.C. et al., 2002. Mouse Af9 is a controller of embryo patterning, like Mll, whose human homologue fuses with Af9 after chromosomal translocation in leukemia. *Molecular and Cell Biology*, 22(20), pp. 7313-7324.
- Cornetta, K., Matheson, L. and Ballas, C., 2005. Retroviral vector production in the National Gene Vector Laboratory at Indiana University. *Gene Therapy*, 12, pp. 28-35.
- Corral, J. et al., 1993. Acute leukemias of different lineages have similar MLL gene fusions encoding related chimeric proteins resulting from chromosomal translocation. *Proceedings of the National Academy of Sciences*, 90(18), pp. 8538-8542.
- Corral, J. et al., 1996. An Mll-AF9 fusion gene made by homologous recombination causes acute leukemia in chimeric mice: a method to create fusion oncogenes. *Cell*, 85(5), pp. 853-861.
- Coutu, D.L. and Galipeau, J., 2011. Roles of FGF signalling in stem cell self-renewal, senescence and aging. *Aging*, 3(10), pp. 920-933.
- Crook, J.M., Hei, D. and Stacey, G., 2010. International Stem Cell Banking Initiative: raising standards to bank on. *In Vitro Cellular & Developmental Biology*, 46, pp. 169-172.
- Dang, C.V., 1999. c-Myc target genes involved in cell growth, apoptosis, and metabolism. *Molecular and Cellular Biology*, 19(1), pp. 1-11.
- Dang, C.V., 2012a. MYC on the path to cancer. *Cell*, 149, pp. 22-35.
- Dang, C.V., 2012b. Cancer cell metabolism: there is no ROS for the weary. *Cancer Discovery*, 2, pp. 304-307.
- Davies, J.A., 1996. Mesenchyme to epithelium transition during development of the mammalian kidney tubule. *Acta Anatomica*, 156(3), pp. 187-201.
- Davis, H.E., Morgan, J.R. and Yarmush, M.L., 2002. Polybrene increases retrovirus gene transfer efficiency by enhancing receptor-independent virus adsorption on target cell membranes. *Biophysical Chemistry*, 97(2), pp. 159-172.

- DeLorey, T.M. et al., 1998. Mice lacking the $\beta 3$ subunit of the GABA_A receptor have the epilepsy phenotype and many of the behavioural characteristics of Angelman syndrome. *The Journal of Neuroscience*, 18(20), pp. 8505-8514.
- Desai, N., Rambhia, P. and Gishto, A., 2015. Human embryonic stem cell cultivation: historical perspective and evolution of xeno-free culture systems. *Reproduction Biology and Endocrinology*, 13, pp. 9-23.
- Dewald, W. et al., 1983. A possible specific chromosome marker for monocytic leukemia: three more patients with t(9;11)(p22;q24) and another with t(11;17)(q24;q21), each with acute monoblastic leukemia. *Cancer Genetics and Cytogenetics*, 8(3), pp. 203-212.
- Ding, S. et al., 2005. Efficient transposition of the piggyBac (PB) transposon in mammalian cells and mice. *Cell*, 122, pp. 473-483.
- Dimos, J.T. et al., 2008. Induced pluripotent stem cells generated from patients with ALS can be differentiated into motor neurons. *Science*. 321, pp. 1218-1221.
- Dobson, C.L. et al., 1999. The *Mll-AF9* gene fusion in mice controls myeloproliferation and specifies acute myeloid leukaemogenesis. *EMBO Journal*, 18, pp. 3564-3574.
- Ebert, A.L. et al., 2009. Induced pluripotent stem cells from a spinal muscular atrophy patient. *Nature*, 457, pp. 277-280.
- El-Sayed, A., Futaki, S. and Harashima, H., 2009. Delivery of macromolecules using arginine-rich cell-penetrating peptides: Ways to overcome endosomal entrapment. *The AAPS Journal*, 11(1), pp.13-22.
- Eminli, S., Utikal, J., Arnold, K., Jaenisch, R. and Hochedlinger, K., 2008. Reprogramming of neural progenitor cells into induced pluripotent stem cells in the absence of exogenous Sox2 expression. *Stem cells*, 26, pp. 2467-2474.
- Esteban, M.A. et al., 2010. Vitamin C enhances the generation of mouse and human induced pluripotent stem cells. *Cell Stem Cell*, 6, pp. 71-79.
- Estey, E.H., 2012. Acute myeloid leukemia: 2012 update on diagnosis, risk stratification, and management. *American Journal of Hematology*, 87, pp. 89-99.
- Evans, P.M. and Liu, C., 2008. Role of Krüppel-like factor 4 in normal homeostasis, cancer, and stem cells. *Acta Biochimica et Biophysica Sinica*, 40(7), pp. 554-564.
- Ezashi, T., Das, P. and Roberts, R.M., 2005. Low O₂ tensions and the prevention of differentiation of hES cells. *Proceedings of the National Academy of Sciences*, 102(13), pp. 4783-4788.

- Fang, R. et al., 2014. Generation of naïve pluripotent stem cells from rhesus monkey fibroblasts. *Cell Stem Cell*, 15(4), pp. 488-496.
- Feltes, B.C. and Bonatto, D., 2013. Combining small molecules for cell reprogramming through an interatomic analysis. *Molecular BioSystems*, 9, pp. 2741-2763.
- Fanning, S.R., Sekeres, M.A. and Theil, K., 2009. *Acute myelogenous leukemia* [Online]. Available at: <http://www.clevelandclinicmeded.com/medicalpubs/diseasemanagement/hematology-oncology/acute-myelogenous-leukemia/> [Accessed: 17 March 2015]
- Feng, C., Jia, Y.-D. and Zhao, X.-Y., 2013. Pluripotency of Induced Pluripotent Stem Cells. *Genomics, Proteomics & Bioinformatics*, 11(5), pp. 299-303.
- Fleischmann, K.K. et al., 2014. RNAi-mediated silencing of MLL-AF9 reveals leukemia-associated downstream targets and processes. *Molecular cancer*, 13, pp. 27-41.
- Foo, L.C. 2013. Purification of astrocytes from transgenic rodents by fluorescence-activated cell sorting. *Cold Spring Harbor Protocols*, 2013, pp. 551-561.
- Fong, H., Hohenstein, K.A. and Donovan, P.J., 2008. Regulation of self-renewal and pluripotency by Sox2 in human embryonic stem cells. *Stem Cells*, 26(8), pp. 1931-1938.
- Forestell, S.P., Bohnlein, E. and Rigg, R.J., 1995. Retroviral end-point titer is not predictive of gene transfer efficiency: implications for vector production. *Gene therapy*, 2(10), pp. 723-730.
- Foster, K.W. et al., 2005. Induction of KLF4 in basal keratinocytes blocks the proliferation-differentiation switch and initiates squamous epithelial dysplasia. *Oncogene*, 24, pp. 1491-1500.
- Fu, J.F., Liang, D.C. and Shih, L.Y., 2007. Analysis of acute leukemias with MLL/ENL fusion transcripts: identification of two novel breakpoints in ENL. *American Journal of Clinical Pathology*, 127(1), pp. 24-30.
- Gan, T., Jude, C.D., Zaffuto, K. and Ernst, P., 2010. Developmentally induced Mll1 loss reveals defects in postnatal haematopoiesis. *Leukemia*, 24(10), pp. 1732-1741.
- Godley, L.A. and Larson, R.A., 2008. Therapy-related myeloid leukemia. *Seminars in Oncology*, 35 (4), pp. 418-429.
- Gonzalez, F., Boue, S. and Izpisua Belmonte, J.C., 2011. Methods for making induced pluripotent stem cells; reprogramming a la carte. *Nature Reviews Genetics*, 12, pp. 231-242.

- Gordan, J.D., Thompson, C.B. and Simon, M.C., 2007. HIF and c-Myc: sibling rivals for control of cancer cell metabolism and proliferation. *Cancer Cell*, 12, pp. 108-113.
- Gutierrez-Aranda, I. et al., 2010. Human induced pluripotent stem cells develop teratoma more efficiently and faster than human embryonic stem cells regardless the site of injection. *Stem Cells*, 28(9), pp. 1568-1570.
- Haase, A. et al., 2009. Generation of induced pluripotent stem cells from human cord blood. *Cell Stem cell*, 5, pp. 434-441.
- Hanahan, D. and Weinberg, R.A., 2011. Hallmarks of cancer: The next generation. *Cell*, 144, pp. 648-674.
- Hanna, J. et al., 2007. Treatment of sickle cell anemia mouse model with iPS cells generated from autologous skin. *Science*. 318(5858), pp. 1920-1923.
- Hanna, J. et al., 2008. Direct reprogramming of terminally differentiated mature B lymphocytes to pluripotency. *Cell*, 133, pp. 250-264.
- Hanna, J. et al., 2010. Human embryonic stem cells with biological and epigenetic characteristics similar to those of mouse ESCs. *Proceedings of the National Academy of Sciences*, 107, pp. 9222-9227.
- Hass, R., Kasper, C., Böhm, S. and Jacobs, R. 2011. Different populations and sources of human mesenchymal stem cells (MSC): A comparison of adult and neonatal tissue-derived MSC. *Cell Communication and Signaling*, 9, pp. 12-25.
- He, S., Nakada, D. and Morrison, S.J. 2009. Mechanisms of stem cell self-renewal. *Annual Review of Cell and Developmental Biology*, 25, pp. 377-406.
- He, H., Hua, X. and Yan, J., 2011. Epigenetic regulations in hematopoietic Hox code. *Oncogene*, 30(4), pp. 379-388.
- Heim, S. et al., 1987. A new specific chromosomal rearrangement, t(8;16) (p11;p13), in acute monocytic leukaemia. *British Journal of Haematology*, 66(3), pp. 323-326.
- Hochedlinger, K. and Plath, L., 2009. Epigenetic reprogramming and induced pluripotency. *Development*, 136, pp. 509-523.
- Hottam A. and Ellis, J., 2008. Retroviral vector silencing during iPS cell induction: An epigenetic beacon that signals distinct pluripotent states. *Journal of Cellular Biology*, 105(4), pp. 940-948.
- Houbaviy, H.B., Murray, M.F. and Sharp, P.A., 2003. Embryonic stem cell specific microRNAs. *Developmental Cell*, 5, pp. 351-358.

- Hovatta, O. et al., 2003. A culture system using human foreskin fibroblasts as feeder cells allows production of human embryonic stem cells. *Human Reproduction*, 18(7), pp. 1404-1409.
- Hsieh, J.J., Ernst, P., Erdjument-Bromage, H., Tempst, P. and Korsmeyer, S.J., 2003. Proteolytic cleavage of MLL generates a complex of N- and C-terminal fragments that confers protein stability and subnuclear localization. *Molecular and Cell Biology*, 23(1), pp. 186-194.
- Hu, K. and Slukvin, I., 2013. Generation of transgene-free iPSC lines from human normal and neoplastic blood cells using episomal vectors. *Methods in Molecular Biology*, 997, pp. 163-176.
- Huangfu, D. et al., 2008a. Induction of pluripotent stem cells by defined factors is greatly improved by small-molecule compounds. *Nature Biotechnology*, 26(7), pp. 795-797.
- Huangfu, D. et al., 2008b. Induction of pluripotent stem cells from primary human fibroblast with only *Oct4* and *Sox2*. *Nature Biotechnology*, 26(11), pp. 1269-1275.
- Huang, M. et al., 2009. Novel minicircle vector for gene therapy in murine myocardial infarction. *Circulation*, 120, pp. 230-237.
- Ichida, J.K. et al., 2009. A small-molecule inhibitor of tgf-Beta signalling replaces *sox2* in reprogramming by inducing *nanog*. *Cell Stem Cell*, 5, pp. 491-503.
- Jaso, J.M., Wang, S.A., Jorgensen, J.L. and Lin, P., 2014. Multi-color flow cytometric immunophenotyping for detection of minimal residual disease in AML: past, present and future. *Bone Marrow Transplantation*, 49, pp. 1129-1138.
- Jia, F. et al., 2010. A nonviral minicircle vector for deriving human iPS cells. *Nature Methods*, 7, pp. 197-199.
- Jiang, J. et al., 2008. A core Klf circuitry regulates self-renewal of embryonic stem cells. *Nature Cell Biology*, 10(3), pp. 353-360.
- Johnson, J.J. et al., 2003. Prenatal and postnatal myeloid cells demonstrate stepwise progression in the pathogenesis of MLL fusion gene leukemia. *Blood*, 101, pp. 3229-3235.
- Judson, R.L., Babiarz, J.E., Venere, M. and Belloch, R., 2009. Embryonic stem cell-specific microRNAs promote induced pluripotency. *Nature Biotechnology*, 27, pp. 459-461.
- Jung, D.W., Kim, W.H. and Williams, D.R., 2014. Reprogram or reboot: small molecule approaches for the production of induced pluripotent stem cells and direct cell reprogramming. *ACS Chemical Biology*, 9(1), pp. 80-95.

- Kaji, K. et al., 2009. Virus-free induction of pluripotency and subsequent excision of reprogramming factors. *Nature*, 458, pp. 771-775.
- Kamachi, Y. and Kondoh, H., 2013. Sox proteins: regulators of cell fate specification and differentiation. *Development*, 140, pp. 4129-4144.
- Kawamura, T. et al., 2009. Linking the p53 tumour suppressor pathway to somatic cell reprogramming. *Nature*, 460, pp. 1140-1144.
- Kay, M.A., He, C.Y. and Chen, Z.Y., 2010. A robust system for production of minicircle DNA vectors. *Nature Biotechnology*, 28, pp. 1287-1289.
- Kheyrodin, H. and Ghazvinian, K., 2011. DNA purification and isolation of genomic DNA from bacterial species by plasmid purification system. *African Journal of Agricultural Research*, 7(3), pp. 433-442.
- Kim, J.B. et al., 2008. Pluripotent stem cells induced from adult neural stem cells by reprogramming with two factors. *Nature*, 454, pp. 646-650.
- Kim, D.H. et al., 2009. Generation of human induced pluripotent stem cells by direct delivery of reprogramming proteins. *Cell Stem cell*, 4, pp. 472-476.
- Kim, J.S. et al., 2013. An iPSC line from human pancreatic ductal adenocarcinoma undergoes early to invasive stages of pancreatic cancer progression. *Cell Reports*, 3, pp. 2088-2099.
- King, R.C., Stansfield, W.D. and Mulligan, P.K., 2006. *A dictionary of genetics*, 7th ed. London: Oxford University Press.
- Kohlmann, A. et al., 2005. New insights into MLL gene rearranged acute leukemias using gene expression profiling: shared pathways, lineage commitment, and partner genes. *Leukemia*, 19, pp.953-964.
- Krampera, M., Franchini, M., Pizzolo, G. and Aprili, G. 2007. Mesenchymal stem cells: from biology to clinical use. *Blood Transfusion*, 5(3), pp. 120-129.
- Kulcenty, K., Wróblewska, J., Mazurek, S., Liszewska, E. and Jaworski, J., 2015. Molecular mechanisms of induced pluripotency. *Contemporary Oncology*, 19(1A), pp. 22-29.
- Kumano, K. et al., 2012. Generation of induced pluripotent stem cells from primary chronic myelogenous leukemia patient samples. *Blood*, 119(26), pp. 6234-6242.
- Kumar, C.C., 2011. Genetic abnormalities and challenges in the treatment of acute myeloid leukemia. *Genes and Cancer*, 2(2), pp. 95-107.
- Kurosawa, H., 2007. Methods for inducing embryoid body formation: in vitro differentiation system of embryonic stem cells. *Journal of Bioscience and Bioengineering*, 103(5), pp. 389-398.

- Lai, J.L. et al., 1992. Acute monocytic leukemia with (8;22) (p11;q23) translocation. Involvement of 8p11 as in classical t(8;16) (p11;p13). *Cancer Genetics and Cytogenetics*, 60(2), pp. 180-182.
- Lane, S.W., Williams, D.A. and Watt, F.M., 2014. Modulating the stem cell niche for tissue regeneration. *Nature Biotechnology*, 32, pp. 795-803.
- Lapasset, L. et al., 2011. Rejuvenating senescent and centenarian human cells by reprogramming through the pluripotent state. *Genes & Development*, 25, pp. 2248-2253.
- Lee, R.C., Feinbaum, R.L. and Ambros, V., 1993. The *C. elegans* heterochronic gene *lin-4* encodes small RNAs with antisense complementarity to *lin-14*. *Cell*, 75, pp. 843-854.
- Lee, D.H. and Chung, H.M., 2011. Differentiation into endoderm lineage: pancreatic differentiation from embryonic stem cells. *International Journal of Stem Cells*, 4(1), pp. 35-42.
- Lee, G. and Studer, L., 2011. Modelling familial dysautonomia in human induced pluripotent stem cells. *Philosophical Transactions of the Royal Society Biological Sciences*, 366, pp. 2286-2296.
- Levenberg, S., 2002. Endothelial cells derived from human embryonic stem cells. *Proceedings of the National Academy of Sciences*, 99(7), pp. 4391-4396.
- Lewinski, M.K. et al., 2006. Retroviral DNA integration: Viral and cellular determinants of target-site selection. *PLoS Pathogens*, 2(6), pp. 611-622.
- Li, L. and Xie, T., 2005. Stem cell niche: structure and function. *Annual Review of Cell and Developmental Biology*, 21, pp. 605-631.
- Li, J., Shen, Y., Liu, A., Wang, X. and Zhao, C. 2008. Transfection of the DAAO gene and subsequent induction of cytotoxic oxidative stress by D-alanine in 9L cells. *Oncology Reports*, 20, pp. 341-346.
- Li, W. et al., 2009. Generation of human-induced pluripotent stem cells in the absence of exogenous Sox2. *Stem Cell*, 27, pp. 2992-3000.
- Li, Y. et al., 2011. Generation of iPSCs from mouse fibroblasts with a single gene, Oct4, and small molecules. *Cell Research*, 21(1), pp. 196-204.
- Lichtman, M.A., 1995. Acute myelogenous leukemia. In: Beutler, E., Lichtman, M.A., Coller, B.S. and Kipps, T.J. (eds). *Williams Hematology*. New York; McGraw-Hill, pp. 272-298.
- Lida, S. et al., 1993. *MLLT3* gene on 9p22 involved in t(9;11) leukemia encodes a serine/proline rich protein homologous to *MLLT1* on 19p13. *Oncogene*, 11, pp. 3085-3092.

Lim, D.A. et al., 2000. Noggin antagonizes BMP signalling to create a niche for adult neurogenesis. *Neuron*, 28, pp. 713-726.

Lin, S.L. et al., 2008. Mir-302 reprograms human skin cancer cells into a pluripotent ES-cell-like state. *RNA*, 14, pp. 2115-2124.

Lin, T. et al., 2009. A chemical platform for improved induction of human iPSCs. *Nature Methods*, 6, pp. 805-808.

Lin, T. et al., 2011. Regulation of somatic cell reprogramming through inducible mir-302 expression. *Nucleic Acids Research*, 39, pp. 1054-1065.

Lin, T. and Wu, S., 2015. Reprogramming with small molecules instead of exogenous transcription factors. *Stem Cells International*, 13(9), pp. 1-11.

Liu, X.S. et al., 2008. Yamanaka factors critically regulate the developmental signalling network in mouse embryonic stem cells. *Cell Research*, 18, pp. 1177-1189.

Liu, H., Cheng, E.H. and Hsieh, J.J., 2009. MLL fusions: pathways to leukemia. *Cancer Biology and Therapy*, 8, pp. 1204-1211.

Liu, H. et al., 2010. Generation of endoderm-derived human induced pluripotent stem cells from primary hepatocytes. *Hepatology*, 51, pp. 1810-1819.

Liu, Y. et al., 2013. Reprogramming of MLL-AF9 leukemia cells into pluripotent stem cells. *Leukemia*, 2013, pp. 1-10.

Loh, Y.H. et al., 2006. The Oct4 and Nanog transcription network regulates pluripotency in mouse embryonic stem cells. *Nature Genetics*, 38, pp. 431-440.

Loh, Y.H. et al., 2009. Generation of human induced pluripotent stem cells from human blood. *Blood*, 113, pp. 5476-5479.

Lowry, W.E. et al., 2008. Generation of human induced pluripotent stem cells from dermal fibroblasts. *Proceedings of the National Academy of Sciences*, 105, pp. 2883-2888.

Löwenberg, B., Downing, J.R. and Burnett, A., 1999. Acute myeloid leukemia. *The New England Journal of Medicine*, 341(14), pp. 1051-1062.

Lyssiotis, C.A. et al., 2009. Reprogramming of murine fibroblasts to induced pluripotent stem cells with chemical complementation of Klf4. *Proceedings of the National Academy of Sciences*, 106(22), pp. 8912-8917.

Ma, H. and Young, M., 2014. The octamer-binding transcription factor 4 (Oct-4) and stem cell literatures. *Stem Cell*, 5(3), pp. 26-41.

- Mahalingam, D. et al., 2012. Reversal of aberrant cancer methylome and transcriptome upon direct reprogramming of lung cancer cells. *Scientific Reports*, 2, pp. 592-599.
- Maherali, N. et al., 2007. Directly reprogrammed fibroblasts show global epigenetic remodelling and widespread tissue contribution. *Cell Stem Cell*, 1, pp. 55-70.
- Maherali, N. and Hochedlinger, K., 2008. Guidelines and techniques for the generation of induced pluripotent stem cells. *Cell Stem Cells*, 3, pp. 595-605.
- Maherali, N. et al., 2008. A high-efficiency system for the generation and study of human induced pluripotent stem cells. *Cell Stem cell*, 3, pp. 340-345.
- Maherali, N. and Hochedlinger, K., 2009. Tgfbeta signal inhibition cooperates in the induction of iPSCs and replaces Sox2 and cMyc. *Current Biology*, 19, pp. 374-382.
- Malik, B. and Hemenway, C.S., 2013. CBX8, a component of the Polycomb PRC1 complex, modulates DOT1L-mediated gene expression through AF9/MLLT3. *FEBS Letters*, 587(18), pp. 3038-3044.
- Mandal, P.K. and Rossi, D.J., 2013. Reprogramming human fibroblasts to pluripotency using modified mRNA. *Nature Protocols*, 8, pp. 568-582.
- Marión, R.M. et al., 2009. A p53-mediated DNA damage response limits reprogramming to ensure iPS cell genomic integrity. *Nature*, 460, pp. 1149-1153.
- Marson, A. et al., 2008. Wnt signalling promotes reprogramming of somatic cell to pluripotency. *Cell Stem Cell*, 3, pp. 132-135.
- Marti, M. et al., 2013. Characterization of pluripotent stem cells. *Nature Protocol*, 8(2), pp. 223-253.
- Masaki, H. et al., 2008. Heterogeneity of pluripotent marker gene expression in colonies generated in human iPS cell induction culture. *Stem Cell Research*, 2008(1), pp. 105-115.
- Masui, S. et al., 2007. Pluripotency governed by Sox2 via regulation of Oct3/4 expression in mouse embryonic stem cells. *Nature Cell Biology*, 9(6), pp. 625-635.
- McCormack, E., Bruserud, O. and Gjertsen, B.T., 2008. Review: genetic models of myeloid leukaemia. *Oncogene*, 27, pp. 3765-3779.
- Medvedev, S.P., Shevchenko, A.I. and Zakian, S.M., 2010. Induced pluripotent stem cells: Problems and advantages when applying them in regenerative medicine. *Acta Naturae*, 2(2), pp. 18-28.

- Mikkelsen, T.S. et al., 2008. Dissecting direct reprogramming through integrative genomic analysis. *Nature*, 454, pp. 49-55.
- Mimasu, S. et al., 2008. Crystal structure of histone demethylase LSD1 and tranlycypromine at 2.25 Å. *Biochemical and Biophysical Research Communications*, 366, pp. 15-22.
- Miyoshi, N. et al., 2010. Defined factors induce reprogramming of gastrointestinal cancer cells. *Proceedings of the National Academy of Science*, 107(1), pp. 40- 45.
- Miyoshi, N. et al., 2011. Reprogramming of mouse and human cells to pluripotency using mature microRNAs. *Cell Stem Cell*, 8, pp. 633-638.
- Mohyeldin, A., Garzón-Muvdi, T. and Quinones-Hinojosa, A., 2010. Oxygen in stem cell biology: A critical component of the stem cells niche. *Cell Stem Cell*, 7(2), pp. 150-161.
- Montes, R. et al., 2009. Feeder-free maintenance of hESCs in mesenchymal stem cell-conditioned media: distinct requirements for TGF-beta and IGF-II. *Cell Research*, 19(6), pp. 698-709.
- Moriya, K. et al., 2012. Development of a multi-step leukemogenesis model of MLL-rearranged leukemia using humanized mice. *PLoS ONE*, 7(6), pp. 1-12.
- Mrózek, K. and Bloomfield, C.D., 2012. Acute myeloid leukemia with adverse cytogenetic risk. *Oncology (Williston Park)*, 26(8), pp. 714-723.
- Murnmery, C.L. et al., 2012. Differentiation of human embryonic stem cells and induced pluripotent stem cells to cardiomyocytes. *Circulation Research*, 111, pp. 344-358.
- Müller, F.J. et al., 2011. A bioinformatics assay for pluripotency in human cells. *Nature Methods*, 8, pp. 315-317.
- Nakagawa, M. et al., 2008. Generation of induced pluripotent stem cells without Myc from mouse and human fibroblasts. *Nature Biotechnology*, 26, pp. 101-106.
- Nakagawa, M. et al., 2010. Promotion of direct reprogramming by transformation-deficient Myc. *Proceedings of the National Academy of Science*, 107(32), pp. 14152-14157.
- Nakatake, Y. et al., 2006. Klf4 cooperates with Oct3/4 and Sox2 to activate the Lefty1 core promoter in embryonic stem cells. *Molecular in Cell Biology*, 26(20), pp. 7772-7782.
- Narsinh, K. et al., 2011a. Generation of adult human induced pluripotent stem cells using nonviral minicircle DNA vectors. *Nature Protocols*, 6(1), pp. 78-88.

Narsinh, K., Narsinh, K. H. and Wu, J. C., 2011b. Derivation of human induced pluripotent stem cells for cardiovascular disease modelling. *Circulation Research*, 108, pp. 1146-1156.

National Cancer Registry, 2007. National Cancer Registry Report Malaysia Cancer Statistics – Data and Figure 2007. [Online] Available at: http://www.care.upm.edu.my/dokumen/13603_NCR2007.pdf [Accessed 19 May 2015].

Neff, T. and Armstrong, S.A., 2013. Recent progress toward epigenetic therapies: the example of mixed lineage leukemia. *Blood*, 121(24), pp. 4847-4853.

Nishikawa, S., Goldstein, R.A. and Nierras, C.R., 2008. The promise of human induced pluripotent stem cells for research and therapy. *Nature Reviews Molecular Cell Biology*, 9(9), pp. 725-729.

Nin, D.S. et al., 2012. Role of misfolded N-CoR mediated transcriptional deregulation of Flt3 in acute monocytic leukemia (AML)-M5 subtype. *PLoS ONE*, 7 (4), pp. 1-11.

Niwa, H., Miyazaki, J. and Smith, A.G., 2000. Quantitative expression of Oct-3/4 defines differentiation, dedifferentiation or self-renewal of ES cells. *Nature Genetic*, 24, pp. 372-376.

Ohnishi, K. et al., 2014. Premature termination of reprogramming in vivo leads to cancer development through altered epigenetic regulation. *Cell Stem Cell*, 4(3), pp. 269-271.

Okano, M., Bell, D. W., Haber, D. A. and Li, E., 1999. DNA Methyltransferases Dnmt3a and Dnmt3b are essential for de novo methylation and mammalian development. *Cell*, 99(3), pp. 247-257.

Okita, K., Ichisaka, T. and Yamanaka, S., 2007. Generation of germline-competent induced pluripotent stem cells. *Nature*, 448, pp. 313-317.

Osten, P., Grinevich, V. and Cetin, A., 2007. Viral vectors: a wide range of choices and high levels of service. *Handbook of Experimental Pharmacology*, 178, pp. 177-202.

Palmqvist, L. et al., 2005. Correlation of murine embryonic stem cell gene expression profiles with functional measures of pluripotency. *Stem Cells*, 23, pp. 663-680.

Pan, G., Chang, Z.Y., Scholer, H.R. and Pei, D., 2002. Stem cell pluripotency and transcription factor Oct4. *Cell Research*, 12, pp. 321-329.

Pan, G., Li, J., Zhou, Y., Zheng, H. and Pei, D., 2006. A negative feedback loop of transcription factors that controls stem cell pluripotency and self-renewal. *The FASEB Journal*, 20(10), pp. 1730-1732.

- Pan, G. and Thomson, J. A., 2007. Nanog and transcriptional networks in embryonic stem cell pluripotency. *Cell Research*, 17, pp. 42-49.
- Papapetrou, E.P., et al., 2009. Stoichiometric and temporal requirements of Oct4, Sox2, Klf4, and c-Myc expression for efficient human iPSC induction and differentiation. *Proceedings of the National Academy of Science*, 106, pp. 12759-12764.
- Papapetrou, E.P. and Sadelain, M., 2011. Generation of transgene-free human induced pluripotent stem cells with an excisable single polycistronic vector. *Nature Protocols*, 6(9), pp.1251-1273.
- Park, E.T. et al., 2008. Aberrant expression of SOX2 upregulates MUC5AC gastric foveolar mucin in mucinous cancers of the colorectum and related lesions. *International Journal of Cancer*, 122, pp. 1253-60.
- Park, I.H. et al., 2008. Disease-specific induced pluripotent stem cells. *Cell*. 134(5), pp. 877-886.
- Pera, M.F., Reubinoff, B. and Trounson, A. 2000. Human embryonic stem cells. *Journal of Cell Science*, 113(1), pp. 5-10.
- Pession, A. et al., 2003. MLL-AF9 oncogene expression affects cell growth but not terminal differentiation and is downregulated during monocyte-macrophage maturation in THP-1 cells. *Oncogene*, 22, pp. 8671-8676.
- Pina, C. et al., 2008. MLLT3 regulates early human erythroid and megakaryocytic cell fate. *Cell Stem Cell*, 2(3), pp. 264-273.
- Polak, U. et al., 2012. Selecting and isolating colonies of human induced pluripotent stem cells reprogrammed from adult fibroblasts. *Journal of Visualized Experiments*, 60, pp. 1-5.
- Pui, C.H. et al., 1985. Central nervous system leukemia in children with acute nonlymphoblastic leukemia. *Blood*, 66(5), pp. 1062-1067.
- Qian, S.W. et al., 2010. Characterization of adipocyte differentiation from human mesenchymal stem cells in bone marrow. *BMC Developmental Biology*, 10, pp. 47-57.
- Qu, C., Brinck-Jensen, N., Zang, M. and Chen, K., 2014. Monocyte-derived dendritic cells: targets as potent antigen-presenting cells for the design of vaccines against infectious diseases. *International Journal of Infectious Diseases*, 19, pp. 1-5.
- Ramirez, J.M. et al., 2011. Brief report: benchmarking human pluripotent stem cell markers during differentiation into three germ layers unveils a striking heterogeneity: all markers are not equal. *Stem Cells*, 29, pp. 1469-1474.

- Raya, A. et al., 2009. Disease-corrected haematopoietic progenitors from Fanconi anaemia induced pluripotent stem cells. *Nature*, 460(7251), pp. 53-59.
- Rehman, J. et al., 2004. Secretion of angiogenic and antiapoptotic factors by human adipose stromal cells. *Circulation*, 109, pp. 1292-1298.
- Richards, M., Fong, C.Y., Chan, W.K., Wong, P.C. and Bongso, A., 2002. Human feeders support prolonged undifferentiated growth of human inner cell masses and embryonic stem cells. *Nature Biotechnology*, 20(9), pp. 933-936.
- Rizzino, A., 2009. Sox2 and Oct-3/4: A versatile pair of master regulators that orchestrate the self-renewal and pluripotency of embryonic stem cells by functioning as molecular rheostats. *Wiley Interdisciplinary Reviews: Systems Biology and Medicine*, 2, pp. 228-236.
- Rizzino, A., 2013. The Sox2-Oct4 connection: Critical players in a much larger interdependent network integrated at multiple levels. *Stem cells*, 31(6), pp. 1033-1039.
- Robinton, D.A. and Daley, G.Q., 2012. The promise of induced pluripotent stem cells in research and therapy. *Nature*, 481, pp. 295-305.
- Roboz, G.J., 2011. Novel approaches to the treatment of acute myeloid leukemia. *ASH Education Book*, 2011(1), pp. 43-50.
- Rodda, D.J. et al., 2005. Transcriptional regulation of *Nanog* by OCT4 and SOX2. *The Journal of Biological Chemistry*, 280, pp. 24731-24737.
- Rowland, B.D., Bernards, R. and Peeper, D.S., 2005. The KLF4 tumour suppressor is a transcriptional repressor of p53 that acts as a context-dependent oncogene. *Nature cell biology*, 7, pp. 1074-1082.
- Rubnitz, J.E., Behm, F.G. and Downing, J.R., 1996. 11q23 rearrangements in acute leukemia. *Leukemia*, 10(1), pp. 74-82.
- Rubnitz, J.E., Gibson, B. and Smith, F.O., 2010. Acute myeloid leukemia, *Hematology oncology clinics of North America*, 24, pp. 35-63.
- Ruvkun, G., 2001. Molecular biology. Glimpses of a tiny RNA world. *Science*, 294, pp. 797-799.
- Rybouchkin, A., Kato, Y. and Tsunoda, Y., 2006. Role of histone acetylation in reprogramming of somatic nuclei following nuclear transfer. *Biology of Reproduction*, 74, pp. 1083-1089.
- Saida, F., Uzan, M., Odaert, B. and Bontems, F., 2006. Expression of highly toxic genes in *E. coli*: special strategies and genetic tools. *Current Protein and Peptide Science*, 7(1), pp. 47-56.

- Scadden, D.T., 2006. The stem cell niche as an entity of action. *Nature*, 441(7097), pp. 1075-1079.
- Schlenk, R.F., 2014. Post-remission therapy for acute myeloid leukemia. *Haematologica*, 99(11), pp. 1663-1670.
- Schmidt, R. and Plath, K., 2012. The roles of the reprogramming factors Oct4, Sox2 and Klf4 in resetting the somatic cell epigenome during induced pluripotent stem cell generation. *Genome Biology*, 13(10), pp. 251-261.
- Schopperle, W.M. and DeWolf, W.C., 2006. The TRA-1-60 and TRA-1-81 human pluripotent stem cell markers are expressed on podocalyxin in embryonal carcinoma. *Stem Cells*, 25(3), pp. 723-730.
- Schrök, E. et al., 1996. Multicolor spectral karyotyping of human chromosomes. *Science*, 273, pp. 494-497.
- Schulz, T.C. et al., 2003. Directed neural differentiation of human embryonic stem cells. *BMC Neuroscience*, 4, pp. 27-39.
- Schwahnässer, B. et al., 2011. Global quantification of mammalian gene expression control. *Nature*, 473, pp. 337-342.
- Seki, T. et al., 2010. Generation of induced pluripotent stem cells from human terminally differentiated circulating T cells. *Cell Stem Cell*, 7, pp. 11-14.
- Semi, K., Matsuda, Y., Ohnisi, K. and Yamada, Y., 2012. Cellular reprogramming and cancer development. *International Journal of Cancer*, 132(6), pp.1240-1248.
- Seo, E.J. et al., 2013. Efficient production of retroviruses using PLGA/bPEI-DNA nanoparticles and application for reprogramming somatic cells. *PLoS ONE*, 8(9), pp.1-12.
- Seuntjens, E. et al., 2009. Transforming growth factor type beta and Smad family signaling in stem cell function. *Cytokine Growth Factor Review*, 20(5-6), pp. 449-458.
- Shahjahan Miah, S.M. and Campbell, K.S., 2010. Expression of cDNAs in human natural killer cell lines by retroviral transduction. *Methods in Molecular Biology*, 612, pp. 199-208.
- Shamblott, M.J. et al., 1998. Derivation of pluripotent stem cells from cultured human primordial germ cells. *Proceedings of the National Academy of Science*, 95, pp. 13726-13731.
- Si-Tayeb, K. et al., 2010. Generation of human induced pluripotent stem cells by simple transient transfection of plasmid DNA encoding reprogramming factors. *BMC Developmental Biology*, 10, pp. 81-90.

- Sidney, L.E., Kirkham, G.R. and Buttery, L.D., 2014. Comparison of osteogenic differentiation of embryonic stem cells and primary osteoblasts revealed by responses to IL-1 β , TNF- α , and IFN- γ . *Stem Cells and Development*, 23(6), pp. 605-617.
- Singh, U. et al. 2012. Novel Live Alkaline Phosphatase Substrate for Identification of Pluripotent Stem Cells. In: *Stem Cell Reviews and Reports*. New York City: Humana Press Inc., pp. 1021-1029.
- Slany, R.K., 2009. The molecular biology of mixed lineage leukemia. *Haematologica*, 94(7), pp. 984-993.
- Sojitra, P. et al., 2013. Chronic myelomonocytic leukemia monocytes uniformly display a population of monocytes with CD11c underexpression. *American Journal of Clinical Pathology*, 140, pp. 686-692.
- Soldner, F. et al., 2009. Parkinson's disease patient-derived induced pluripotent stem cells free of viral reprogramming factors. *Cell*, 136, pp. 964-977.
- Somervaille, T.C.P. and Clearly, M.L., 2006. Identification and characterization of leukemia stem cells in murine MLL-AF9 acute myeloid leukemia. *Cancer Cell*, 10(4), pp. 257-268.
- Sommer, C.A. et al., 2009. Induced pluripotent stem cell generation using a single lentiviral stem cell cassette. *Stem cells*, 27, pp. 543-549.
- Song, B. et al., 2011. Generation of induced pluripotent stem cells from human kidney mesangial cells. *Journal of the American Society of Nephrology*, 22, pp. 1213-1220.
- Sridharan, R. et al., 2009. Role of the murine reprogramming factors in the induction of pluripotency. *Cell*, 136, pp. 364-377.
- Stadtfeld, M. and Hochedlinger, K., 2010. Induced pluripotency: history, mechanisms, and applications. *Genes & development*, 24, pp. 2239-2263.
- Stam, R.W., 2012. MLL-AF4 driven leukemogenesis: what are we missing? *Cell Research*, 22, pp. 948-949.
- Sugii, S. et al., 2010. Human and mouse adipose-derived cells support feeder independent induction of pluripotent stem cells. *Proceedings of the National Academy of Science*, 107, pp. 3558-3563.
- Sulzbacher, S., Schroeder, I.S., Truong, T.T. and Wobus, A.M., 2009. Activin A-induced differentiation of embryonic stem cells into endoderm and pancreatic progenitors- the influence of differentiation factors and culture conditions. *Stem Cell Review*, 5(2), pp. 159-173.

- Svendsen, C.N., 2013. Back to the future: how human induced pluripotent stem cells will transform regenerative medicine. *Human Molecular Genetics*, 22(1), pp. 32-38.
- Swift, S., Lorens, J., Achacoso, P. and Nolan, G.P., 1999. Rapid production of retroviruses for efficient gene delivery to mammalian cells using 293T cell-based systems. In: Coligan, J.E., Kruisbeek, A.M., Margulies, D.H., Shevach, E.M. and Strober, W. (eds.). *Current Protocols in Immunology*. New York: Wiley, Vol 1. 17C, pp, 1-17.
- Tallman, M.S. et al., 2004. Acute monocytic leukemia (French-American-British classification M5) does not have a worse prognosis than other subtypes of acute myeloid leukemia: A report from the Eastern Cooperative Oncology Group. *Journal of Clinical Oncology*, 22, pp. 1276-1286.
- Takahashi, K. and Yamanaka, S., 2006. Induction of pluripotent stem cells from mouse embryonic and adult fibroblast cultures by defined factors. *Cell*, 126, pp. 663-676.
- Takahashi, K. et al., 2007. Induction of pluripotent stem cells from adult human fibroblasts by defined factors. *Cell*, 131, pp. 861-872.
- Takahashi, K., Narita, M., Yokura, M., Ichisaka, T. and Yamanaka, S., 2009. Human induced pluripotent stem cell on autologous feeder. *PLoS ONE*, 4(12), pp. 1-6.
- Tanabe, K. et al., 2013. Maturation, not initiation, is the major roadblock during reprogramming toward pluripotency from human. *Proceedings of the National Academy of Sciences*, 110(30), pp. 12171-12179.
- Tanaka, T. S. et al., 2006. Esg1, expressed exclusively in preimplantation embryos, germline, and embryonic stem cells, is a putative RNA-binding protein with broad RNA targets. *Development, Growth and Differentiation*, 48(6), pp. 381-390.
- Tetreault, M., Yang, Y. and Kats, J.P., 2013. Krüppel-like factors in cancer. *Nature Reviews Cancer*, 13, pp. 701-713.
- Thirman, M.J. et al., 1993. Rearrangement of the MLL gene in acute lymphoblastic and acute myeloid leukemias with 11q23 chromosomal translocations. *The New England Journal of Medicine*, 329, pp. 909-914.
- Thomas, E.D. et al., 1979. Marrow transplantation for acute nonlymphoblastic leukemia in first remission. *The New England Journal of Medicine*, 301, pp. 597-599.
- Thomson, J.A. et al., 1998. Embryonic stem cell lines derived from human blastocyst. *Science*, 282, pp. 1145-1147.

- Tiscornia, G., Vivas, E.L. and Belmonte, J.C.I., 2011. Diseases in a dish: modelling human genetic disorders using induced pluripotent cells. *Nature Medicine*, 17, pp. 1570-1576.
- Truong, T.T, Huynh, K., Nakatsu, M.N., and Deng, S.X., 2011. SSEA4 Is a Potential Negative Marker for the Enrichment of Human Corneal Epithelial Stem/Progenitor Cells. *Investigative Ophthalmology Visual Science*, 52(9), pp. 6315-6320.
- Tsuchiya, S. et al., 1980. Establishment and characterization of a human acute monocytic leukemia cell line (THP-1). *International Journal of Cancer*, 26(2), pp. 171-176.
- Tsukiyama, T. et al., 2014. A comprehensive system for generation and evaluation of induced pluripotent stem cells using PiggyBac transposition. *PLoS ONE*, 9(3), pp. 1-8.
- Utikal, J. et al., 2009. Sox2 is dispensable for the reprogramming of melanocytes and melanoma cells into induced pluripotent stem cells. *Journal of Cell Science*, 122(19), pp. 3502-3510.
- Van Der Sanden, B., Dhobb, M., Berger, F. and Wion, D., 2010. Optimizing stem cell culture. *Journal of Cell and Biochemistry*, 111(4), pp. 801-807.
- Verlinsky, Y. et al., 2005. Human embryonic stem cell line with genetic disorders. *Reproductive Biomedicine*, 10(1), pp. 105-110.
- Verschuur, A., 2004. Acute monocytic leukemia. *Orphanet Encyclopedia*, 2204, pp. 1-5.
- Vogel, C. et al., 2010. Sequence signatures and mRNA concentration can explain two-thirds of protein abundance variation in a human cell line. *Molecular Systems Biology*, 6, pp. 1-9.
- Vogel, C. and Marcotte, E.M. 2012. Insights into the regulation of protein abundance from proteomic and transcriptomic analyses. *Nature Review Genetic*, 13(4), pp. 227-232.
- Wan, W. et al., 2014. Applications of induced pluripotent stem cells in studying the neurodegenerative diseases. *Stem Cells International*, 2015, pp.1-11.
- Wang, J., Levasseur, D.N. and Orkin, S.H. 2008. Requirement of Nanog dimerization for stem cell self-renewal and pluripotency. *Proceedings of the National Academy of Science*, 105(17), pp. 6326-6331.
- Wakao, S. et al., 2012. Morphologic and gene expression criteria for identifying human induced pluripotent stem cells. *PLoS One*, 7(12), pp. 1-9.

- Warren, L. et al., 2010. Highly efficient reprogramming to pluripotency and directed differentiation of human cells with synthetic modified mRNA. *Cell Stem Cell*, 7(5), pp. 618-630.
- Washington State University., 2008, *CD15s* [Online]. Available at <https://apps.vetmed.wsu.edu/tkp/report.aspx?ID=21> [Accessed: 8 May 2015].
- Watanabe, D., Suetake, I., Tada, T. and Tajima, S., 2002. Stage- and cell-specific expression of Dnmt3a and Dnmt3b during embryogenesis. *Mechanisms of Development*, 118(1-2), pp. 187-190.
- Weh, H.J. et al., 1986. Translocation (9;11)(p21;q23) in a child with acute monoblastic leukemia following 2 ½ years after successful chemotherapy for neuroblastoma. *Journal of Clinical Oncology*, 4(10), pp. 1518-1520.
- Wei, F., Schöder, H.R. and Atchison, M.L., 2007. Sumoylation of Oct4 enhances its stability, DNA binding, and transactivation. *The Journal of Biological Chemistry*, 282(29), pp. 21551-21560.
- Woltjen, K. et al., 2009. A PiggyBac transposition reprograms fibroblasts to induced pluripotent stem cells. *Nature*, 458, pp. 766-770.
- Wu, G. and Schöder, H.R., 2014. Role of Oct4 in the early embryo development. *Cell Regeneration*, 3(1), pp. 7-16.
- Xu, D. et al., 2009. Phenotypic correction of murine haemophilia A using an iPS cell-based therapy. *Proceedings of the National Academy of Science*, 106, pp. 808-813.
- Xu, Y. et al., 2010. Revealing a core signalling regulatory mechanism for pluripotent stem cell survival and self-renewal by small molecules. *Proceedings of the National Academy of Science*, 107(18), pp. 8129-8134.
- Yamaguchi, S. et al., 2011. Sox2 expression effects on direct reprogramming efficiency as determined by alternative somatic cell fate. *Stem Cell Research*, 6, pp. 177-186.
- Yamanaka, S., 2012. Induced pluripotent stem cells: Past, present, and future. *Cell Stem Cell*, 10, pp. 678-684.
- Yamasaki, S. et al., 2014. Generation of human induced pluripotent stem (iPS) cells in serum and feeder-free defined culture and TGF- β 1 regulation of pluripotency. *PLoS ONE*, 9(1), pp. 1-13.
- Yan, X.J. et al., 2011. Exome sequencing identifies somatic mutations of DNA methyltransferase gene DNMT3A in acute monocytic leukemia. *Nature genetics*, 34 (4), pp. 309-317.

- Yang, J.Y. et al., 2014. Culture of pig induced pluripotent stem cells without direct feeder contact in serum free media. *Journal of Stem Cell Research Therapy*, 4(2), pp. 1-8.
- Ying, Q. et al., 2008. The ground state of embryonic stem cell self-renewal. *Nature*, 453, pp. 519-523.
- Yokoyama, A., Kitabayashi, I., Ayton, P.M., Cleary, M.L. and Ohki, M., 2002. Leukemia proto-oncoprotein MLL is proteolytically processed into 2 fragments with opposite transcriptional properties. *Blood*, 100, pp. 3710-3718.
- Yoshida, Y., Takahashi, K., Okita, K., Ichisaka, T. and Yamanaka, S., 2009. Hypoxia enhances the generation of induced pluripotent stem cells. *Cell Stem Cell*, 5, pp. 237-241.
- Yu, B.D. et al., 1995. Altered Hox expression and segmented identity in Mll-mutant mice. *Nature*, 378(6556), pp. 505-508.
- Yu, B.D. et al., 1998. MLL, a mammalian trithorax-group gene, functions as a transcriptional maintenance factor in morphogenesis. *Proceedings of the National Academy of Sciences*, 95(18), pp. 10632-10636.
- Yu, J. et al., 2007. Induced pluripotent stem cell lines derived from human somatic cells. *Science*, 318, pp. 1917-1920.
- Yu, J. et al., 2009. Human induced pluripotent stem cells free of vector and transgene sequences. *Science*, 324, pp. 797-801.
- Yu, J. et al., 2011. Efficient feeder-free episomal reprogramming with small molecules. *PLoS ONE*, 6(3), pp. 1-10.
- Zhang, et al., 2012a. Terminal differentiation and loss of tumorigenicity of human cancers via pluripotency-based reprogramming. *Oncogene*, 2012, pp. 1-12.
- Zhang, Y., Li, W., Laurent, T. and Ding, S., 2012b. Small molecules, big roles-the chemical manipulation of stem cell fate and somatic cell reprogramming. *Journal of Cell Science*, 125, pp. 5609-5620.
- Zhang, S. and Cui, W., 2014. Sox2, a key factor in the regulation of pluripotency and neural differentiation. *World Journal of Stem Cells*, 6(3), pp. 305-311.
- Zhao, H.X. et al., 2010. Rapid and efficient reprogramming of human amnion-derived cells into pluripotency by three factors OCT4/SOX2/NANOG. *Differentiation*, 80(2-3), pp. 123-129.
- Zhao, W. et al., 2012. Embryonic stem cells markers. *Molecules*, 17, pp. 6196-6236.

Zhou, T. et al., 2011. Generation of induced pluripotent stem cells from urine. *Journal of the American Society of Nephrology*, 22, pp. 1221-1228.

Zhu, S. et al., 2010. Reprogramming of human primary somatic cells by oct4 and chemical compounds. *Cell Stem Cell*, 7, pp.651-655.

Ziegler, A. et al., 2005. The cationic cell-penetrating peptide CPP (TAT) derived from the HIV-1 protein TAT is rapidly transported into living fibroblasts: optical, biophysical, and metabolic evidence. *Biochemistry*, 44(1), pp. 138-148.

Zuk, P.A. et al., 2002. Human adipose tissue is a source of multipotent stem cells. *Molecular Biology of the Cells*, 13(12), pp. 4279-4295.

APPENDICES

APPENDIX A

Measurement of plasmid concentration

Quantification of recombinant plasmids.

Plasmids Wavelength	pMXs- hOCT3/4	pMXs- hSOX2	pMXs- hKLF4	pMXs- hc-MYC	pMX-GFP
A230	0.071	0.101	0.077	0.091	0.056
A260	0.174	0.203	0.144	0.187	0.120
A280	0.096	0.113	0.078	0.103	0.066
A320	0.002	0.003	0.001	0.010	0.000
A260/280	1.813	1.796	1.846	1.816	1.818
A260/230	2.251	2.010	1.870	2.055	2.143
Concentration (ng/μl)	435	508	360	468	300

APPENDIX B

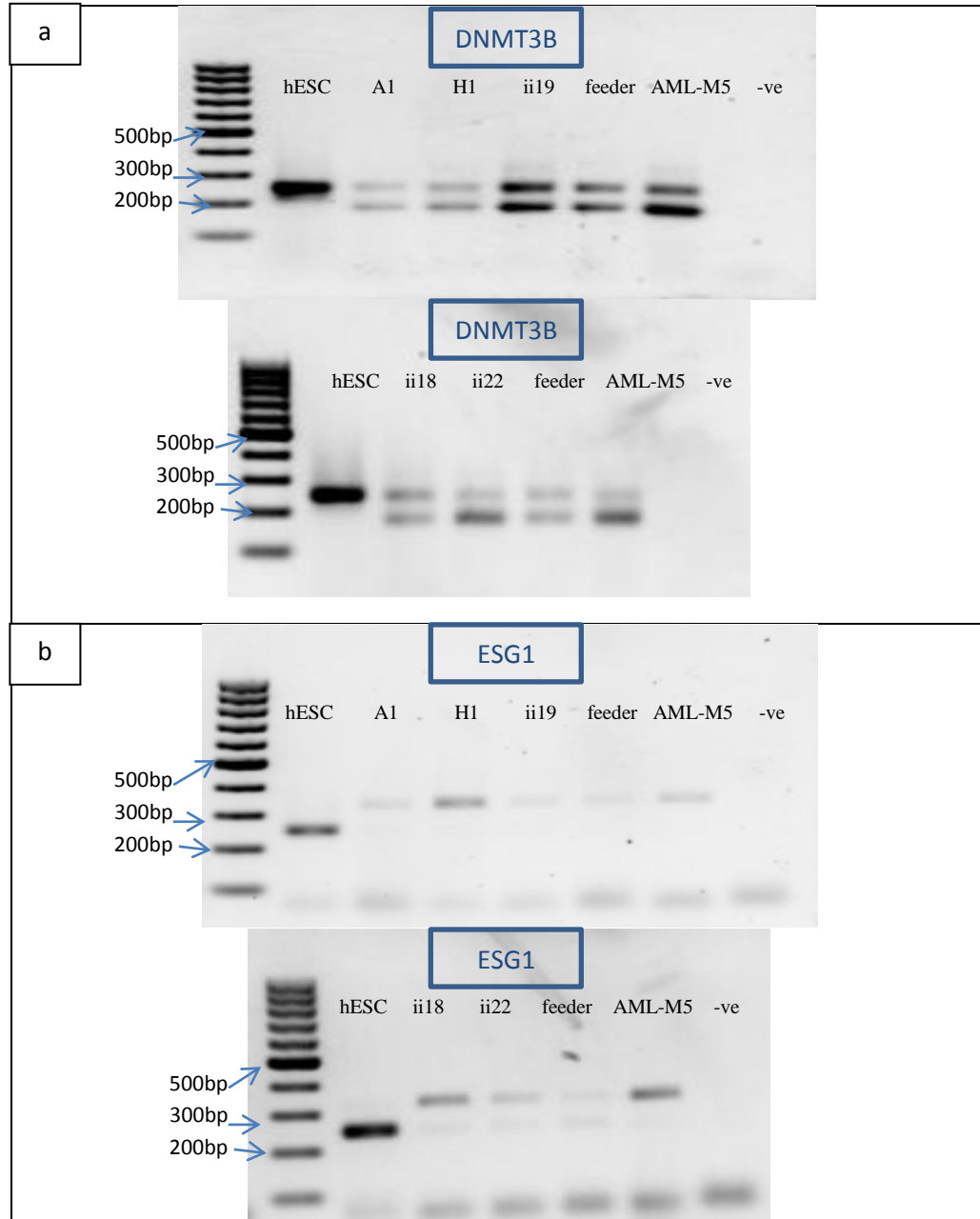
Measurement of RNA Concentration

RNA quantification of hESC, AML-M5-derived iPSC clones, feeder and AML-M5 cells.

Samples Wavelength	hESC	AML-M5-derived iPSC clones					feeder	Parent al AML- M5
		A1	H1	ii18	ii19	ii22		
A230	0.401	0.420	0.170	0.175	0.234	0.173	0.237	0.741
A260	0.378	0.428	0.131	0.090	0.427	0.355	0.246	0.511
A280	0.198	0.225	0.068	0.050	0.222	0.177	0.129	0.752
A320	0.001	0.005	0.001	0.002	0.001	0.001	0.001	0.009
A260/ 280	1.909	1.923	1.913	1.769	1.928	2.000	1.914	1.997
A260/ 230	0.942	1.019	0.772	0.520	1.828	2.046	1.038	2.027
Conce ntratio n(ng/ μl)	789	169	264	184	852	712	490	608

APPENDIX C

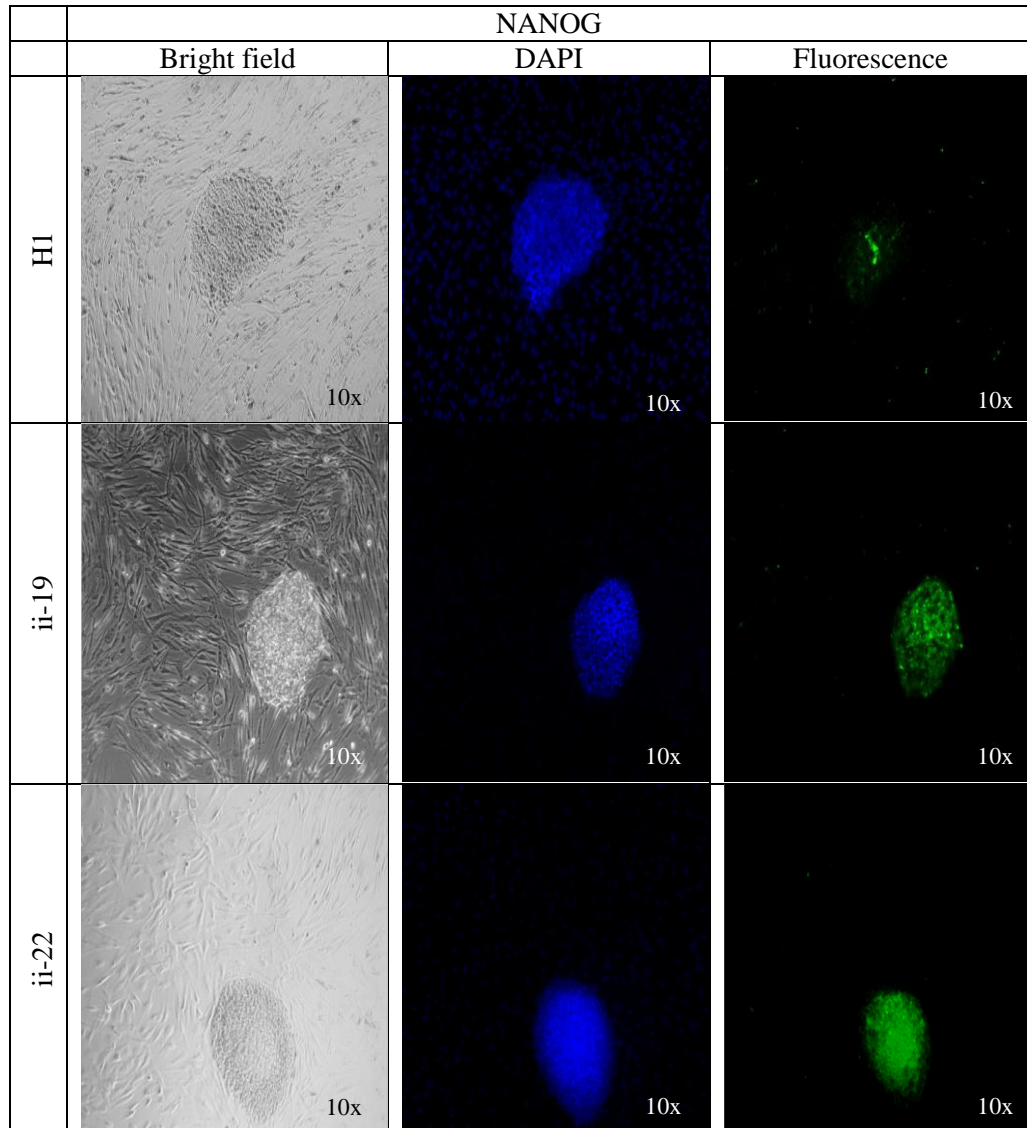
Detection of Pluripotency Markers using RT-PCR



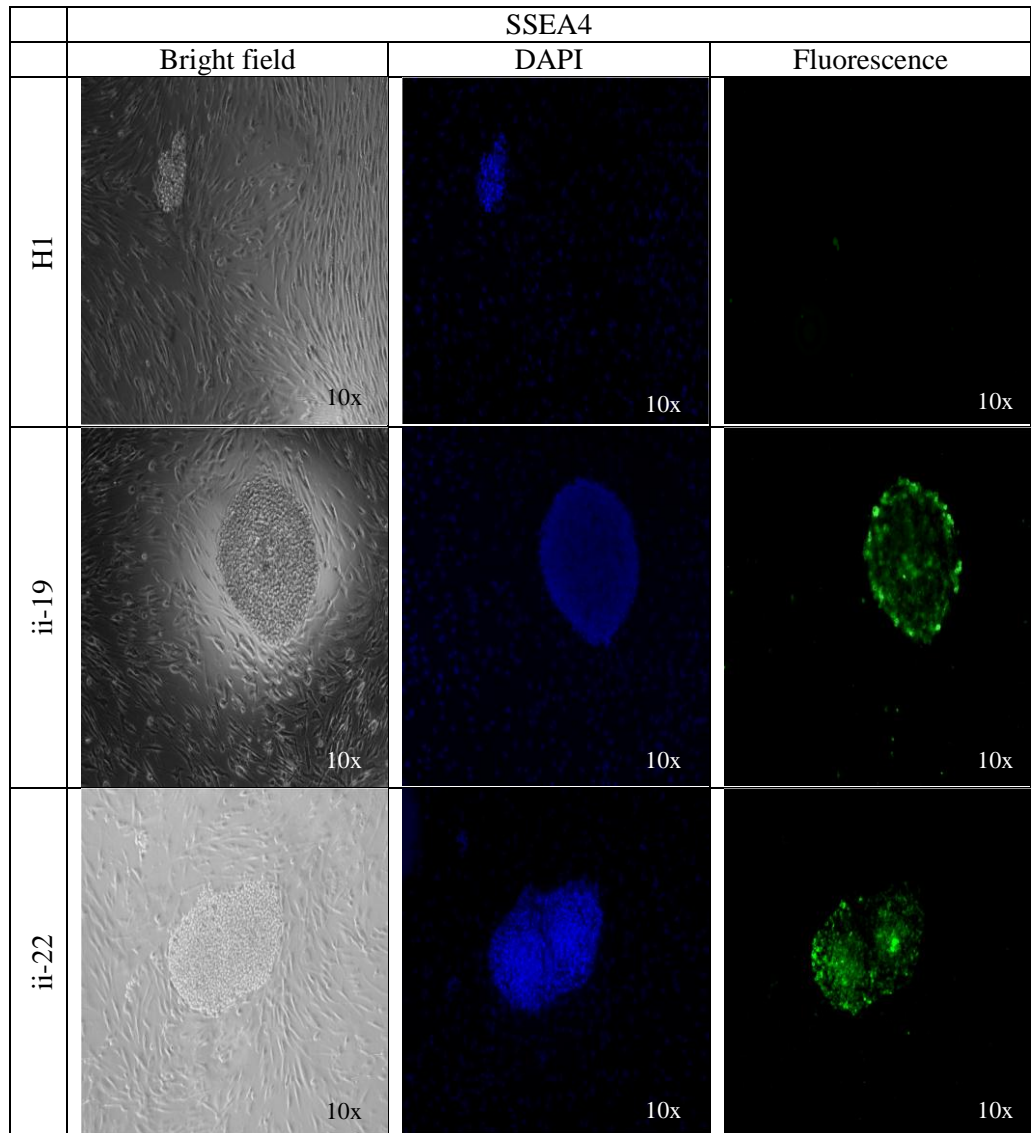
Detection of DNMT3B and ESG1 using RT-PCR. Gel Images showed the RT-PCR result of (a) DNMT3B, (b) ESG1 in hESC (Positive Control), AML-M5-derived iPSC clones (A1, H1, ii18, ii19 and ii22), feeder cells (hAd-MSC), parental AML-M5 cell line (Negative Control) and '-ve' as a non-template control. Multiple bands for the DNMT3B were detected in AML-M5-derived iPSC clones, feeder and parental AML-M5 cells. On the other hand, no expression of ESG1 was detected in AML-M5-derived iPSC clones, feeder and parental AML-M5 cells. The 100bp DNA ladder was used to determine the size of the PCR product.

APPENDIX D

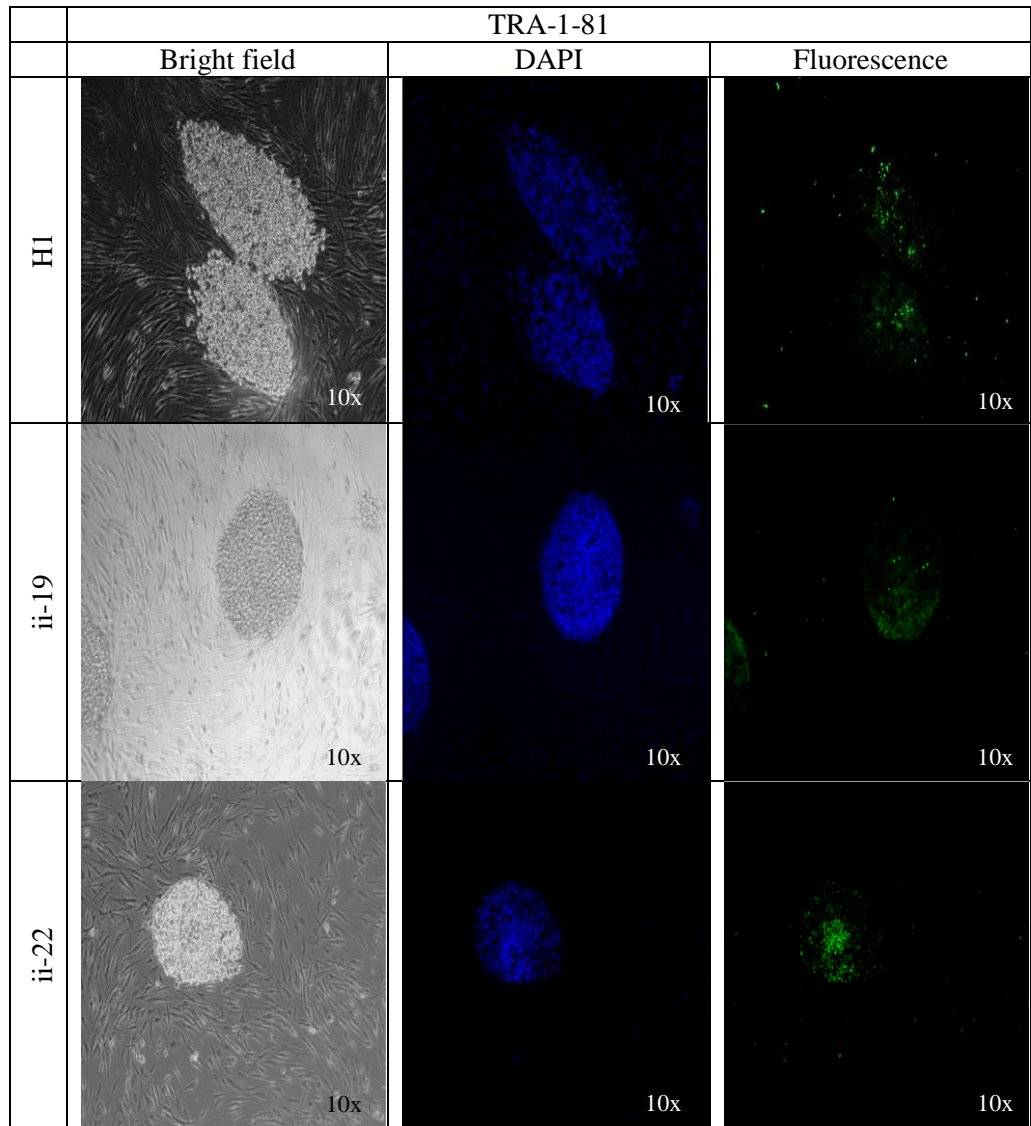
Detection of Pluripotency Markers using Immunofluorescence Staining



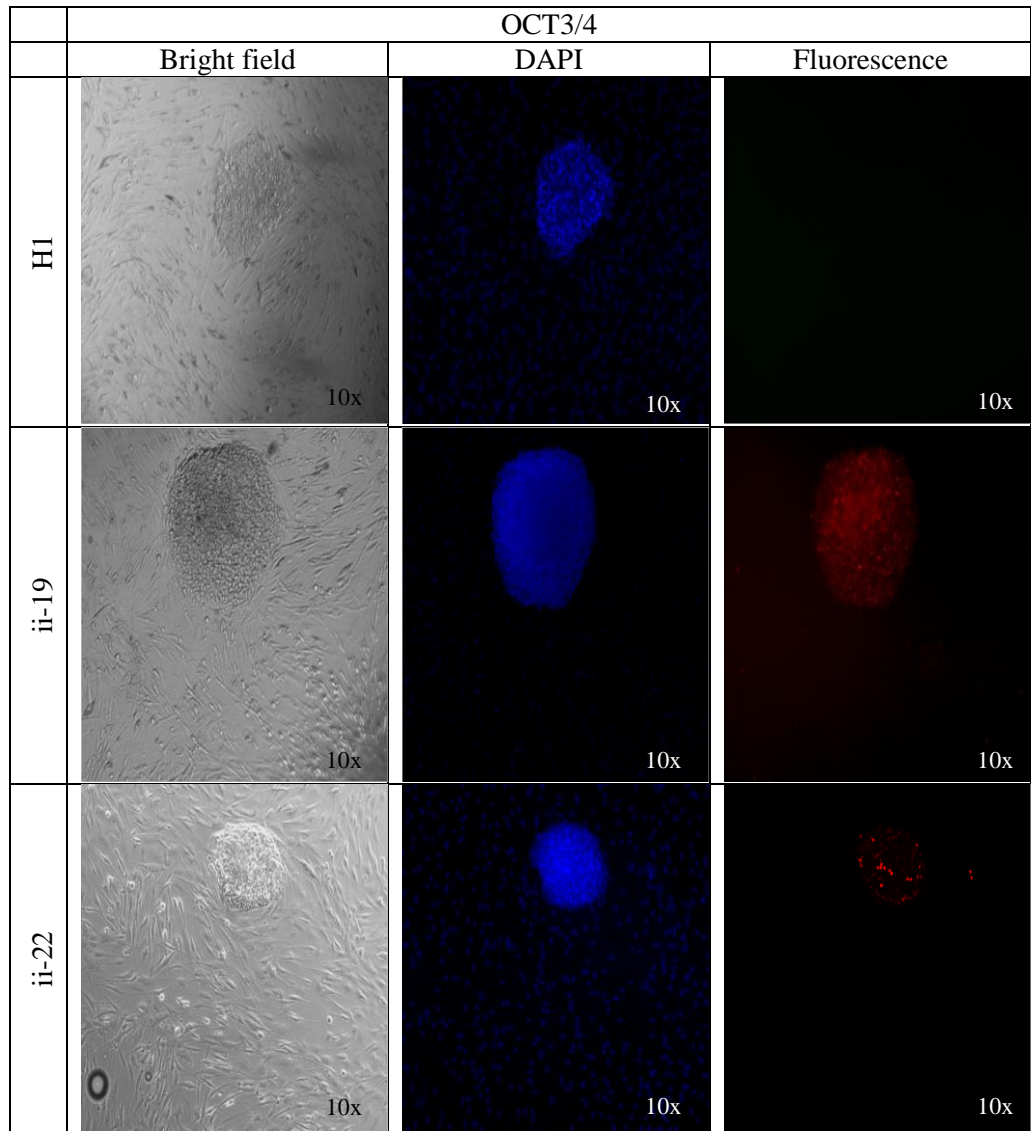
Detection of NANOG using immunofluorescence staining on other AML-M5-derived iPSC clones. Pseudo-green fluorescence signal indicates positive staining for NANOG marker. NANOG was homogenously expressed in clone ii-19 and clone ii-22, and expressed only in center region of clone H1. DAPI was used to indicate the presence of nuclei acid.



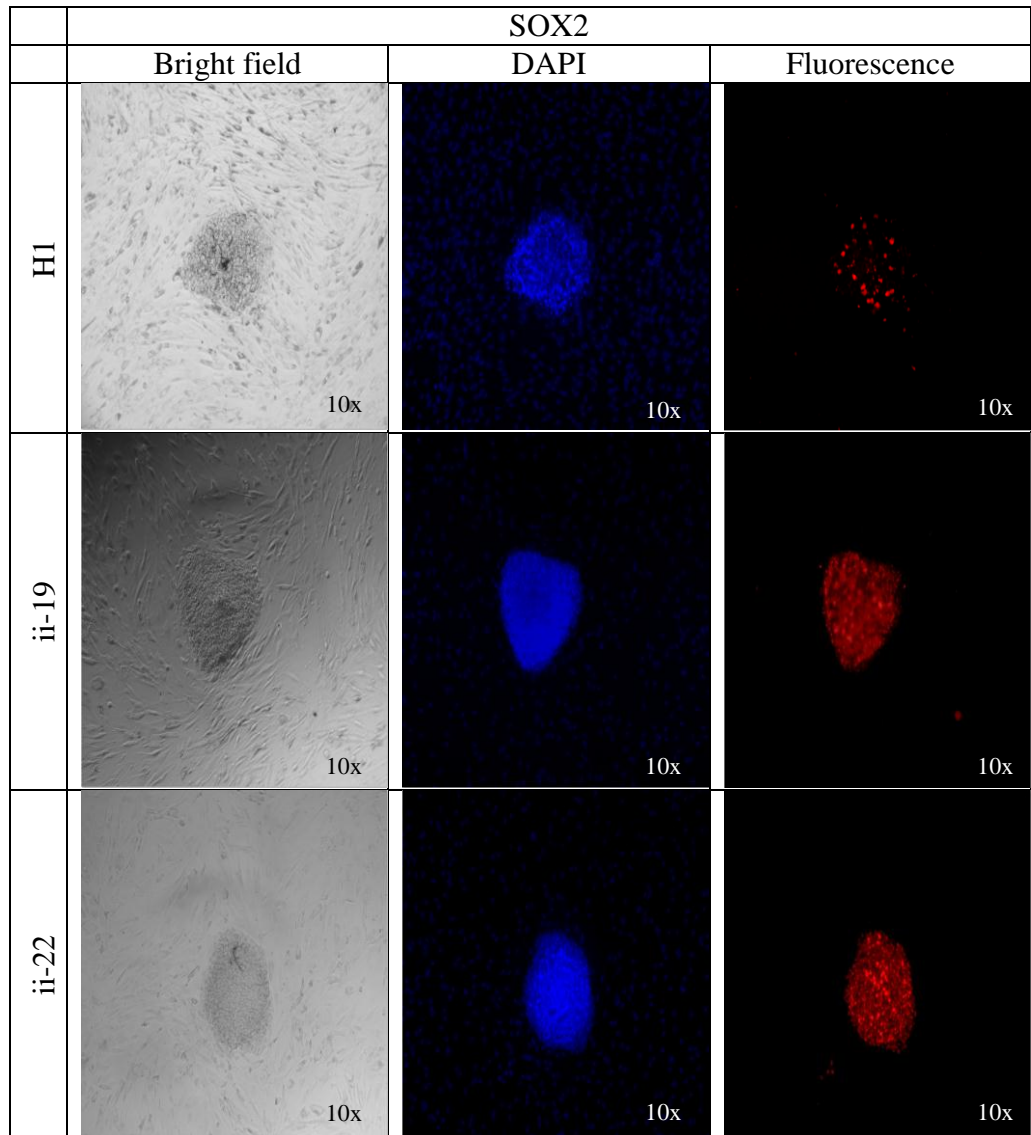
Detection of SSEA4 using immunofluorescence staining on other AML-M5-derived iPSC clones. Pseudo-green fluorescence signal indicates positive staining for SSEA4 marker. SSEA4 was homogenously expressed in clone ii-19 and clone ii-22, but no expression in clone H1. DAPI was used to indicate the presence of nuclei acid.



Detection of TRA-1-81 using immunofluorescence staining on other AML-M5-derived iPSC clones. Pseudo-green fluorescence signal indicates positive staining for TRA-1-81 marker. TRA-1-81 was expressed in all AML-M5-derived iPSC clones. DAPI was used to indicate the presence of nuclei acid.



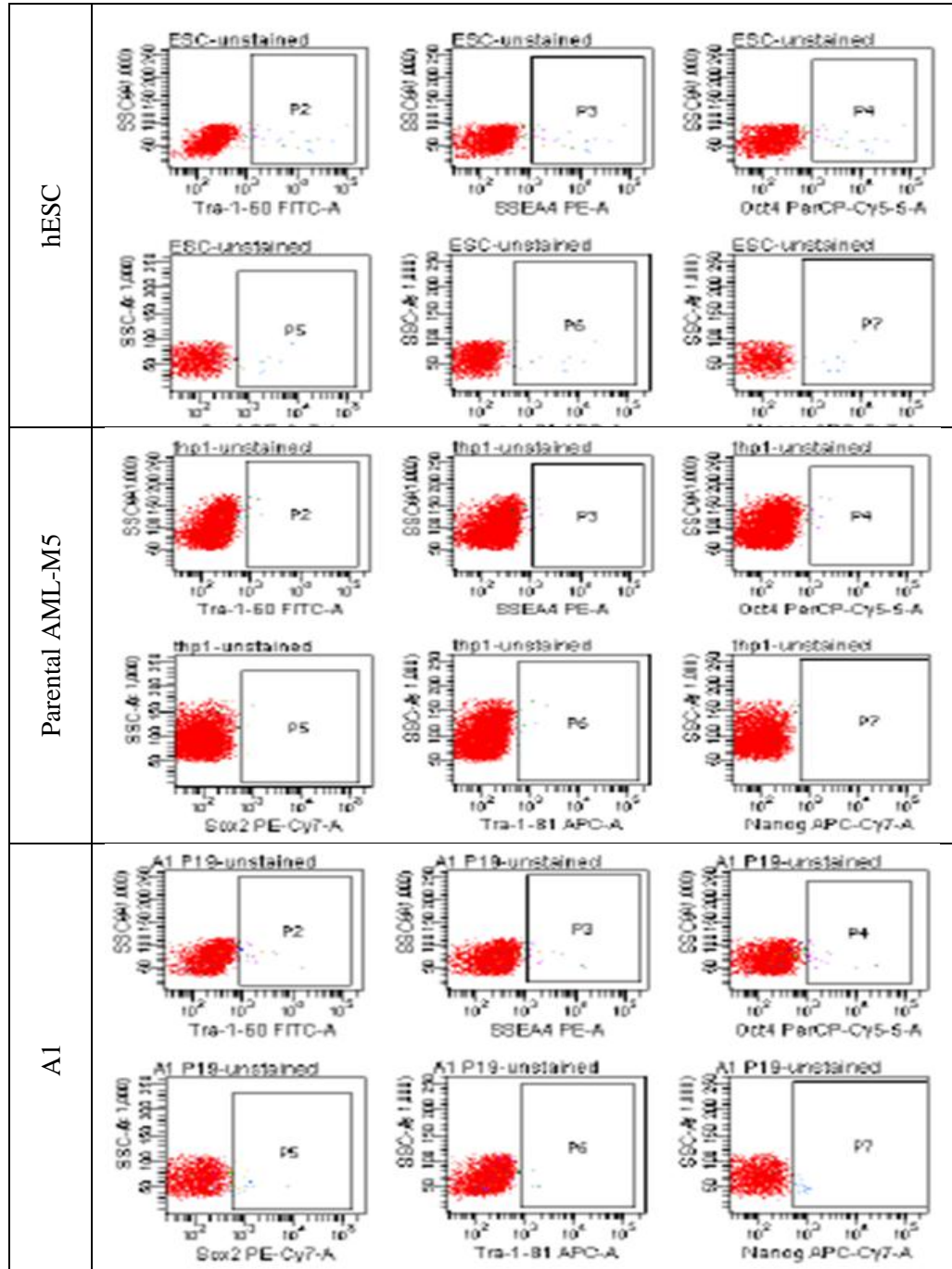
Detection of OCT3/4 using immunofluorescence staining on other AML-M5-derived iPSC clones. Pseudo-red fluorescence signal indicates positive staining for OCT3/4 marker. OCT3/4 was homogenously expressed in clone ii-18, whereas expressed in small population of cells in clone ii-22 and no expression in clone H1. DAPI was used to indicate the presence of nuclei acid.



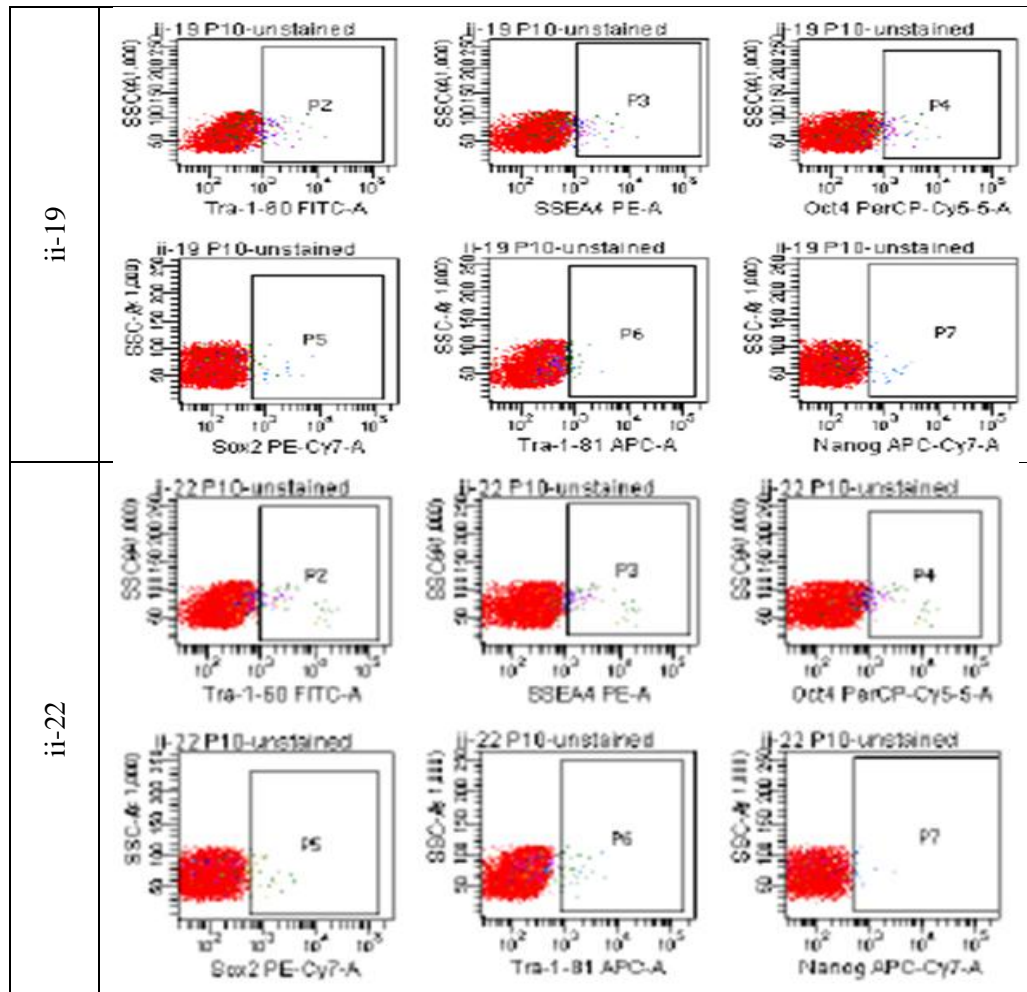
Detection of SOX2 using immunofluorescence staining on other AML-M5-derived iPSC clones. Pseudo-red fluorescence signal indicates positive staining for SOX2 marker. SOX2 was homogenously expressed in clone ii-19 and clone ii-22, whereas expressed in small population of cells in clone H1. A small population of parental AML-M5 cell line was stained positively with SOX2. DAPI was used to indicate the presence of nuclei acid.

APPENDIX E

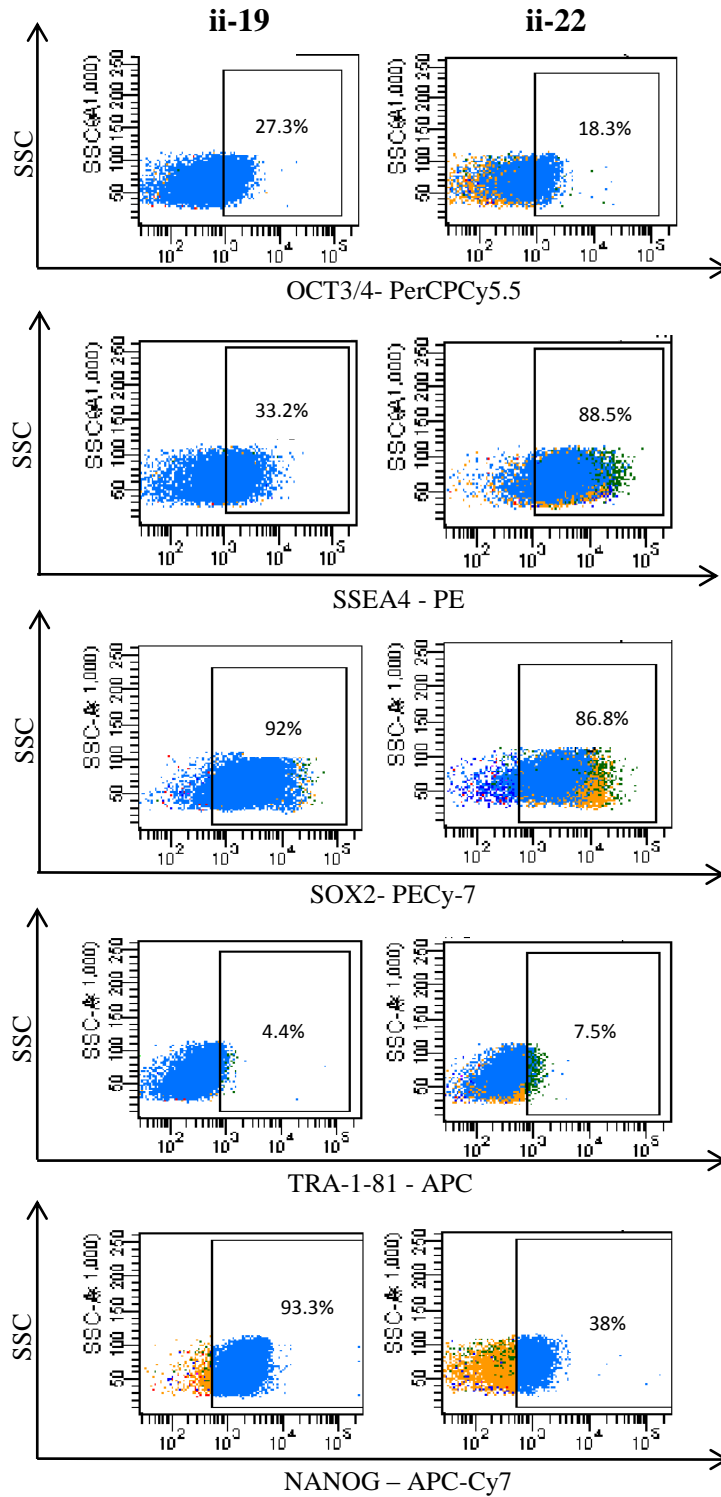
Detection of Pluripotency Markers using Immunophenotyping



FACS unstained controls of pluripotency markers. Representative histogram obtained from FACS profile showed low auto-fluorescence background of pluripotent markers NANOG, SSEA4, OCT3/4, SOX2 and TRA-1-81 on AML-M5-derived iPSCs, hESC and parental AML-M5 cells.



FACS unstained controls of pluripotency markers (continued). Representative histogram obtained from FACS profile showed low auto-fluorescence background of pluripotent markers NANOG, SSEA4, OCT3/4, SOX2 and TRA-1-81 on other AML-M5-derived iPSC clones (ii-19 and ii22).



Flow cytometry analysis of expression of pluripotency markers on other AML-M5-derived iPSC clones. Representative dot plots showed expression of pluripotency markers (a) OCT3/4, (b) SSEA4, (c) SOX2, (d) TRA-1-81, and (e) NANOG on AML-M5-derived iPSC clones (ii-19 and ii-22).

APPENDIX F

SPSS Data Set

Mann-Whitney Test

		Ranks		
sample		N	Mean Rank	Sum of Ranks
TRA181	positive control	3	2.00	6.00
	iPSCs	3	5.00	15.00
	Total	6		

		TRA181
Mann-Whitney U		.000
Wilcoxon W		6.000
Z		-1.964
Asymp. Sig. (2-tailed)		.050
Exact Sig. [2*(1-tailed Sig.)]		.100 ^a

- a. Not corrected for ties.
b. Grouping Variable: sample

```
T-TEST GROUPS=sample (1 2)
/MISSING=ANALYSIS
/VARIABLES=TRA181
/CRITERIA=CI (.95) .
```

T-Test

[DataSet1] C:\ah bee's info\research lab\SPSS\data key in template.sav

Group Statistics				
sample	N	Mean	Std. Deviation	Std. Error Mean
TRA181 positive control	3	.5667	.40415	.23333
iPSCs	3	10.5333	8.08847	4.66988

		Levene's Test for Equality of Variances		t-test for Equality of Means						
		F	Sig.	t	df	Sig. (2-tailed)	Mean Difference	Std. Error Difference	95% Confidence Interval of the Difference	
									Lower	Upper
TRA181	Equal variances assumed	10.769	.030	-2.132	4	.100	-9.96667	4.67571	-22.94851	3.01517
	Equal variances not assumed			-2.132	2.010	.166	-9.96667	4.67571	-29.98912	10.05579

SPSS data set of TRA-1-81. Representative data was showed statistical analysis of TRA-1-81 on AML-M5-derived iPSC and parental AML-M5 cell line using Mann-Whitney Test and Independent T-Test.

Mann-Whitney Test

Ranks

sample	N	Mean Rank	Sum of Ranks
SSEA4 positive control	3	2.00	6.00
iPSCs	3	5.00	15.00
Total	6		

Test Statistics^b

	SSEA4
Mann-Whitney U	.000
Wilcoxon W	6.000
Z	-1.964
Asymp. Sig. (2-tailed)	.050
Exact Sig. [2*(1-tailed Sig.)]	.100 ^a

a. Not corrected for ties.

b. Grouping Variable: sample

```
T-TEST GROUPS=Sample (1 2)
/MISSING=ANALYSIS
/VARIABLES=SSEA4
/CRITERIA=CI (.95) .
```

T-Test

[DataSet1] C:\ah bee's info\research lab\SPSS\data key in template.sav

Group Statistics

sample	N	Mean	Std. Deviation	Std. Error Mean
SSEA4 positive control	3	.3667	.30551	.17638
iPSCs	3	68.7667	30.86330	17.81893

Independent Samples Test

		Levene's Test for Equality of Variances		t-test for Equality of Means						
								95% Confidence Interval of the Difference		
		F	Sig.	t	df	Sig. (2-tailed)	Mean Difference	Std. Error Difference	Lower	Upper
SSEA4	Equal variances assumed	15.152	.018	-3.838	4	.018	-68.40000	17.81981	-117.87572	-18.92428
	Equal variances not assumed			-3.838	2.000	.062	-68.40000	17.81981	-145.05805	8.25805

SPSS data set of SSEA4. Representative data was showed stastictical analysis of SSEA4 on AML-M5-derived iPSC and parental AML-M5 cell line using Mann-Whitney Test and Independent T-Test.

Mann-Whitney Test

		Ranks		
sample		N	Mean Rank	Sum of Ranks
OCT4	positive control	3	2.00	6.00
	iPSCs	3	5.00	15.00
	Total	6		

Test Statistics ^b		OCT4
Mann-Whitney U		.000
Wilcoxon W		6.000
Z		-1.964
Asymp. Sig. (2-tailed)		.050
Exact Sig. [2*(1-tailed Sig.)]		.100 ^a

a. Not corrected for ties.

b. Grouping Variable: sample

```
T-TEST GROUPS=Sample (1 2)
/MISSING=ANALYSIS
/VARIABLES=OCT4
/CRITERIA=CI (.95) .
```

T-Test

[DataSet1] C:\ah bee's info\research lab\SPSS\data key in template.sav

Group Statistics					
sample	N	Mean	Std. Deviation	Std. Error Mean	
OCT4	positive control	3	.9667	.85049	.49103
	iPSCs	3	20.0333	6.51869	3.76357

Independent Samples Test										
		Levene's Test for Equality of Variances		t-test for Equality of Means						
		F	Sig.	t	df	Sig. (2-tailed)	Mean Difference	Std. Error Difference	95% Confidence Interval of the Difference	
									Lower	Upper
OCT4	Equal variances assumed	7.269	.054	-5.024	4	.007	-19.06667	3.79547	-29.60457	-8.52877
	Equal variances not assumed			-5.024	2.068	.035	-19.06667	3.79547	-34.89280	-3.24053

SPSS data set of OCT3/4. Representative data was showed stastictical analysis of OCT3/4 on AML-M5-derived iPSC and parental AML-M5 cell line using Mann-Whitney Test and Independent T-Test.

Mann-Whitney Test

		Ranks		
sample		N	Mean Rank	Sum of Ranks
SOX2	positive control	3	2.00	6.00
	iPSCs	3	5.00	15.00
	Total	6		

		SOX2
Mann-Whitney U		.000
Wilcoxon W		6.000
Z		-1.964
Asymp. Sig. (2-tailed)		.050
Exact Sig. [2*(1-tailed Sig.)]		.100 ^a

a. Not corrected for ties.

b. Grouping Variable: sample

```
T-TEST GROUPS=Sample (1 2)
/MISSING=ANALYSIS
/VARIABLES=SOX2
/CRITERIA=CI (.95) .
```

T-Test

[DataSet1] C:\ah bee's info\research lab\SPSS\data key in template.sav

Group Statistics					
sample	N	Mean	Std. Deviation	Std. Error Mean	
SOX2	positive control	3	62.0000	.95394	.55076
	iPSCs	3	89.6333	2.63122	1.51914

Independent Samples Test										
		Levene's Test for Equality of Variances		t-test for Equality of Means						
								95% Confidence Interval of the Difference		
		F	Sig.	t	df	Sig. (2-tailed)	Mean Difference	Std. Error Difference	Lower	Upper
SOX2	Equal variances assumed	2.469	.191	-17.101	4	.000	-27.63333	1.61589	-32.11977	-23.14689
	Equal variances not assumed			-17.101	2.517	.001	-27.63333	1.61589	-33.38205	-21.88461

SPSS data set of SOX2. Representative data was showed stastical analysis of SOX2 on AML-M5-derived iPSC and parental AML-M5 cell line using Mann-Whitney Test and Independent T-Test.

Mann-Whitney Test

Ranks

sample	N	Mean Rank	Sum of Ranks
NANOG positive control	3	3.00	9.00
iPSCs	3	4.00	12.00
Total	6		

Test Statistics^b

	NANOG
Mann-Whitney U	3.000
Wilcoxon W	9.000
Z	-.655
Asymp. Sig. (2-tailed)	.513
Exact Sig. [2*(1-tailed Sig.)]	.700 ^a

a. Not corrected for ties.

b. Grouping Variable: sample

```
T-TEST GROUPS=Sample (1 2)
/MISSING=ANALYSIS
/VARIABLES=NANOG
/CRITERIA=CI (.95) .
```

T-Test

[DataSet1] C:\ah bee's info\research lab\SPSS\data key in template.sav

Group Statistics

sample	N	Mean	Std. Deviation	Std. Error Mean
NANOG positive control	3	70.5000	.78102	.45092
iPSCs	3	73.9000	31.12411	17.96951

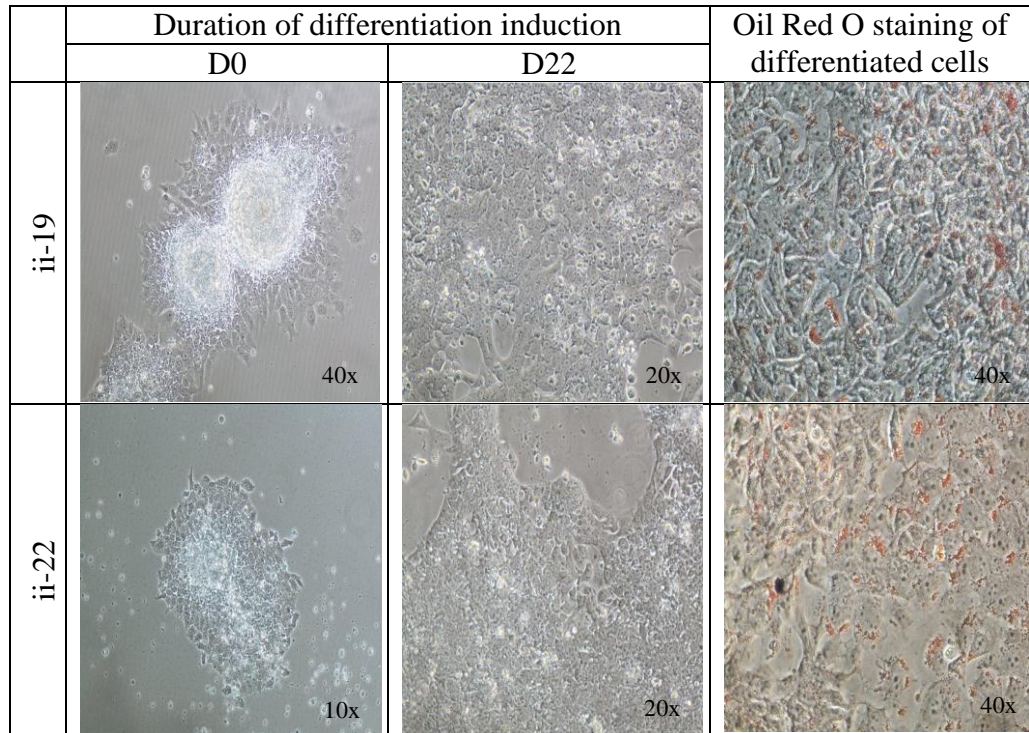
Independent Samples Test

		Levene's Test for Equality of Variances		t-test for Equality of Means						
									95% Confidence Interval of the Difference	
		F	Sig.	t	df	Sig. (2-tailed)	Mean Difference	Std. Error Difference	Lower	Upper
NANOG	Equal variances assumed	14.906	.018	-.189	4	.859	-3.40000	17.97517	-53.30707	46.50707
	Equal variances not assumed			-.189	2.003	.867	-3.40000	17.97517	-80.64776	73.84776

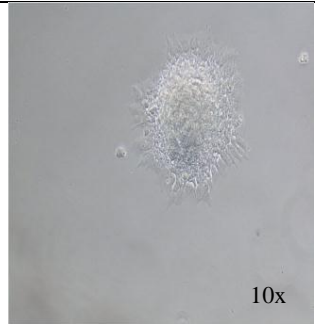
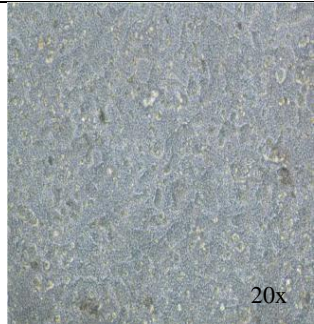
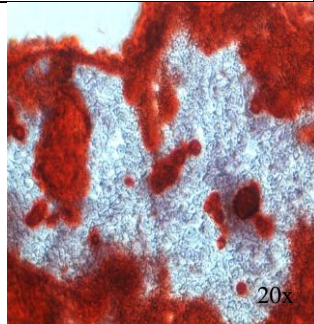
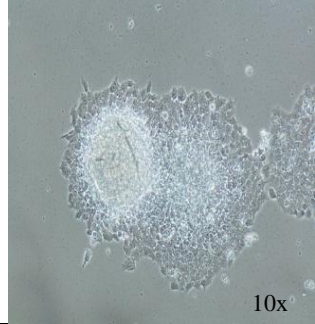
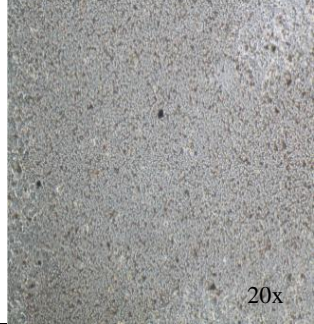
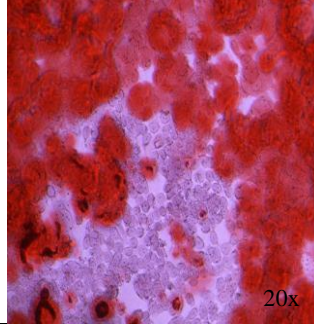
SPSS data set of NANOG. Representative data was showed stastical analysis of NANOG on AML-M5-derived iPSC and parental AML-M5 cell line using Mann-Whitney Test and Independent T-Test.

APPENDIX G

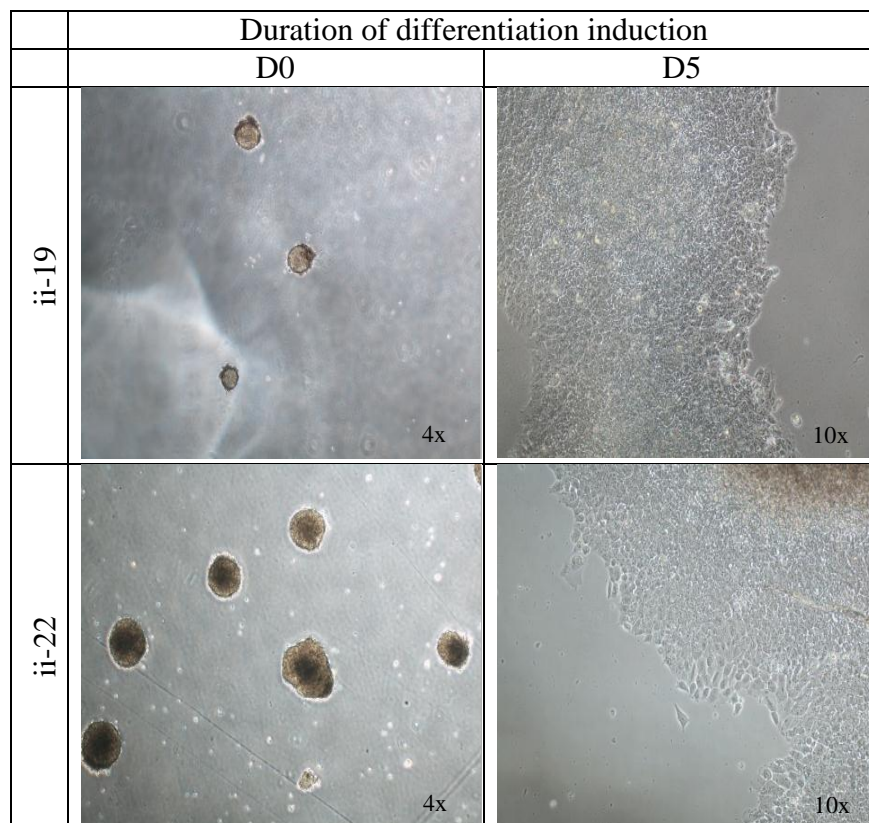
Three Germ Layers Differentiation Assays



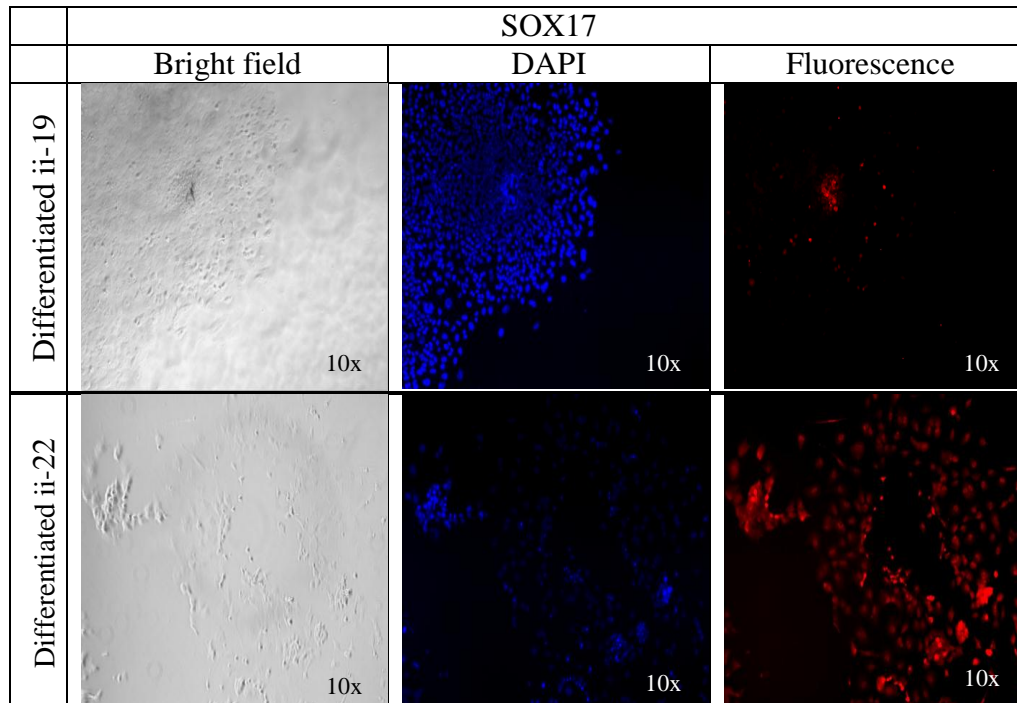
Induction of adipogenesis differentiation. Phase contrast images showed morphological changes of AML-M5-derived iPSC clones (ii-19 and ii-22) from day 0 to day 22. Presence of oil droplets in differentiated AML-M5-derived iPSC clones (ii-19 and ii-22) were stained by Oil Red O staining, as indicated in red colour staining.

	Duration of differentiation induction		Alizarin Red staining of differentiated cells
	D0	D22	
ii-19			
ii-22			

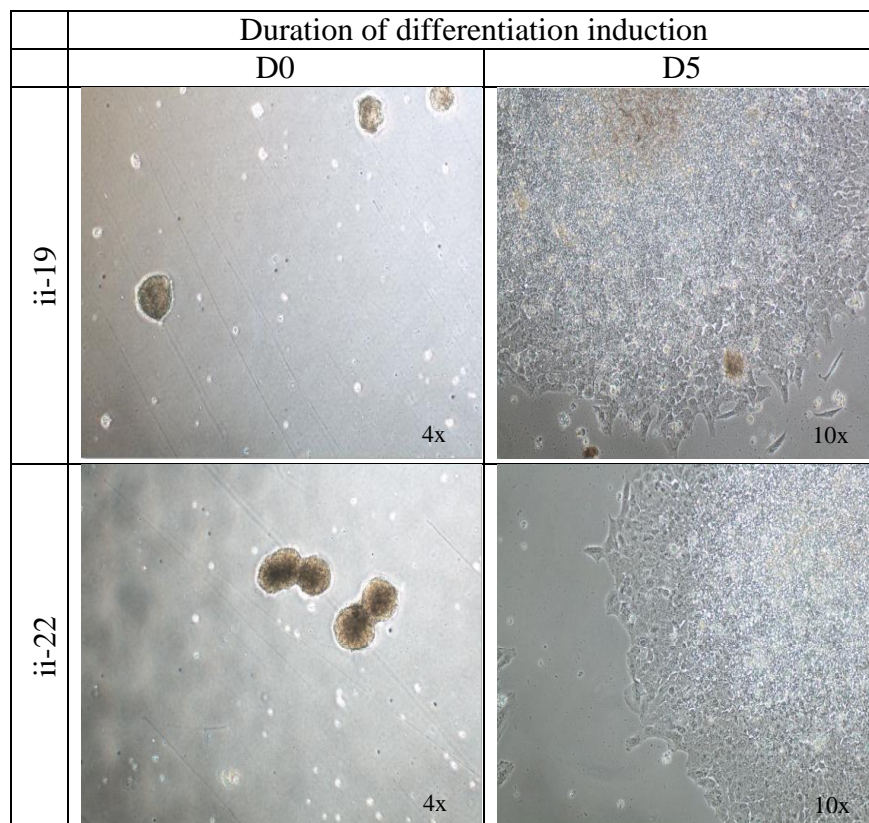
Induction of osteogenesis differentiation. Phase contrast images showed morphological changes of AML-M%-derived iPSC clones (ii-19 and ii-22) from day 0 to day 22. Accumulation of calcium ions in all differentiated cells were positively stained by Alizarin Red stain, as indicated by red precipitate.



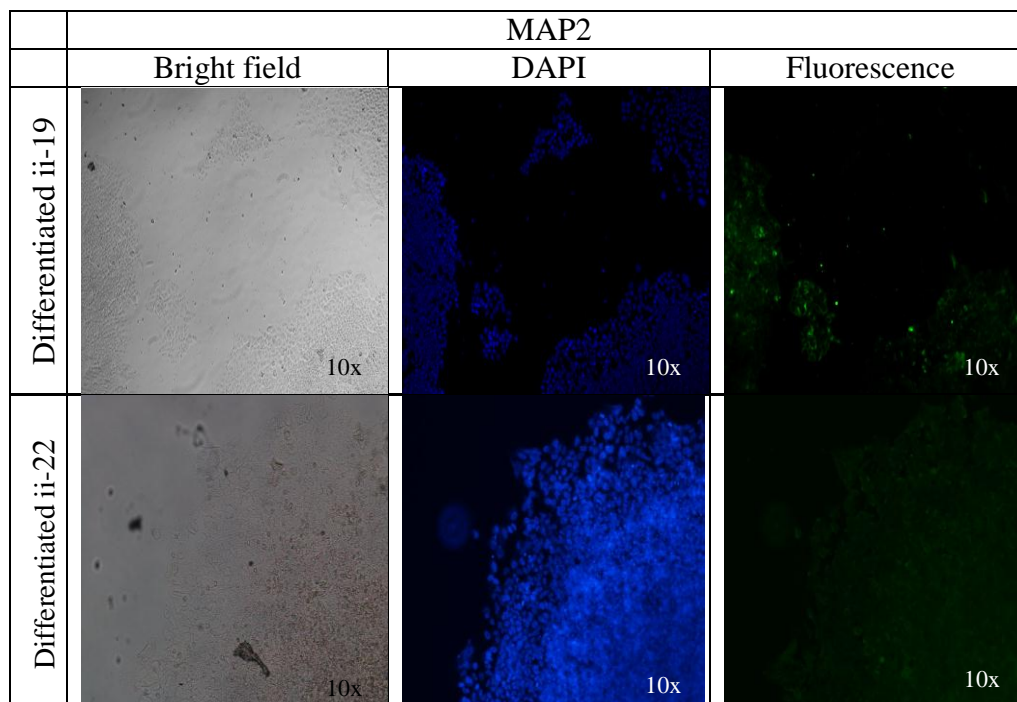
Activin A-induced endoderm differentiation of AML-M5-derived iPSCs. Phase contrast images showed morphological changes of AML-M5-derived EBs from day zero to day five of differentiation induction. Cell outgrowths were formed from AML-M5-derived EBs.



Detection of definitive endoderm marker SOX17 using immunofluorescence staining. Phase contrast and fluorescent images were captured from differentiated cells. DAPI was counterstained to indicate the presence of nuclei acid. Pseudo-red fluorescence signal indicated positive staining of SOX17 in differentiated cells. Expression of SOX17 was confined in outgrowth region of differentiated ii-19, whereas homogenously expressed in differentiated ii-22.



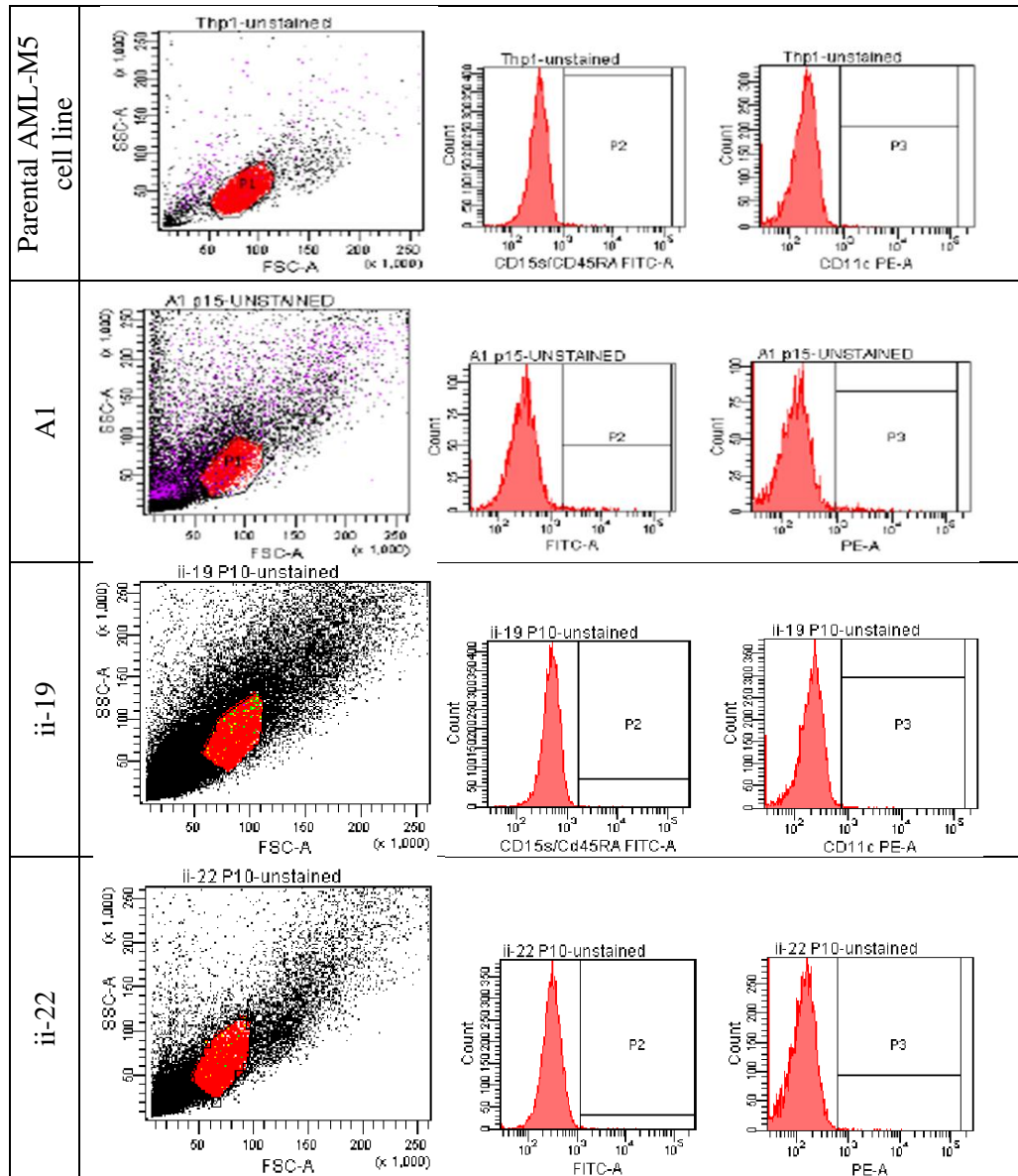
Noggin-induced ectoderm differentiation of AML-M5-derived iPSC. Phase contrast images showed morphological changes of AML-M5-derived EBs from day zero to day five of differentiation induction. Cell outgrowths were formed from AML-M5-derived EBs.



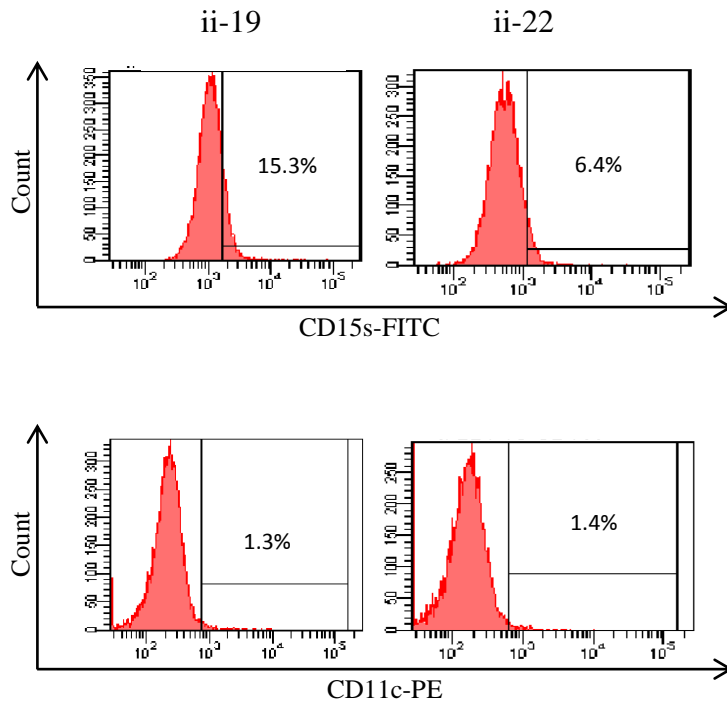
Detection of ectoderm marker MAP2 using immunofluorescence staining. Phase contrast and fluorescent images were captured from differentiated cells. DAPI was counterstained to indicate the presence of nuclei acid. Pseudo-green fluorescence signal indicated positive staining of MAP2 in differentiated cells. Result showed dim but homogenous expression of MAP2 in differentiated-22 cells, whereas expression of MAP2 was detected in small population of differentiated ii-19 cells.

APPENDIX H

Detection of Monocytic-specific Markers using Immunophenotyping



FACS unstained controls of monocytic markers on parental AML-M5 cell and AML-M5-derived iPSC clones. Representative histogram obtained from FACS profile showed low auto-fluorescence background of CD11c and CD15s on parental AML-M5 cell line and AML-M5-derived iPSC clones (A1, ii-19 and ii-22).



FACS analysis of monocytic-specific markers on other AML-M5-derived iPSC clone. Histograms displayed expression of monocytic-specific marker CD15s on ii-19 and ii-22 was 15.3% and 6.4%, respectively. On the other hand, expression of monocytic-specific marker CD11c on ii-19 and ii-22 was 1.3% and 1.4%, respectively.

APPENDIX I

SPSS Data Set

Mann-Whitney Test

		Ranks		
sample		N	Mean Rank	Sum of Ranks
CD15s	positive control	3	5.00	15.00
	iPSCs	3	2.00	6.00
	Total	6		

		CD15s
Mann-Whitney U		.000
Wilcoxon W		6.000
Z		-1.964
Asymp. Sig. (2-tailed)		.050
Exact Sig. [2*(1-tailed Sig.)]		.100 ^a

a. Not corrected for ties.

b. Grouping Variable: sample

```
T-TEST GROUPS=sample ( 1 2 )
/MISSING=ANALYSIS
/VARIABLES=CD15s
/CRITERIA=CI (.95) .
```

T-Test

[DataSet1] C:\ah bee's info\research lab\SPSS\data key in template.sav

Group Statistics					
sample	N	Mean	Std. Deviation	Std. Error Mean	
CD15s	positive control	3	98.4333	1.26623	.73106
	iPSCs	3	14.8000	8.16149	4.71204

Independent Samples Test										
		Levene's Test for Equality of Variances		t-test for Equality of Means						
								95% Confidence Interval of the Difference		
		F	Sig.	t	df	Sig. (2-tailed)	Mean Difference	Std. Error Difference	Lower	Upper
CD15s	Equal variances assumed	3.268	.145	17.539	4	.000	83.63333	4.76841	70.39409	96.87257
	Equal variances not assumed			17.539	2.096	.003	83.63333	4.76841	63.99312	103.27354

SPSS data set of CD15s. Representative data was showed statistical analysis of CD15s on AML-M5-derived iPSC and parental AML-M5 cell line using Mann-Whitney Test and Independent T-Test.

Mann-Whitney Test

Ranks

sample	N	Mean Rank	Sum of Ranks
CD11c positive control	3	5.00	15.00
iPSCs	3	2.00	6.00
Total	6		

Test Statistics^b

	CD11c
Mann-Whitney U	.000
Wilcoxon W	6.000
Z	-1.993
Asymp. Sig. (2-tailed)	.046
Exact Sig. [2*(1-tailed Sig.)]	.100 ^a

a. Not corrected for ties.

b. Grouping Variable: sample

```
T-TEST GROUPS=Sample (1 2)
/MISSING=ANALYSIS
/VARIABLES=CD11c
/CRITERIA=CI (.95) .
```

T-Test

[DataSet1] C:\ah bee's info\research lab\SPSS\data key in template.sav

Group Statistics

sample	N	Mean	Std. Deviation	Std. Error Mean
CD11c positive control	3	79.2000	.95394	.55076
iPSCs	3	1.3667	.05774	.03333

Independent Samples Test

		Levene's Test for Equality of Variances		t-test for Equality of Means						
								95% Confidence Interval of the Difference		
		F	Sig.	t	df	Sig. (2-tailed)	Mean Difference	Std. Error Difference	Lower	Upper
CD11c	Equal variances assumed	4.766	.094	141.063	4	.000	77.83333	.55176	76.30139	79.36528
	Equal variances not assumed			141.063	2.015	.000	77.83333	.55176	75.47575	80.19092

SPSS data set of CD11c. Representative data was showed statistical analysis of CD11c on AML-M5-derived iPSC and parental AML-M5 cell line using Mann-Whitney Test and Independent T-Test.